The Cardioprotective Effect of a Lanosteryl Triterpene from *Protorhus Longifolia* on H9c2 Cardiomyoblasts

Dissertation submitted in fulfilment of the requirements for the degree of

Master of Science in Biochemistry (December 2017) Candidate:

NONHLAKANIPHO F. SANGWENI (201148985)

Supervisors': Dr R.A Mosa and Dr R Johnson

Co-Supervisors': Prof C.J.F Muller and Prof A. Kappo

Department of Biochemistry and Microbiology, Faculty of Science and Agriculture, University of Zululand, KwaDlangezwa, KwaZulu Natal, South Africa

DECLARATION

I, Nonhlakanipho F. Sangweni declare that the entirety of the work contained herein is my own and that it has not been submitted for any degree or examination in any other University and that all the sources I have used have been acknowledged by complete references.

Signature: ……..

Nonhlakanipho F. Sangweni (201148985)

Date: ……

ABSTRACT

Introduction: Diabetes mellitus is a predisposing factor of cardiovascular diseases (CVDs). Globally, CVDs are the prominent cause of death in both diabetic and nondiabetic individuals. In an effort to fight the disease burden, more researchers are looking into natural-products as adjunctive therapies to use with the current treatment regimen against diabetes and concomitant cardiovascular complications. For decades, herbalists in the Zululand region of KwaZulu-Natal have been using *Protorhus longifolia* as a blood-thinning agent. Recently, Mosa and colleagues have demonstrated that methyl-3β-hydroxylanosta-9,24-dien-21-oate (RA3) derived from the stem barks of *P. longifolia* can act as a nutraceutical to control hyperglycemia, hyperlipidemia and reduce insulin resistance in a diabetic animal model. However, no mechanism associated with its cardioprotective potential has been proposed.

Aim: In this study, we aimed to assess the mechanism by which methyl-3βhydroxylanosta-9,24-dien-21-oate (RA3) is able to improve glucose uptake, whilst decreasing lipotoxicity, oxidative stress, insulin resistance and apoptosis in H9c2 cardiomyoblasts exposed to high glucose.

Methodology: H9c2 cardiomyoblasts were cultured in either normal (NG- 5.5 mM) or high (HG- 33 mM) glucose for 24 hrs. Subsequently, cells exposed to HG were treated with RA3 (1 µM), n-acetyl cysteine (NAC, 1 mM), metformin (MET, 1 µM), a combination of MET+RA3 (both at 2 µM) as well as MET+NAC (at 2µM and 2 mM, respectively) for a further 24 hrs. Time and dose response as well metabolic activity were assessed using ATP assays. While, the cardioprotective potential of RA3 to attenuate high glucose induced, shift in substrate preference, where investigated using various biochemical assays and protein expression analysis.

Results: Data from this study accentuated the anti-diabetic properties of RA3 through its ability to improve shift in substrate preference and insulin signaling in the H9c2 cardiomyoblasts. We further demonstrated the capability of RA3 to mitigate high glucose induced oxidative stress and accelerated apoptosis in these cells. Interestingly the results from this study showed a synergistic cardioprotective effect with the treatment of

MET+RA3. However, the combination of MET+NAC was not as effective as MET alone to alleviate high-glucose-induced cardiac dysfunction.

Conclusion: Data presented in this study provides a plausible mechanism by which RA3 protects the myocardium against hyperglycemic-induced oxidative stress and apoptosis.

Acknowledgements

For I know the plans I have for you," declares the LORD, "plans to prosper you and not to harm you, plans to give you hope and a future (Jerimiah 29:11)

This research was funded in part by the National Research Foundation (NRF) Thuthuka Programme Grant 87836 and the South Africa Medical Research Council's Biomedical Research and Innovation Platform.

To my Supervisor's: The successful completion of this project would not have been possible without the impeccable supervision I have received.

It is very rare that you come across strangers with an open heart, willing to go beyond the bare minimum in order to see you succeed. Dr Johnson and Dr Mosa, you have become dear to me. Having been supervised by the best I truly believe there could not have been a better fitting. From the very 1st day, I have been in awe of your work ethic, empathy, poise and natural enthusiast for research. As such, I can only hope to become as great of a scientist as you are.

To my co-supervisor's: Prof. Muller and Prof Kappo, thank you for your invaluable guidance, words of encouragement and contribution throughout this project. I am forever grateful.

BRIP Director: To Prof. Louw, your overall fairness in the way you lead is something I have never seen before and the reason you are respected by everyone, including myself. I am grateful for all the opportunities you have exposed too. Thank you for everything.

BRIP Staff and Cardio-metabolism group: Thank you for all the assistance you have provided throughout this project. To Charna, thank you for editing and polishing my manuscript. To Kwazi, thank you for always having your door open and assisting me where possible. To Samira, thank you for all the technical assistance you have provided.

To Dr. Dludla: I treasure the influence you have had in my growing career. Your support, valuable input and always going the extra mile throughout this journey is something I will forever be grateful too. Thanks Phiwa.

Family, friends and colleagues: To my friends and colleagues, thank you for the consistent support and making this journey bearable. To Samke and Sihle, thank you for all your help and times spent laughing throughout.

To my amazing family, thank you for the love, constant encouragement and overall support.

To my Moms (Thembalihle and Zinhle), you did this! Everything that I am is through your selfless love, patience and strength.

OUTPUTS

Symposiums, conference proceeding and workshop(s)

Symposium

N.F. Sangweni, R. Johnson, P.V. Dludla, C.J.F Muller, J. Louw and R.A. Mosa. The cardioprotective potential of a lanosteryl triterpene on H9c2 cardiomyoblasts. SABI River Sun, Nelspruit, University of Limpopo symposium, 26 August 2017

N.F. Sangweni, R. Johnson, P.V. Dludla, C.J.F Muller, J. Louw and R.A. Mosa. The cardioprotective potential of a lanosteryl triterpene on H9c2 cardiomyoblasts. Biomedical Research and Innovation Platform symposium. Cape town, South Africa, 16 October 2016.

Conference

N.F. Sangweni, R. Johnson, P.V. Dludla, C.J.F Muller, J. Louw and R.A. Mosa. The cardioprotective potential of a lanosteryl triterpene on H9c2 cardiomyocytes. The South African Annual Pharmacology Conference. Bloemfontein, South Africa, 1st - 4th October 2017.

Workshop

N.F. Sangweni. Novartis Healthcare Professional University – Grant-writing Workshop-: Johannesburg, South Africa, 8-9 December 2017

Table of Contents

LIST OF TABLES

LIST OF FIGURES

LIST OF ABBREVIATION

Akt	Protein kinase B
AMP	Adenosine monophosphate
AMPK	Adenosine monophosphate-activated protein kinase
ANOVA	Analysis of variance
ATP	Adenosine triphosphate
BSA	Bovine serum albumin
Ca^{2+}	Calcium
CAT	Catalase
CVDs	Cardiovascular diseases
Cyt c	Cytochrome c
DCFH-DA	Dichlorodihydrofluorescein diacetate
DCM	Diabetic cardiomyopathy
DdH2O	Double distilled water
DM	Diabetes mellitus
DMEM	Dulbecco’s Modified Eagle’s Medium
DMSO	Dimethyl sulfoxide
DNA	Deoxyribonucleic acid
DPBS	Dulbecco’s phosphate buffered saline
ER	Endoplasmic reticulum
ERK	Extracellular signal-regulated protein kinase
FBS	Foetal bovine serum

GDP	Gross domestic product
GSH	Glutathione
H_2O_2	Hydrogen peroxide
H9c2	Embryonic ventricular rat heart-derived myogenic cell line
HCl	Hydrochloride
HF	Heart Failure
HPLC	High Performance liquid chromatography
IDF	International Diabetes Federation
JNK	c-Jun N-terminal kinase
MDA	Malondialdehyde
MS	Mass Spectrometry
NAC	N-acetyl cysteine
NAD	Nicotinamide adenine dinucleotide
NADH	Nicotinamide adenine dinucleotide hydrate
NaOH	Sodium hydroxide
NCDs	Non-communicable diseases
NF-kB	Nuclear factor kappa-B
NRF	National Research Foundation
O_2	Oxygen
$O_2^{\bullet-}$	Superoxide radical
$OH^{\bullet}$	Hydroxyl radical
PBS	Phosphate-buffered saline
Pen/strep	Penicillin-streptomycin
PI	Propidium iodide
PI3K	Phosphatidylinositol 3-phosphate kinase
PMSF	Phenylmethylsulfonyl fluoride
PVDF	Polyvinylidene fluoride
Resv	Resveratrol
ROS	Reactive oxygen species

RT	Room temperature
SAMRC	South African medical Research Council
SDS-Page	Sodium dodecyl sulfate poly-acrylamide gel electrophoresis
SOD	Superoxide dismutase
STATS SA	Statistics South Africa
TBARS	Thiobarbituric Acid Reactive Substances
TBST	Tris-buffered saline containing Tween-20
TC	Tissue culture
Tris	Trizma
WHO	World Health Organization
β-ME	Beta-Mercaptoethanol

CHAPTER ONE

INTRODUCTION TO THE CURRENT STUDY

1.0 Introduction

The medicinal usage of herbal derivatives as pharmaceutical products has been the major focus of increasing investigation, with the main focus being on reducing noncommunicable diseases (NCDs) through therapeutic invention. For thousands of years, our ancestors have relied on herbal medicine, also known as phytomedicine, to treat diseases such as diabetes mellitus (DM). Plants such as *Allium sativum*, *Gymnema sylvestre* and *Pterocarpus marsupium*, to name a few, have been traditionally consumed and scientifically validated for their therapeutic effect against diabetes mellitus (DM) and resultant complications (Srivastava, Lal and Pant, 2012). Of particular interest is *Galega officinalis,* a herbal plant that was used in traditional medicine to treat the now known Type 2 DM (T2DM). The hypoglycemic effect of *G. officinalis,* which was established in 1918, was attributed to its rich source of guanidine. However, it was later found that this compound possessed cytotoxic effects and had a limited efficacy. From this, several other biguanides were investigated which led to the discovery of dimethylbiguanide, an antidiabetic agent now commonly known as metformin/glucophage. To date, metformin is the most widely prescribed first line antidiabetic drug with known cardioprotective properties. However, cumulative evidence suggests that the efficacy of metformin against diabetes and associated cardiovascular complications diminishes over time.

As such, there has been renewed interest in herbal medicine as alternative or adjunctive therapeutics to the current synthetic anti-diabetic drugs (Lozano-Mena *et al.*, 2014). Southern Africa is known for its diverse flora kingdom that is a rich source of polyphenols with known medicinal properties (Enshasy *et al.*, 2013; Street and Prinsloo, 2013). An example is *Aspalathus linearis,* commonly known as rooibos, a leguminous shrub native to the Cedarberg region of South Africa. The regular consumption of rooibos has been linked with the reduction of serum triglycerides and cholesterol in human subjects (Schloms *et al.*, 2011)]. In addition, compounds found in rooibos such as aspalathin, a *C*glucosyl dihydrochalcone as well as the phenylpropenoic acid, phenylpyruvic acid-2-*O*-β$_D$-glucoside (PPAG) have been shown to display an enhanced effect in reducing

hyperglycemia thereby, preventing diabetes and its associated cardiovascular complications (Johnson *et al.*, 2017; P. V. Dludla *et al.*, 2017).

Of particular interest, to this study, is *Protorhus longifolia* (Benrh.) Engl. a plant native to Southern Africa with reported anti-diabetic properties. The major biological activities of this plant may be attributed to its lanosteryl triterpenes, which include methyl-3βhydroxylanosta-9, 24-dien-21-oate (RA3) and 3β-hydroxylanosta-9, 24-dien-21-oic acid (RA5). Mosa and colleagues have progressively reported on the antidiabetic and cardioprotective properties of lanosteryl triterpenes, extracted from the stem barks of *Protorhus longifolia* (Mosa *et al.*, 2015, 2016). However, currently no study has summarized evidence relating to the metabolic benefits of these triterpenes in preventing diabetes-induced cardiovascular dysfunction. In this study, we elaborated on the therapeutic potential as well as the proposed mechanism associated with the protective effect of these compounds against diabetes-induced myocardial dysfunction. Furthermore, a brief overview of the pathophysiology associated with the development of diabetic cardiomyopathy (DCM) is provided to accentuate the cardioprotective potential of these triterpenes.

1.1 STUDY OULINE

1.1.1 Aim

In the present study, we aimed to investigate the mechanism associated with the cardioprotective potential of lanosteryl triterpenes from the stem barks of *Protorhus longifolia* on H9c2 cardiomyoblasts.

1.1.2 Objectives

- To isolate the triterpenes (RA3 and RA5) from the chloroform extract of plant material.
- To determine the effect of RA3 on oxidative stress and apoptosis
- To study the effects of RA3 on hyperglycemia and hyperlipidemia in H9c2 cells
- To establish a relationship between RA3 and metformin as a combination treatment

1.1.3 Intended contribution to the body of knowledge

This study will add to the current body of knowledge on the cardioprotective effect of methyl-3β-hydroxylanosta-9, 24-dien-21-oate against diabetic stressors as well as elaborate on its potential mechanism.

This dissertation will be divided into 6 chapters:

1. Introduction
2. Literature Review
3. Materials and Methodology
4. Results
5. Discussion
6. Conclusion

CHAPTER TWO

LITERATURE REVIEW

2.1 Literature Review Introduction

2.1.1 Diabetes and associated cardiovascular disease

Diabetes mellitus (DM) is a complex metabolic disease that is distinguished by chronic hyperglycemia, hyperlipidemia and insulin resistance. The International Diabetes Federation (IDF, 2017) reports that globally, over 425 million people currently have diabetes and this number will escalate to over 629 million by the year 2045 (IDF, 2017). Furthermore, in Africa approximately 16 million individuals have diabetes of which 10.7 million are undiagnosed and it is predicted that the prevalence of DM in this region will rise by 156% (i.e.41 million diabetic patients) by 2045 (IDF, 2017). Alarmingly, this estimated increase supersedes Western Pacific, which currently have the highest diagnosed diabetic prevalence for 2017 (IDF, 2017). Interestingly, more than a decade ago DM was not ranked amongst the top 10 leading causes of mortality worldwide (Figure 2.1) and this was widely attributed to traditional lifestyles. However, as a result of urbanization and unhealthy lifestyle a shift in the top 10 leading causes of death has been observed with DM ranking sixth, globally (WHO, 2017). Similarly, in South Africa, DM is among the top ten leading causes of mortality being responsible for approximately 460 236 deaths, as recorded in 2015 (WHO, 2017). According to STATS South Africa, diabetes is now ranked 2nd amongst the prominent cause of mortality, in this region (STATS SA, 2017). With the increased prevalence of DM, a concomitant increase in the incidence of coronary artery disease and diabetic cardiomyopathy, is expected, as DM is a predisposing factor for the development of myocardial dysfunction.

Cardiovascular diseases (CVDs) are the leading cause of morbidity and mortality in individuals with and without diabetes, globally. A projected 17.7 million deaths in 2015 were attributed to CVDs, demonstrating 31% of all global mortalities (WHO, 2017) (Figure 2.1), of these, approximately 7.4 million were due to ischemic heart disease, commonly known as coronary artery disease (CAD). Globally, more deaths are attributed to CVDs than TB, HIV and malaria combined (STATS SA, 2017). In South Africa (SA), CVDs are the 4th leading cause of mortality and the recorded incidence being ascribed to an unhealthy lifestyle as SA has the highest levels of obese and overweight cases in the

world. Furthermore, in SA it has been reported that more than 5 people die of myocardial infarction every hour with half of these deaths occurring before the age of 65 (STATS SA, 2017). In addition, the reported premature deaths in the working age groups (35-64 years) is currently 41.3% and is expected to increase by 41% by the year 2030 (STATS SA, 2017).

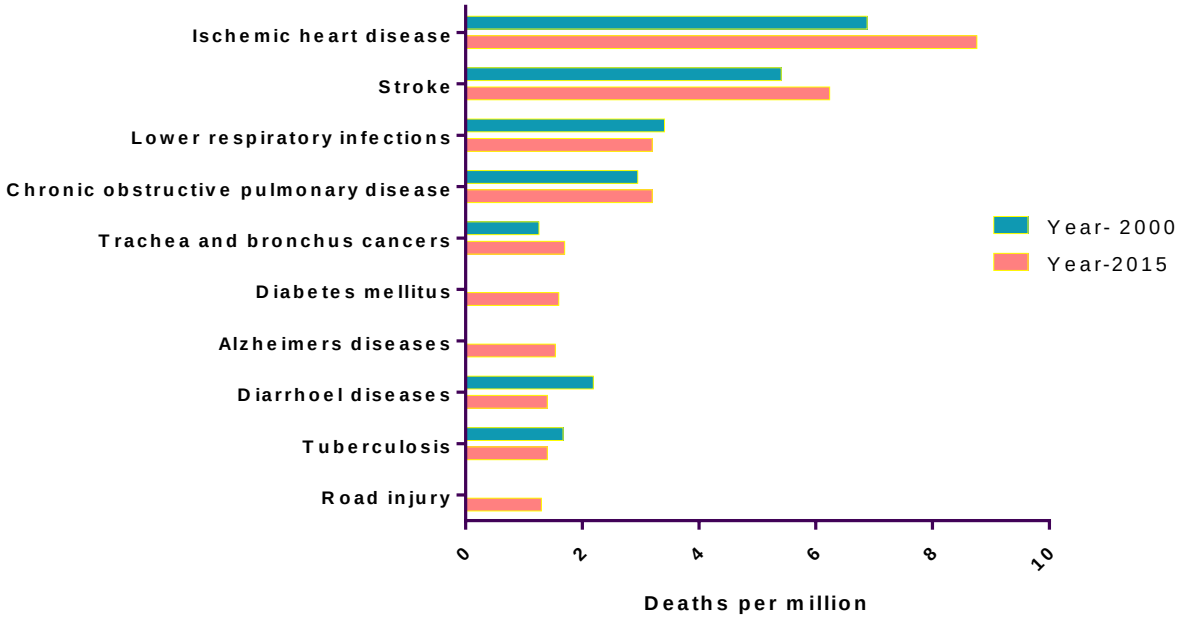

Figure 2.1: The top 10 global mortality rate for 2015. Cardiac diseases are the prominent cause of mortality, worldwide, with most deaths being caused by ischemic heart disease, followed by stroke. Resultant myocardial infarction accounts for the death of 3 individuals in every 10 reported mortalities, constituting to approximately 17.7 million deaths globally (WHO, 2017). More than a decade ago diabetes mellitus was not ranked amongst the 10 leading causes of death. However, the prevalence of DM has drastically increased placing it as the sixth major cause of mortality. (Adapted from the World Health Organization (2017)).

2.1.2 The effect of Diabetes and associated cardiovascular complications on health expenditure

In light of these global burdens characterized by premature mortality and the reduced quality of life, diabetes and related cardiovascular complications inflict a significant economic impact on a country's healthcare system and more importantly, individual

households. The current total healthcare expenditure for DM and heart diseases is estimated to be $ 673 billion and $ 555 billion, respectively. However, with the coming years the economic burden of these diseases is expected to escalate to $ 958 billion (DM- in 2045) and $ 1.1 trillion (CVDs- in 2035) (IDF, 2017; Khavjou *et al.*, 2016), respectively. In addition, the total cost of healthcare as a percentage of gross domestic product (GDP) spent in South Africa (SA) is 8.80%, which is equivalent to that of the United Kingdom (GDP- 9.12%) but 8.34% less than that of the United States of America (USA) (GDP- 17.14%)(Figure 2.2). Nonetheless, it is worth noting that the total cost of healthcare as a percentage of GDP for both private and government healthcare in SA (51.76% and 48.24%) is comparable with that of the USA (51.70% and 48.30%) (WHO, 2016).

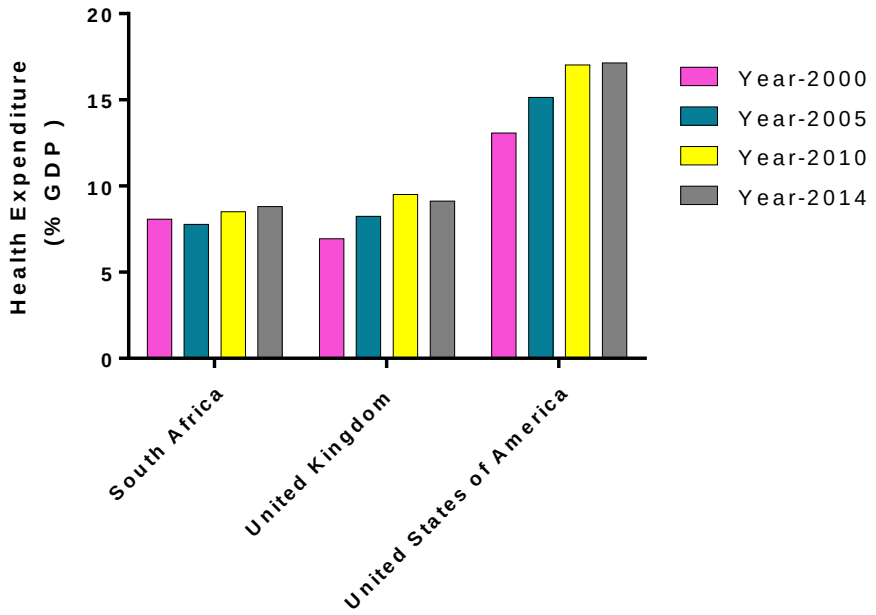

Figure 2.2: Diabetes-related healthcare expenditure in 2000-2014. Diabetes mellitus (DM) has an economic impact that warrants intervention. In the last decade, the total health care expenditure has become a serious economic burden. United States of America spends the most on healthcare expenditure as a percent of gross domestic product (GDP) ranging from 13-17.14%. Over the past years, the total expenditure as a percent of GDP for South Africa and the United Kingdom has steadily increased between 7-8.34% and 6.94-9.12%, respectively. (Adapted from the World Health Organization, 2016).

2.2 The role diabetes plays in the development of coronary artery disease and diabetic cardiomyopathy

2.2.1 Diabetes-induced coronary artery disease

Coronary artery disease (CAD), also referred to as ischaemic heart disease, is characterized by plaque build-up inside the walls of the arteries which restricts blood flow to the heart (Leon, 2015). This accelerated plaque build-up in the walls of the arteries has been linked to obesity induced inflammation and lipogenesis. It has been well reported that diabetic individuals have a 3 times increased risk for the development of CAD. The imbalance between food intake and energy expenditure has been described as the major contributing factor for the observed increase in obesity-induced inflammation and circulating free fatty acids (FFAs), as observed in diabetic patients with heart failure (HF) (Lopaschuk *et al.*, 2010; Ferrannini *et al.*, 2014). This increase in *de novo* FFA synthesis (lipogenesis) is a common abnormality associated with peripheral insulin resistance, which leads to chronic hyperglycemia, the driving force associated with the development of T2DM and CVDs. It has been reported by Mazibuko *et al.*, (2013) that prolonged elevated FFAs like palmitate, leads to an abnormal increase in intracellular lipid metabolites such as ceramide and diacylglycerol (DAG). Consequently, these metabolites result in the phosphorylation of protein kinase C, a major kinase known to inhibit the insulin receptor substrate 1 and thereby decreasing insulin stimulated glucose uptake in peripheral tissue (Mazibuko *et al.*, 2015). Literature has shown that the aforementioned along with excessive generation of reactive oxygen species (ROS) and inflammation, aggravates the formation of atherosclerosis in the diabetic patient (Hansson, 2005; Chait and Bornfeldt, 2009; Velayutham *et al.*, 2017).

2.2.2 Diabetes-induced cardiomyopathy

More than 4 decades ago, a unique clinical entity has been defined as diabetic cardiomyopathy (DCM) which exists in the absence of CAD or hypertension (Khavandi *et al.*, 2009; Kiencke *et al.*, 2010). Rubler (1972) was the first to define DCM after a postmortem study on the hearts of four diabetic patients, in which he observed a

significant increase in left ventricular wall thickness (Rubler *et al.*, 1972; Freire and Moura, 2007; Tarquini *et al.*, 2011). As such, the disease is distinctly characterised by a disproportionately enlarged left ventricular mass and diastolic dysfunction which is associated with reduced cardiac efficiency (CF) and ejection fraction (EF) (Figure 2.3) (Stanley, Recchia and Lopaschuk, no date; Fotbolcu *et al.*, 2010; Sharma and Kass, 2014). This decrease in CF and EF impairs the heart's ability to pump blood into the circulatory system thereby leading to fluid build-up in the lungs (pulmonary oedema) and legs (peripheral oedema) (Szwejkowski *et al.*, 2013; Velagaleti *et al.*, 2014). Unlike CAD which remains the most prominent type of CVD, the lower incidence of DCM can be obscured by its nebulous nature and lack of specific biomarkers for its early detection Kiencke *et al.*, 2010; Dandamudi *et al.*, 2014). Currently, DCM is detected at its late stages with diabetic patients already displaying symptoms similar to CAD such as ischemia and systolic dysfunction (Sanchis-Gomar *et al.*, 2016). While these diseases are distinctively different, numerous studies have reported on the interlinking pathophysiological mechanisms involving hyperglycemia-induced oxidative stress and impaired inflammatory response in the development of DCM and CAD (Figure 2.4) (Kayama *et al.*, 2015; Dludla *et al.*, 2017).

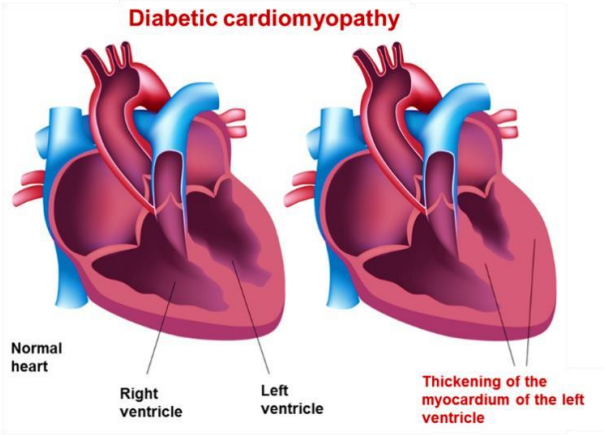

Figure 2.3: Representation of diabetes-induced cardiomyopathy. Diabetic cardiomyopathy is described as a disease of the cardiac muscle developing exclusively in people with diabetes. It is characterised by left ventricular dysfunction, resulting from the thickening of the cardiac walls and subsequent thinning of the left ventricle. This then impairs the hearts ability to pump blood into the circulatory system thereby leading to fluid build-up in the lungs (pulmonary oedema) and legs (peripheral oedema). Adapted from the Australian Heart registry (AGHDR, 2016).

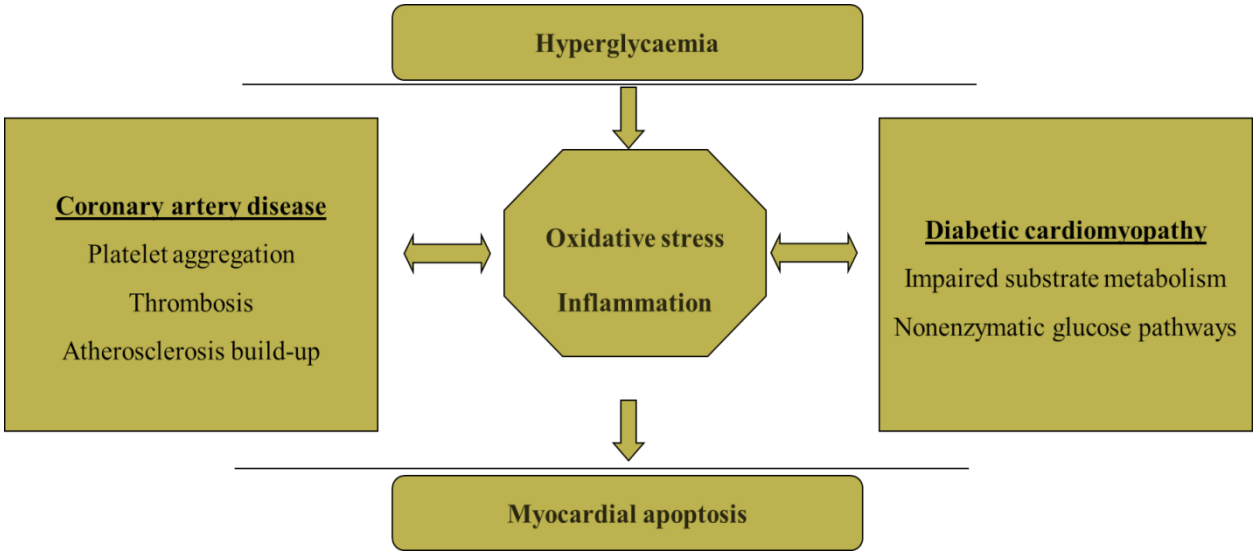

Figure 2.4: Interlinking pathophysiology of diabetic cardiomyopathy (DCM) and coronary artery disease (CAD). Diabetic cardiomyopathy and CAD remain the leading cardiovascular complications implicated in accelerated myocardial infarction within a diabetic state. The mechanism explaining the pathophysiology leading to myocardial infarction, especially distinguishing between the development of CAD and DCM, in a diabetic state are still to be fully elucidated. Although inflammation and non-enzymatic glucose pathways are identified in the development of both CAD and DCM, atherosclerosis build-up is absence in DCM.

2.2.3 Role of oxidative stress and inflammation in diabetes-induced cardiomyopathy

Although other mechanisms including actions of the polyol and hexosamine biosynthetic pathways, production of advanced glycation end products and stimulation of protein kinase C have been linked to the development of DCM, the alteration of the myocardial substrate preference is increasingly recognized as the key initial step in the onset of DCM (Rijzewijk *et al.*, 2009; Liu, Wang and Cai, 2014; Faria and Persaud, 2017). It is well established that substrate metabolism is impaired during the early developmental stage of DCM, with the heart becoming almost completely reliant on FFA as an energy source (Lopaschuk *et al.*, 2010; Johnson *et al.*, 2016). This consequence was initially described by Randle and colleagues, where they showed that increased flux of FFA into the myocardium inhibits uptake and oxidation of glucose (Randle *et al.*, 1963) (Figure 2.5).

Similarly, in a study performed by our group we reported on the accelerated lipid uptake with a subsequent decrease in glucose uptake in embryonic rat heart derived H9c2 cells cultured in high glucose (HG) (Johnson *et al.*, 2016). Even though its utilization is low compared to that of FFAs in the non-diabetic heart, glucose provides better energy efficiency due to its reduced use of oxygen per ATP molecule produced (Long and Zierath, 2006; Menard *et al.*, 2010; Forbes and Cooper, 2013). Thus far, *in vitro* and *in vivo* studies performed on H9c2 cardiomyocytes exposed to high glucose on type 2 diabetic animal models as well as human subjects have confirmed this phenomenon (Tsai *et al.*, 2013; Dhar *et al.*, 2016; Johnson *et al.*, 2016). Asymptomatic diabetic patients without cardiac ischaemia present altered myocardial substrate metabolism concomitant to impaired left ventricular diastolic function when compared to non-diabetic control subjects (Taegtmeyer *et al*., 2002; Bugger and Dale Abel, 2014). Cumulative literature has been presented that impaired myocardial substrate preference can contribute to left ventricular diastolic function through the activation of oxidative stress and proinflammatory processes that eventually lead to myocardial apoptosis (Valen, Yan and Hansson, 2001; Cai *et al.*, 2002; Freire and Moura, 2007; Peng *et al.*, 2013).

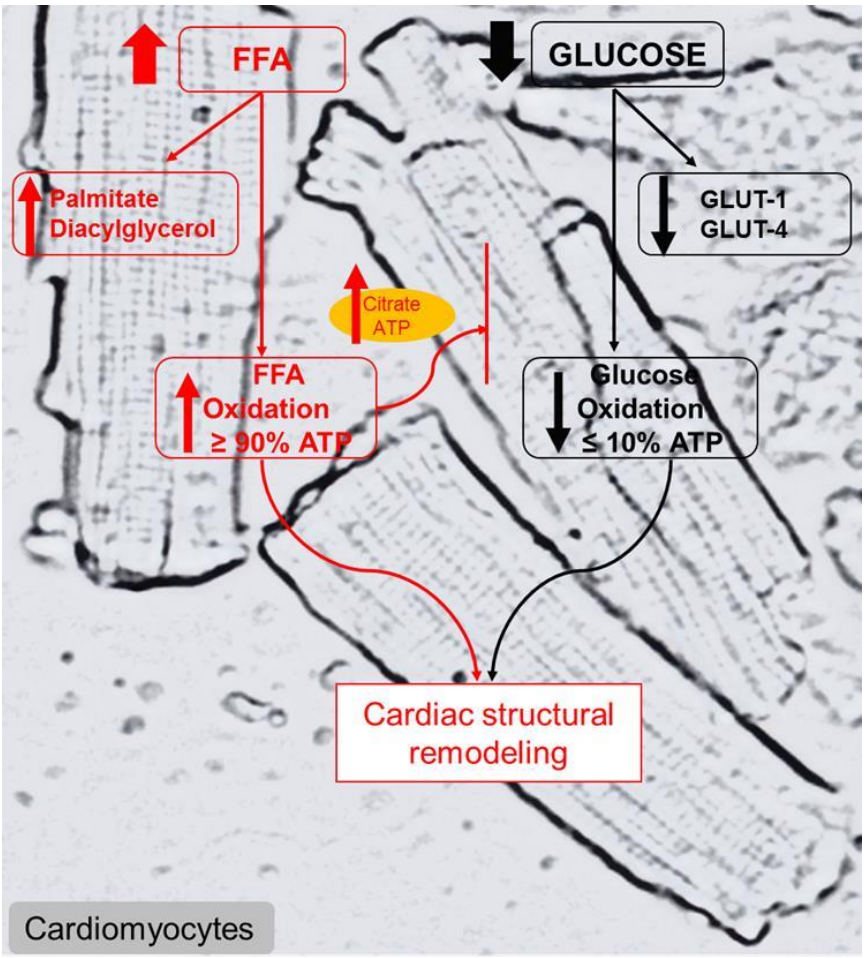

Figure 2.5: Free fatty acid oxidation and glucose uptake in the diabetic heart. Cardiac structural remodeling as a consequence of impaired cardiac substrate metabolism is associated with enhanced fatty acid uptake and oxidation (up to 90%) and repressed glucose uptake and oxidation (to less than 10%). GLUT-1 and GLUT-4 are the main glucose transporters compromised in the diabetic heart, while palmitate and DAG are the main intermediates indicative of enhanced intra-myocardial lipid accumulation. Adenosine triphosphate; **DAG**: diacylglycerol; **FFAs**: free fatty acids; **GLUT-1**: glucose transporter 1; **GLUT-4:** glucose transporter 4.

The excessive use of oxygen, due to impaired substrate metabolism of the myocardium corresponds to enhanced generation of ROS, which triggers cell apoptosis (Loor and Schumacker, 2008; Younce *et al.*, 2013). In the cardiomyocytes, elevated ROS production and impaired mitochondrial membrane potential has been reported in several hyperglycemic studies as reviewed by Dludla and colleagues (P. V. Dludla *et al.*, 2017). Here, increased activity of NADPH oxidases and depolarized mitochondrial membrane were associated with accelerated oxidative damage in a glycemic state. Also, the

activation of nuclear factor (erythroid-derived 2)-like 2 (Nrf2) and its downstream targets such as uncoupling proteins and antioxidant enzymes were revealed to be key players in protecting the heart against oxidative damage (Kowaltowski *et al.*, 2009; Tsai *et al.*, 2013; P. Dludla *et al.*, 2017). In agreement, a recent review by Satta and colleagues provided compelling evidence that "targeted activation of Nrf2, or downstream genes may prove to be a useful avenue in developing therapeutics to reduce the impact of cardiovascular disease" (Satta *et al.*, 2017).

The activation of oxidative stress within a diabetic state is linked to the initiation of proinflammatory factors (Varga *et al.*, 2015). Obesity or diabetes-induced chronic inflammation and subsequent activation of cytokines and chemokines such as interleukin6 (IL-6), tumor necrosis factor alpha (Tnf-α) and nuclear factor kappa-light-chain enhancer of activated B cells (NF-kB) in combination with increased ROS and shift in substrate preference can result in augmented LV hypertrophy and EF, a morphological hallmark of DCM (Neri *et al.*, 2015; Esser *et al.*, 2014). Another important factor, c-Jun Nterminal kinases (JNKs), belonging to mitogen-activated protein kinase family, have been demonstrated as major role players in the regulation of diabetes-induced inflammation. Increased ROS can cause activation of JNKs via double phosphorylation of threonine and tyrosine residues, leading to the elevation of NF-κB and Tnf-α levels and subsequent increase in apoptosis (Evans *et al.*, 2002; Battiprolu *et al.*, 2013).

2.3 Effect of hyperglycemia on insulin signaling in the heart

2.3.1 Insulin dependent pathway

Much evidence has been presented that a diabetic heart can be salvaged through the effective control of glucose and lipid metabolism. Insulin remains a vital hormone for not just lowering raised blood glucose levels, but also for the control of energy metabolism within different cell types. Insulin is known to promote glucose uptake and utilization in the myocardium through the activation of glucose transporter four (GLUT4). By binding to an insulin receptor, insulin can phosphorylate insulin receptor substrate one and two (IRS-1 or 2), which are essential for the activation of phosphoinositide 3-kinase (PI3K) and

protein kinase B (Akt). Basal glucose uptake can be facilitated via GLUT1, activation of the PI3K/AKT pathway and has been linked with enhanced translocation of GLUT4 into the cell membrane to increase diffusion of glucose into the myocardium. In a study done by Fueger *et al.* (2007) they demonstrated that mice lacking GLUT4 have an impaired capacity to take up glucose from the peripheral tissue, correlating with the commencement of insulin resistance and DM. Similarly, animals lacking PI3K and AKT, two of the critical genes for insulin response, develop the same characteristics (Braccini *et al.*, 2015).

In the pathophysiological state of diabetes, impairment of insulin signaling is a key abnormality associated with the development of DCM. The shift in substrate preference in the hearts of diabetic patients often leads to a complete reliance on the oxidation of free fatty acids, thereby suppressing glucose oxidation. Recent studies have clearly illustrated that hyperglycemia and FFAs selectively inhibit insulin action via the dysregulation of IRS/PI3K kinase and AKT pathways (Ansley and Wang, 2013; Li *et al.*, 2014). Elevated FFAs such as diacylglycerol, in the cardiac muscle can activate PKC, a kinase enzyme that is involved in regulating the function of other proteins which promotes insulin resistance through augmented serine phosphorylation of the critical insulin signaling inhibitor, IRS-1(Ser307) (Figure 2.6). This phosphorylation impairs tyrosine phosphorylated PI3K engagement and AKT stimulation in the cardiac muscle (Jia et al., 2015) thereby improving glucose metabolism. Therefore, targeted regulation of insulin signaling has emerged as an important field of research to improve glucose metabolism and reverse impaired cardiac function.

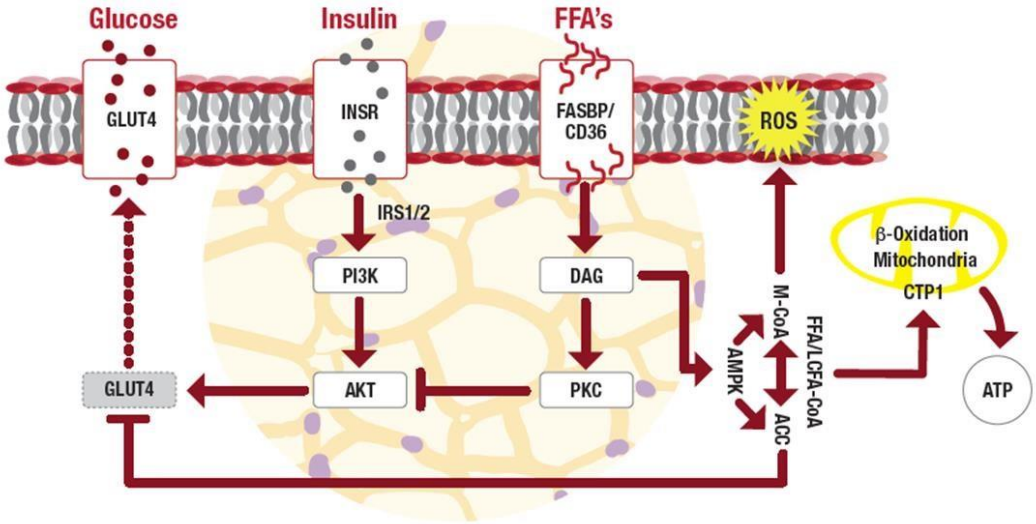

Figure 2.6: Abnormal insulin signaling in the diabetic heart. Under physiological conditions, insulin is known to activate insulin receptor substrate 1 and 2 **(IRS-1/2)**, which in turn activates phosphoinositide 3kinase **(PI3K)** and protein kinase B **(Akt) (PI3K/Akt)** signaling pathway. The activation of these two important kinases is known to result in the translocation of **GLUT4** to the plasma membrane. Under pathophysiological conditions, negative inflammatory response and elevated free fatty acids increase the activation of protein kinase C **(PKC)**, which in turn stimulates serine phosphorylation of IRS (307). Subsequently, the latter disrupts tyrosine phosphorylation of PI3K/Akt thereby preventing GLUT4 translocation to the plasma membrane which impairs glucose metabolism.

2.3.2 Insulin-independent pathway

Apart from the insulin-dependent pathways, the regulation of substrates (glucose and lipids) in the cardiomyocytes may also be facilitated through an insulin-independent signaling cascade, such as 5' AMP-activated protein kinase (AMPK). The latter is a crucial regulator of energy homeostasis and balances the supply of nutrients with energy demand. During pathophysiological conditions, threonine phosphorylation of AMPK^{Thr172} plays a crucial role in the activation and translocation of GLUT4 to the plasma membrane independent of insulin action (Heidrich *et al.*, 2010) (Figure 2.7). Furthermore, AMPK hinders the synthesis of glucose and lipid in the liver but elevates the oxidation of lipids and reduces lipolysis and lipogenesis in the adipose tissue (Long and Zierath, 2006; Montessuit and Lerch, 2013). Importantly, the activation of AMPK in these tissues results

in a favorable metabolic milieu to aid in preventing and formulating treatment for T2DM, through the reduction of glucose, FFAs as well as enhanced insulin sensitivity (Kim *et al.*, 2007; Rojas *et al.*, 2011).

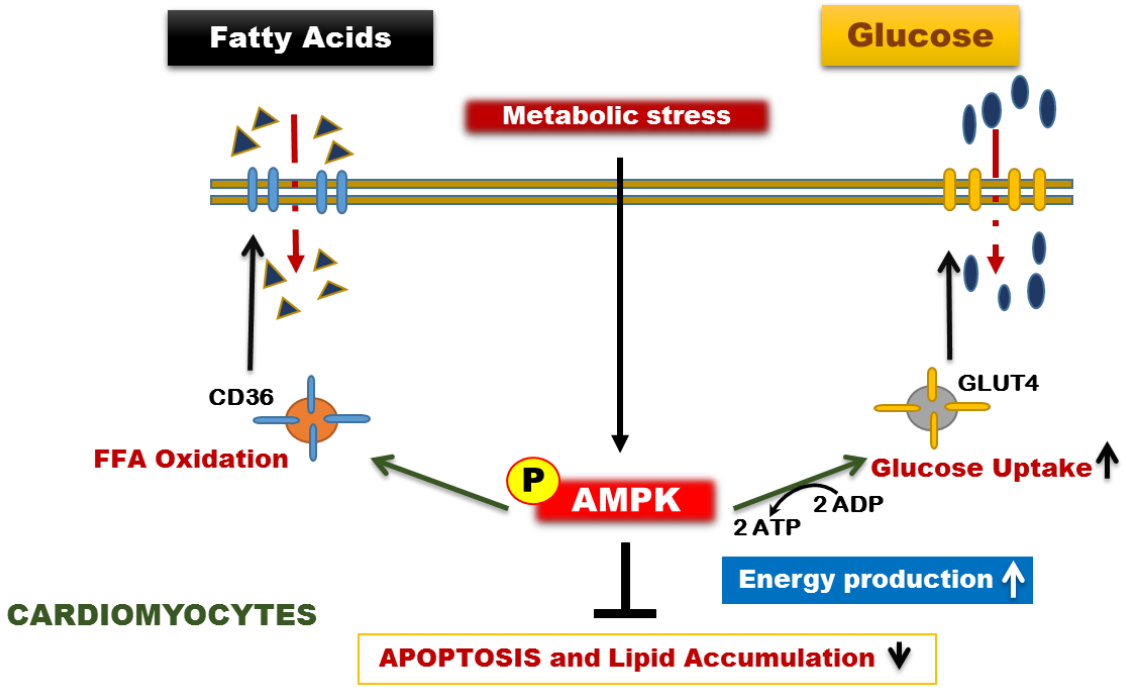

Figure 2.7: Role of 5' adenosine monophosphate-activated protein kinase (AMPK) in the regulation of glucose homeostasis. The phosphorylation of **AMPK** triggers the ATP-production processes, while inhibiting ATP-consuming processes. Metabolic stress stimulates the phosphorylation of AMPK which regulates energy production and expenditure in the cardiomyocytes through increased glucose uptake and reduced lipid storage.

2.3.3 Mitochondrial dysfunction and apoptosis

The mitochondria are the fundamental basis of ATP synthesis in cells, however energy production can be diverted through the expression of catecholamine-regulated uncoupling proteins (UCP). The presence of UCP on the inner mitochondrial membrane alters its proton conductivity and may therefore influence mitochondrial membrane potential (MMP). The importance of maintaining the MMP is fundamental for the proper functioning and survival of cells that have high-energy requirements, such as the cardiomyocytes (Gottlieb *et al.*, 2003). In the diabetic state, changes in MMP have been

linked with increased oxidative and nitrative stress, which may trigger the activation of stress signaling pathways facilitating mitochondrial membrane depolarization in the cardiomyocytes (Webster, 2012). Depolarized mitochondria are key regulators of apoptotic stimuli as they release pro-apoptotic and apoptosis-inducing factors from the intermembrane space to the cytosol and have been shown to be involved in both acute and chronic loss of cardiomyocytes in the hearts of diabetic individuals (Gottlieb *et al.*, 2003).

Apoptosis is a unique process that encompasses morphological and biochemical alterations, such as nuclear condensation and DNA fragmentation (Kitazumi and Tsukahara, 2011). Numerous studies have illustrated an increase in apoptosis in the early and late stages of cardiac injury, suggesting that cell death might play a role in cardiac remodelling and in the subsequent development of DCM (Goldstein *et al.*, 2005; Chen and Knowlton, 2010; Kim and Kang, 2010). Bcl-2 is an anti-apoptotic protein that plays a crucial role in mitochondrial depolarization. Chronic hyperglycemia is known to decrease the expression of Bcl-2, which results in a concomitant increase of mitochondrial depolarization and subsequent release of cytochrome C. This release of cytochrome C, activates caspase 3/7 resulting in its nuclear translocation. Once in the nucleus, caspase 3/7 cleaves poly (ADP-ribose) polymerase (PARP) and the inhibitor of caspase activated DNase (ICAD) (Cardona *et al.*, 2015). The latter induces nuclear DNA fragmentation, which is a hallmark of apoptosis (Kitazumi and Tsukahara, 2011; Cardona *et al.*, 2015) (Figure 2.8).

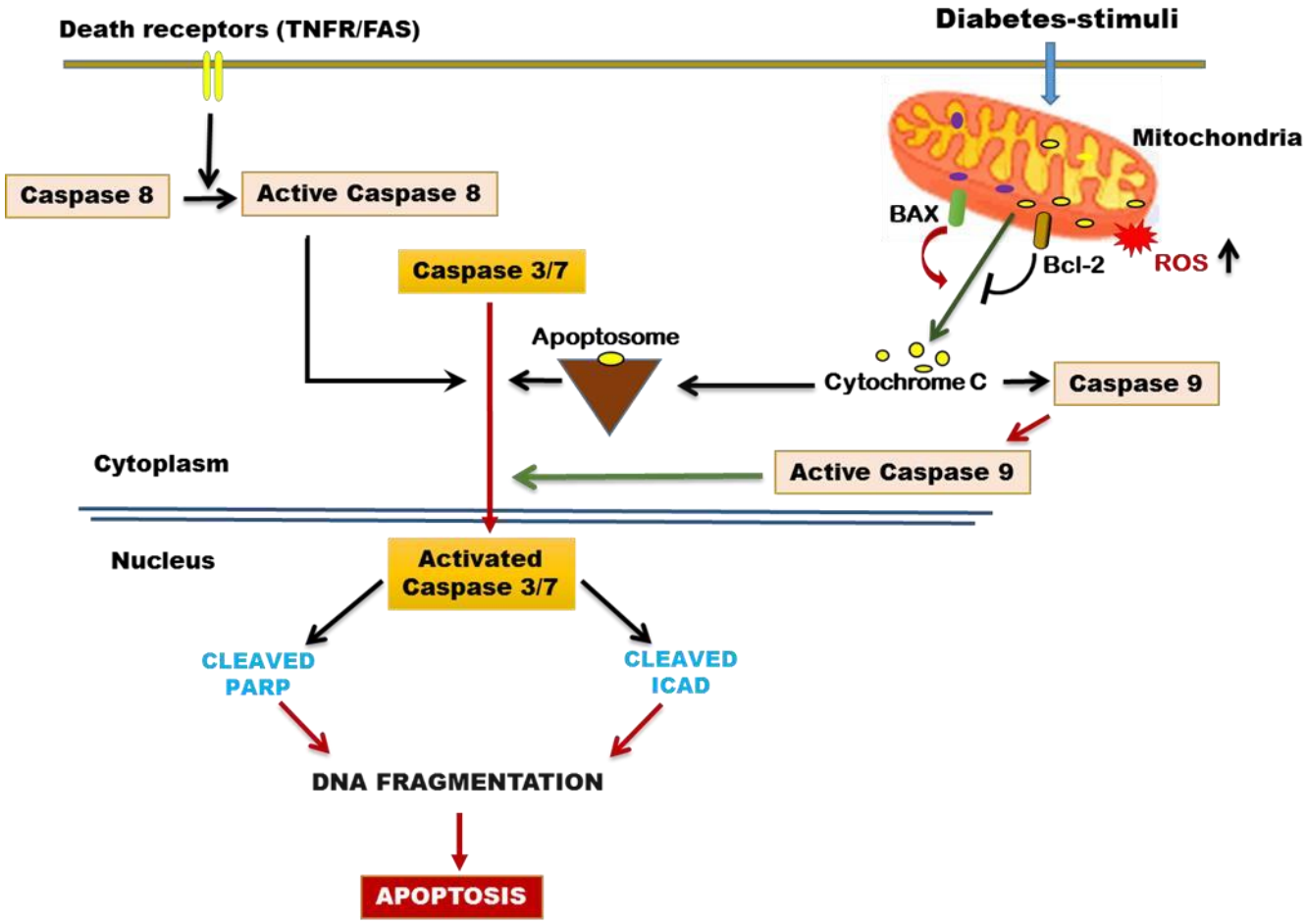

Figure 2.8: Schematic diagram of mitochondrial depolarization. DNA fragmentation and apoptotic signaling. Changes in mitochondrial membrane potential **(MMP)** have been linked with increased oxidative stress and is a key regulator of apoptosis driven by **BAX**. Subsequent, MMP depolarization releases cytochrome C which further activates caspase 3/7 resulting in its nuclear translocation. Once in the nucleus, caspase 3/7 cleaves Poly [ADP-ribose] polymerase **(PARP**) and inhibitor of caspase activated DNase **(ICAD)** which induces nuclear DNA fragmentation, a hallmark of apoptosis.

In a study conducted by Johnson *et al*. (2016), it was reported that high glucose levels have been shown to significantly increase apoptosis in the cardiomyocytes. Also, this increase was reported to accelerate cardiac structural remodeling in the diabetic heart, a crucial component for the development of left ventricular dysfunction (Rota *et al.*, 2006; Battiprolu *et al.*, 2013; Miki *et al.*, 2013).

2.4 Combinational use of current and natural products to protect a diabetic heart

2.4.1 Current synthetic agents

Generally, hyperglycemic control is central to the management of DM and its associated complications. Physical activity and nutrition are some of the essential parts of a healthy lifestyle that are required to maintain low blood glucose levels. This is supported by numerous epidemiological studies showing a convincing association amongst glycemic control and reduced incidence of CVD (Mannucci *et al.*, 2013; Fox *et al.*, 2015). However, an increasing number of CVD-related mortalities are still recorded in individuals with diabetes due to challenges associated with optimal glucose control (Naito and Kasai, 2015). Furthermore, current therapies to protect a diabetic heart at risk of myocardial infarction are limited to those that are used for the treatment of DM (Stone *et al.*, 2014; Green *et al.*, 2015).

Metformin, beta-blockers, glucagon-like peptide 1 receptor agonists, thiazolidinedione's, sulfonylurea and statins are some of the widely-used anti-hyperglycemic therapeutic agents that show limited cardiac protective effects (Table 2.1) (Fox *et al.*, 2015). However, metformin, used as a first-line drug for the treatment of T2DM, and insulin, an accomplished medication for T1DM, are the leading therapeutics that are used to protect patients with diabetes against diabetic complications (May and Schindler, 2016). In addition to alleviating left ventricular dysfunction linked with DM, metformin ameliorates CVD risk factors such as atherosclerosis, platelet aggregation and ischemia (Ferrannini and DeFronzo, 2015; Cheng *et al.*, 2017). Insulin on the other hand has been shown to improve cardiac contractility by improving glucose metabolism through the serine/threonine protein kinase pathway (Volkers *et al.*, 2014). Accumulative evidence on the cardioprotective potential of agents such as metformin and insulin has directed recent therapeutic developments to focus more on the combinational use of these therapies with natural products to enhance or prolong their effect (Gawli and Lakshmidevi, 2015; Low Wang *et al.*, 2016).

Table 2.1: The current synthetic drugs used to treat diabetes and concomitant cardiovascular complications.

Class	Compound	Mode of action	Mechanism	Adverse effects	Reference
Biguanides	Metformin	Decrease hepatic glucose outputs and lipogenesis Promotes muscle glucose uptake	AMP-kinase	Kidney complications Lactic acidosis	(Inzucchi *et al.*, 2014)
Beta-blockers	Acebutolol Atenolol Bisoprolol	Blocks neurotransmitters and epinephrine from binding to receptors.	Beta-adrenergic inhibitor	Headache. Diarrhea Weakness	(Tendera *et al.*, 2014)
Thiazolidinedione	Pioglitazone	Increasing insulin sensitivity Increase glycemic control	PPAR-γ	Weight gain Edema **B**ladder cancer	(Balfour, Rodriguez and Ferdinand, 2014)
Statins	Simvastatin	Lowers cholesterol Reduces Inflammation	HMG-CoA reductase inhibitors	Muscle pain Nausea	(Graveline, 2015)
Sulfonylureas	Glipizide	Increase insulin secretion Promote fatty acid uptake	ATP-sensitive Potassium channels	Hypoglycemia Weight loss	(Komatsu *et al.*, 2013)
Glucagon-like peptidase-1	Albiglutide	Increases insulin secretion Inhibiting glucagon release	GLP-1 agonist	Headaches Nausea Increased sweating Constipation	(García-Compeán *et al.*, 2015)

2.4.2 Triterpenoids and Metabolic health

Triterpenes are compounds that are biosynthesized from squalene and possess diverse pharmacological properties. Various types of triterpenes, such as lanostranes, lanosterols and cholesterols, can be synthesized based on the folding configuration of the squalene chain. Several triterpenes have been reported to ameliorate complications related to obesity, DM, inflammation and CVDs (Hamid *et al.*, 2015; Rodriguez-Rodriguez, 2015). In phase 2 clinical trials, triterpenoid derivatives bardoxolone methyl and its analogues improved renal and vascular damage in diabetic rodent models (Pergola *et al.*, 2011). Similarly, Gonzalez-Burgos and Gomez-Serranillos (2012) described the ability of ursolic

acid, an ursane triterpene, to alleviate stress-related myocardial dysfunction *in vitro*, while an oleane triterpenoid, present in *Vitis vinifera*, has been shown to protect against diabetes associated complications (Marica Bakovic, 2015).

Recently, more research has focused on the specific branch of triterpenes, the lanostanes. This cluster of tetracyclic triterpenoid, resulting from lanosterol, are generated through cyclization of squalene-2, 3-epoxide in a chair-boat configuration, resulting in a protosterol (Chen *et al.*, 2014). Lanostanoids, including those from fungi and fruiting bodies of *Ganoderma leucocontextum* are subject to increasing investigations for their ameliorative properties against various metabolic complications as well as their anticancer potential (Unlu *et al.*, 2016). The beneficial effects displayed by some lanostane triterpenoids to ameliorate diabetes-associated complications include vasodilatory, anti-inflammatory, and antithrombotic properties (Yoshikawa *et al.*, 2005; Khathi *et al.*, 2013; Hamid *et al.*, 2015). Of particular interest, are the triterpenes found in the green aboriginal tall tree, *Protorhus longifolia.*

2.5 *Protorhus longifolia* as a nutraceutical to protect the diabetic heart

2.5.1 The genus Protorhus

The genus Protorhus constitutes one of the diverse species of flowering plants that includes *P. ditimena* and *P. longifolia*, which are endemic to Madagascar and Southern Africa, respectively. Despite the limited medicinal knowledge on *P. ditimena*, scientific data on *P. longifolia* has come to the forefront reporting on the traditional health benefits where this species has been used as a blood-thinning agent in addition to treating conditions such as hemiplegic paralysis, heart burn and abdominal haemorrhaging (Mosa, 2011). Although the commercial value of *Protorhus longifolia* (Figure 2.7) has not yet been established globally, its increased traditional usage can potentially add to its commercial value as the bark is retailed in muthi markets, in SA, to manage high blood sugar levels. The international market for botanical and plant-derived therapeutics is expected to escalate from $29.4 billion to approximately $39.6 billion with a compound annual growth rate (CAGR) of 6.1% for the period of 2017-2022 (Lawson, 2017).This has

been related to the recent commercial success of products such as green tea (*Camellia sinensis*) and rooibos (*Aspalathus linearis*). Although previously considered to be of insignificant economic importance, rooibos is now part of the highly consumed beverages worldwide behind green tea (Joubert and de Beer, 2011; Napolitano *et al.*, 2014).

Therefore, scientific validation of medicinal plants such as *P. longifolia* may be of economic value for the development of herbal health care, plant based cosmetics and nutraceutical supplements for the South African market.

Figure 2.9: Representative image of Protorhus longifolia. *P.longifolia* (Benrh.) Engl. (Anacardiaceae), also known as unhlangothi (Zulu) is a green tall tree that is indigenous to Southern Africa, mostly found in the Zululand region of Kwa-Zulu Natal and parts of Swaziland.

Despite the limited studies that have been reported on the leaf extract of Protorhus longifolia, it has been shown to display antimicrobial properties *in vitro* (Penduka *et al.*, 2015). However, more work has focused on the exploration of the stem barks of this plant. The hexane extract of the stem bark of *P. longifolia* reveals it can inhibit thrombin and epinephrine induced platelet-aggregation *in vitro* (Mosa *et al.*, 2011). Whereas air-dried and powdered extracts display improved antioxidant activity to scavenge 2,2-diphenyl-1picrylhydrazyl (DPPH), 2,2'-azino-bis (3-ethylbenzothiazoline-6-sulphonic acid) (ABTS)

radicals as well as demonstrating enhanced iron (Fe^{2+}) chelating activity (Mosa *et al.*, 2011). The biological activity of *Protorhus longifolia* has been attributed to triterpenoids.

2.5.2 Pharmaceutical properties of lanosteryl triterpenes (RA3 and RA5)

Two prominent triterpenes have been previously extracted from the stem barks of *Protorhus longifolia,* namely, methyl-3β-hydroxylanosta-9, 24-dien-21-oate (RA3) and (B) 3β-hydroxylanosta-9, 24-dien-21-oic acid (RA5). These lanosteryl triterpenes have consistently been demonstrated to possess metabolic benefits against diabetes and its associated cardiovascular complications (Table 2.2). Mosa and colleagues elaborated on the *in vitro* anti-inflammatory and anti-platelet aggregation properties exhibited by RA3 and RA5 (Mosa *et al.*, 2011).

In an *in vitro* study, RA5 efficaciously decreased the accumulation of triglycerides in mature differentiated 3T3-L1 adipocytes; this was taken as indication of the compounds ability to suppress adipogenesis (Mosa *et al.*, 2014). While high fat diet-induced hyperlipidemic rats presented with a significant increase in total cholesterol (TC) and low density lipoproteins (LDLs), oral administration of RA3 at a concentration of 100-200 mg/kg body weight for 15 days significantly attenuated both TC and LDLs, subsequently increasing the levels of high density lipoproteins (HDLs) (Machaba *et al.*, 2014). The group further elaborated on the *in vivo* anti-hyperglycemic activity of RA3 (Mosa *et al.*, 2015). In this study, RA3 effectively reduced the levels of blood glucose by 37% and ameliorated glucose tolerance in an STZ-induced diabetic rat model. Furthermore, the RA3-treated diabetic rats presented with increased superoxide dismutase and catalase activity with concomitant reduction in lipid peroxidation.

Table 2.2: The protective effect of *Protorhus longifolia*, and its lanostane triterpenes, including methyl-3βhydroxylanosta-9, 24-dien-21-oate (RA3) and 3β-hydroxylanosta-9, 24-dien-21-oic acid (RA5) against diabetes associated compilations.

Treatment	Model	Outcome	Reference
RA3 and RA5	Thrombin and epinephrine induced platelet-aggregation	Anti-inflammatory effect (IC_{50} of 0.59mg/mL)	(Mosa *et al.*, 2011)
100 and 200 mg/kg of RA3	High fat fed Sprague-Dawley rats	Improved lipid profiles and atherogenic index	(Machaba *et al.*, 2014)
100mg/kg of RA3	Type 2 diabetes was induced through STZ injection and feeding Sprague-Dawley rats a high fat diet	Improved glucose tolerance, pancreatic beta cell ultrastructure, fasting c-peptide levels, whilst reducing oxidative stress and inflammation.	Mabhida *et al.*, 2017
RA3	Cotton pellet-induced granuloma model in rats	Anticoagulant and antiinflammatory activity	(Mosa *et al.*, 2011)
100 mg/kg RA3	Streptozotocin-induced diabetic Sprague-Dawely rats	Improved glucose tolerance and antioxidant while reducing lipid peroxidation	(Mosa, 2011; Mosa *et al.*, 2015)
100 mg/kg RA3	Isoproterenol-induced myocardial injury in hyperlipidemic Sprague-Dawley rats	Decrease fat deposition, LDH, lipid peroxidation while improving antioxidant capacity in the heart	(Mosa *et al.*, 2016)

Further illustrating the medicinal benefits of triterpenes, using an *in vivo* rat model, Mosa *et al*. (2016) demonstrated the cardioprotective potential of RA3 on isoproterenol-induced myocardial injury (Mosa *et al.*, 2016). Here, the animals presented with myocardial necrosis, resulting from ISO toxicity. However, reduced lipid deposition with concomitant amelioration of acute hyaline degeneration was seen in the cardiac muscles of rats pretreated with RA3. These findings were supported by the increase in antioxidant levels in the heart tissues. Recently, Mabhida *et al.* (2017) reported on the potential of RA3 to enhance the ultrastructure of pancreatic beta cells through the attenuation of reduced glucose tolerance, ameliorating oxidative stress and resultant inflammation.

In addition, the aforementioned data elaborated on improved insulin resistance in skeletal muscles (Mabhida *et al.*, 2017). As summarized in Table 1, the pharmaceutical properties exhibited by these triterpenes are indicative of their potential role in the development of diabetes-induced cardiac injury. Although mechanistic insights are yet to be established, we propose that these triterpenes, more importantly RA3, might exert their cardioprotective potential through their apparent inhibition of lipogenesis, improved insulin sensitivity and resultant increase in the uptake of glucose in the liver and the skeletal and heart muscle (Figure 2.10).

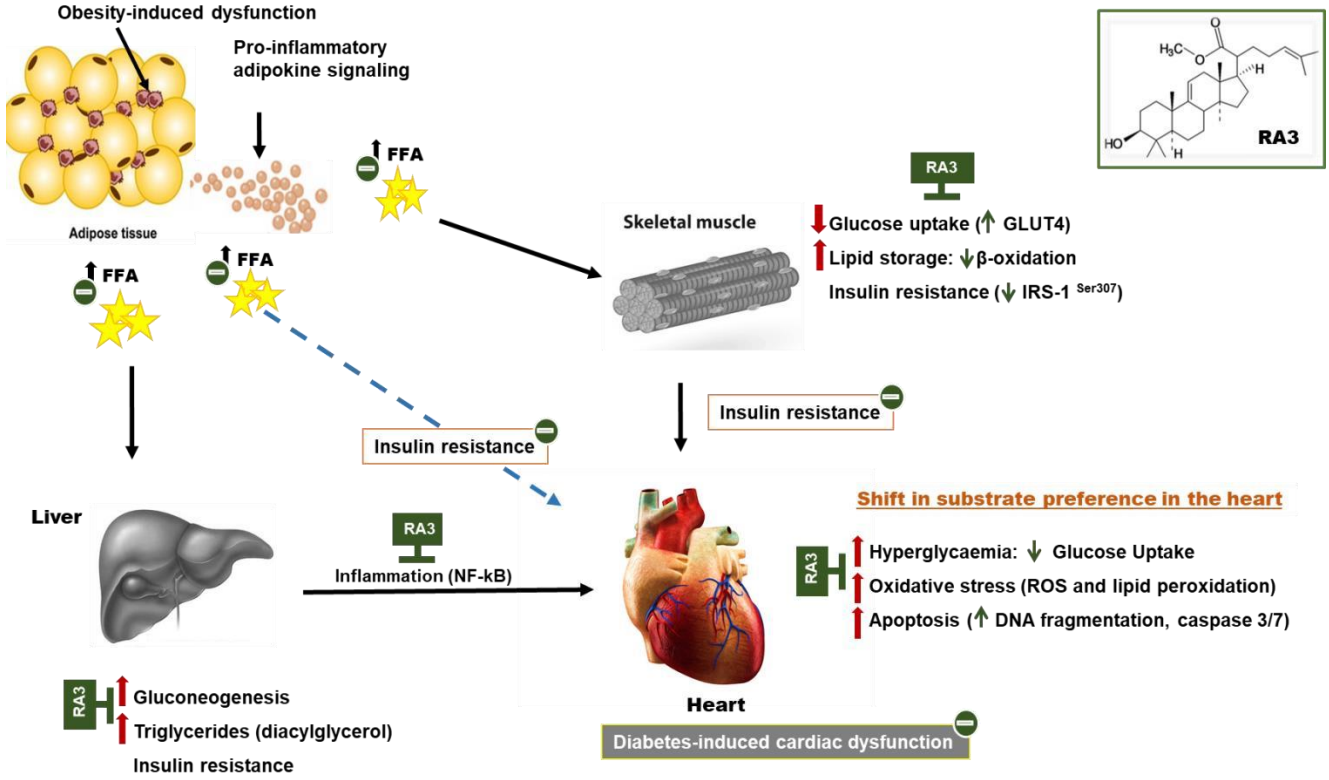

Figure 2.10: Proposed mechanism of action of RA3. Free fatty acids **(FFAs)** and adipokines released from the adipose tissue have been linked with impaired insulin signaling, often resulting from obesity induced-insulin resistance (IR). The latter is associated with the development of type 2 diabetes mellitus (T2DM), which has been shown to increase oxidative stress, inflammation and apoptosis in various tissues. In the skeletal muscles, IR reduces glucose transportation and glycogen synthesis, while selectively stimulating gluconeogenesis and lipogenesis in the liver. This results the shift in substrate preference in the cardiac muscle thereby triggering hyperglycemia-induced oxidative stress and apoptosis subsequently, leading to myocardial dysfunction. Nonetheless, numerous studies from our group have demonstrated the anti-diabetic properties and cardioprotective potential exhibited by RA3. Here, RA3 displayed antihyperlipidemic activities while, improving insulin signaling and glucose uptake.

CHAPTER THREE

METHODOLOGY

The chapter comprises of two sections: A and B.

Section A is a summary of the isolation process of the triterpenes.

Section B summarizes the cardioprotective properties of a lanosteryl triterpene.

All equipment and consumable information can be accessed in appendix A.

Phase 1

3.1 Protorhus longifolia

3.1.1 Collection of stem barks

The stem barks of *Protorhus longifolia* (Benrh.) Engl. were obtained from KwaHlabisa, KwaZulu-Natal, South Africa. *P. longifolia* was confirmed by a Botanist from University of Zululand. Thereafter, stem barks were washed, cut into small pieces and then air dried. Subsequently, the barks were ground into powder and kept in a dark glass container at 4°C until required.

3.1.2 Extraction, isolation and NMR

Triterpenes were extracted and isolated as per Mosa *et al.* (2011b) instructions. Briefly, the ground stem barks were defatted with n-hexane followed by a chloroform extraction (1:5 w/v) (Figure 3.1). Thereafter, the extract (15 g) was placed in a silica gel column chromatography, washed with a ratio of hexane-ethyl acetate (H-EA) solvent (9:1 to 3:7 ratio) to obtain and fractions (20 mL). Subsequently, fractions were assessed with thin layer chromatography (TLC) and, based on their TLC profile, were combined to produce a collective of 18 fractions. The last two fractions were individually purified in n-hexane and ethyl acetate to produce methyl-3β-hydroxylanosta-9, 24-dienoate (RA3) (5 g) and 3β-hydroxylanosta-9, 24-dien-21-oic acid (RA5) (7 g), respectively.

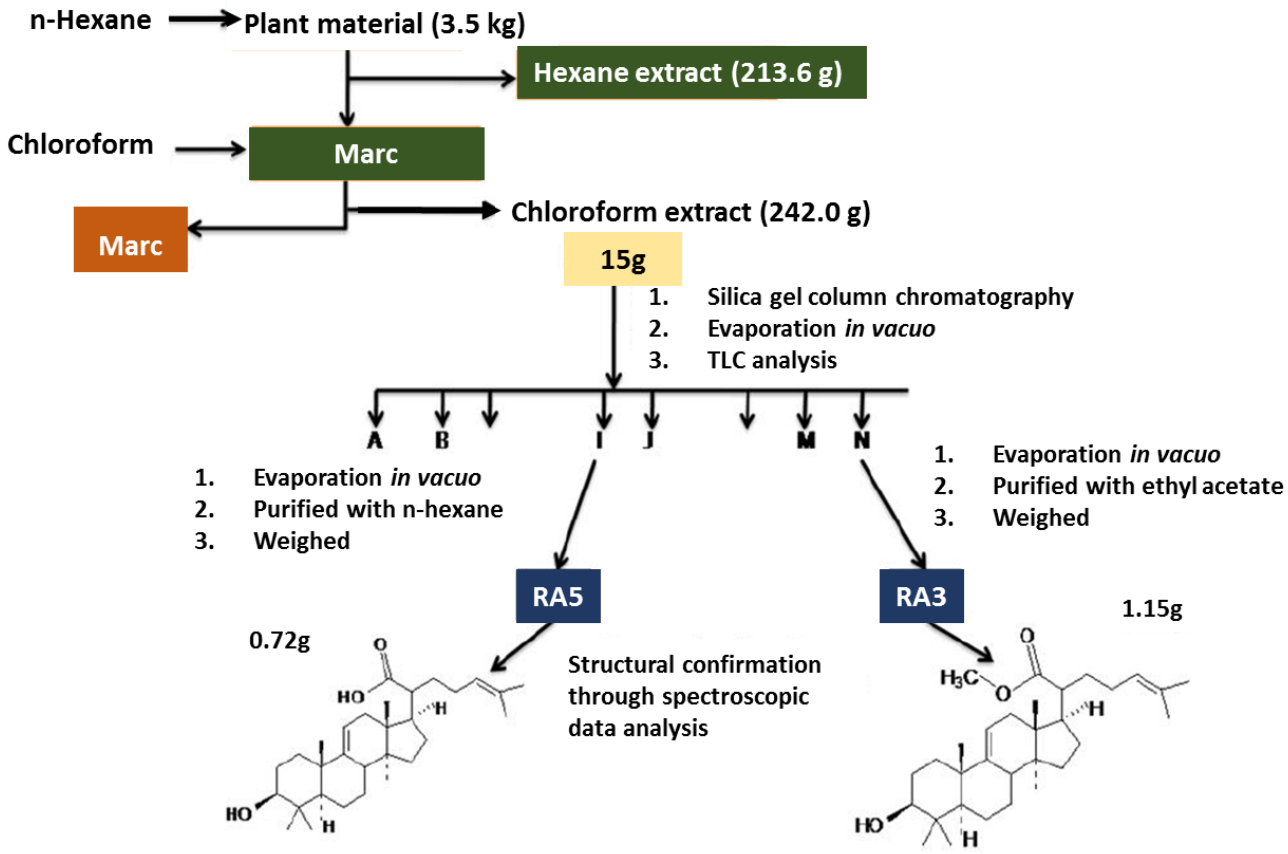

Figure 3.1: Representation of the isolation of the prominent triterpenes from P. longifolia. Spectral data examination was performed to obtain and validate the structures of the triterpenes. Source: Mosa *et al*. (2011), PhD.

Phase 2

3.2 Cell culture

To achieve our objectives, embryonic rat heart derived H9c2 cardiomyoblasts were acquired from the European Collection of Cell Cultures (ECACC No. 8809294) and used to carry out all experiments.

3.2.1 Thawing and resuscitation of cryopreserved cells

The H9c2 rat heart derived cardiomyoblasts, stored in a 1 mL cyrotube, were thawed at room temperature. Once thawed, the cardiomyoblasts were transferred into a 50 mL tube with 10 mL of previously warmed in culturing media- Dulbecco's modified eagle's medium (DMEM) (containing 10% foetal bovine serum (FBS) and 1% penicillin Streptomycin (pen/strep) and centrifuged at 1500 x g for five minutes to eliminate any excess dimethyl sulfoxide (DMSO). Subsequently, cardiomyoblasts were re-suspended in 19 mL culturing media and transferred into a 75 cm^2 flask, which was then incubated under typical tissue culture (TC) conditions (37 ºC, 95% humidified air and 5% CO_2) until 70-80% confluent.

3.2.2 Trypsinizing cardiomyoblasts

Trypsin, stored at -20 ºC, was thawed at room temperature (RT) and Dulbecco's phosphate-buffered saline (DPBS) warmed in a 37 ºC water bath. Thereafter, H9c2 cardiomyoblasts were removed from the CO_2 incubator and washed with pre-warmed DPBS. DPBS was removed and 4 mL trypsin was added to cells in a 75 cm^2 flask. Cells were incubated for 6 minutes in CO_2, under standard TC conditions. To confirm dislodgment, cardiomyoblasts were viewed using a Nikon Eclipse Ti inverted microscope (NETI-microscope) to validate dissociation. To stop trypsinization, 8 mL of culturing media was pipetted into a T75 flask and mixed thoroughly. Thereafter, the cell suspension was transferred into a 50 mL centrifuge tube and centrifuged at 1500 rpm x g for 5 minutes. Subsequently, culturing media was removed and cells re-suspended in 10 mL previously warmed culturing media. Cell viability and density were established (section 3.2.4) prior to seeding cells in their appropriate TC multi-well plates (section 3.2.5) for subsequent biochemical assays

3.2.3 Cell maintenance: sub-culturing

Upon 70 - 80% confluence, H9c2 cells were split and sub-cultured in T75 flasks in previously warmed media to acquire a media to cell ratio of 1:9 and incubated under standard TC conditions. The culturing media was refreshed after 2 days and sub-culturing of H9c2 cardiomyoblasts was retained below 20 passages.

3.2.4 Determination of cell viability

A Countess™ Automated Cell Counter was used to measure cell viability as per manufacturer's instruction. After trypsinization cell pellets were resuspended in 10 mL DMEM (supplemented with 10% FBS and 1% pen/strep). Cellular viability was assessed by pipetting 1 mL of the cells from a 10 mL cell suspension DMEM (supplemented with 10% FBS and 1% pen/strep) into a 2 mL Eppendorf tube. Ten micro litre of the latter was mixed with 10 µL of trypan blue dye, after which 10 µL of the cell/trypan blue sample mixture was pipetted onto the chamber port on one side of the Countess™ cell counting chamber slide. The Countess™ slide was then placed into the slide inlet on the instrument to measure the total number of cells, both dead and alive, as well as the total percentage viable cells. Cell viability above 60% was regarded as seeding worthy.

3.2.5 Seeding of cells in multi-well plates

Following the establishment of the total number of viable cells, H9c2 cardiomyoblasts were then seeded at relative seeding density (Table 3.1.) in the respective TC plates. Thereafter, the plates were incubated under typical TC conditions (37 ºC, 95% humidified air and 5% CO_2) for 3 days in DMEM (containing 10% FBS and 1% pen/strep).

Table 3.1: Seeding of H9c2 cells in multi-well plates

	Multi-well plate (well)	Growth area (cm^2)	Seeding density (cells/well)	Volume (µL)
H9c2	**6**	**10**	**2×10^5**	**3 000**
	24	**2.0**	**5×10^4**	**1 000**
	96	**0.3**	**2×10^4**	**200**

3.3 Treatment preparation

3.3.1 Preparation of Triterpenes (RA3 and RA5)

RA3 (MW: 470.74 g/mol) and RA5 (MW: 455.77g/mol), both at 32 mg, were dissolved in 100 µL DMSO (100%) to yield final stock solutions of 679.7 mM and 700 mM, respectively. The resultant stock solutions were placed at -80ºC until required. A working solution of 1 µM was prepared by mixing 50 µL of the initial stock with 5 mL of 5.5 mM glucose in treatment media (DMEM (without phenol red) supplemented with 0.1% bovine serum albumin (BSA)). Working stock solutions were filter sterilized using a 0.22 µM syringe filter system. A final concentration of 1 µM was prepared by adding 10 µL of the working solution to 10 mL of either 5.5 mM (normal- NG) or 33 mM (high- HG) glucose in treatment media.

3.3.2 Preparation of N-acetylcysteine

A stock solution of N-acetylcysteine (NAC) (MW: 163.19 g/mol) was prepared by weighing 8.16 mg of NAC and dissolving it in 5 mL TC grade water to yield a 10 mM stock solution concentration. Thereafter, the stock solution was filter sterilized before making serial dilutions. A final concentration of 1 mM was prepared using a ratio of 9:1 concentration in either NG or HG glucose in treatment media.

3.3.3 Preparation of Metformin

Metformin stock was formulated by dissolving 6.45 mg/µL metformin (MW: 129.16 g/mol) in 5 mL TC grade water to yield a stock concentration of 10 mM. A 1mM working stock solution was prepared by diluting 0.5 mL of the stock in 4.5 mL of HG in treatment media. The working solution was then filter sterilized using 0.22 µM a syringe filter. Thereafter, 10 µL of the aforementioned was added to 10 mL of HG in treatment media to give a final concentration of 1 µM.

3.4 Treatment

3.4.1 Time and dose response determination of triterpenes

For time and dose response, H9c2 cells were cultured and seeded in a 96 well plate for 2 days. Thereafter, cells were exposed to log concentrations (0.001 - 1000 µM) of either RA3 or RA5 for five different time intervals (3, 6, 12, 24 and 48 hours). The most effective time and dose as well as compound was selected and used for all subsequent experiments.

3.4.2 Methyl-3β-hydroxylanosta-9, 24-dienoate (RA3) post-treatment

To assess the compounds ability to attenuate high glucose-induced cardiac injury, H9c2 cardiomyoblasts exposed to HG or NG were treated with RA3. Cardiomyoblasts were treated for 24 hours with 1 µM of RA3 to evaluate its effect on the physiological state of the cardiomyoblasts and its ability to attenuate HG-induced cardiac damage. The cardiomyoblasts were also treated with 2 µM of a combination of MET+RA3. The purpose was to assess whether RA3 could improve the efficacy of MET and by doing so, establish a synergistic effect from this combination against HG-induced cardiomyopathy.

3.4.2 N-acetylcysteine post-treatment

N-acetylcysteine (NAC) is a known antioxidant stimulant and ROS inhibitor. In the present study, H9c2 cardiomyoblasts exposed to HG for 24 hours were treated with 1 mM of NAC to assess its ability in ameliorating cellular damage resulting from HG and as a comparative tool to determine the antioxidant potential of RA3. The cells were also treated with a combination of 2 mM NAC and 2 µM MET to assess the effect of NAC on enhancing the efficacy of MET.

3.4.3 Metformin post-treatment

Metformin was used to assess the efficacy of RA3 against HG-induced cellular stress. H9c2 cardiomyoblasts exposed to HG were treated with 1 µM of MET for 24 hours to assess its effect against HG-induced cardiac damage. MET was also used in combination with RA3 and NAC, respectively. The purpose for this was to assess a possible synergistic effect from the two treatments.

3.4.4 Treatment of H9c2 cardiomyoblasts

H9c2 cardiomyoblasts, seeded in either 6-well, 24-well or 96-well plates, were washed with DPBS and then exposed to either 5.5 mM normal glucose (NG) or 33 mM high glucose (HG) for 24 hours. Subsequently, cells were exposed to various treatment conditions for a further 24 hours:

- Group 1: Exposed to NG
- Group 2: Exposed to HG
- Group 3: Exposed to NG+RA3
- Group 4: Exposed to HG+RA3
- Group 5: Exposed to HG+NAC
- Group 6: Exposed to HG+MET
- Group 7: Exposed to HG+MET+RA3
- Group 8: Exposed to HG+MET+NAC

Similarly, cardiomyoblasts exposed to NG and HG remained untreated and served as the vehicle and positive control, correspondingly.

3.5. Biochemical analysis

3.5.1 H9c2 metabolic activity assessment

H9c2 cellular metabolic activity was determined by measuring intracellular ATP production using the ViaLight plus ATP kit (Lonza, Walkersville, MD, USA), following manufacturer's guidelines. Briefly, 150 µL of the culture media was aspirated from the treated cells seeded in a white 96-well plate, leaving 50 µL. The cells were then lysed with 50 µL ATP cell lysis buffer and incubated at RT for 10 minutes. Thereafter, ATP monitoring reagent (ATP plus reaction mixture) was added and then incubated for a further 2 minutes at RT. Resultant luminescence was then read in a BioTek® FLx800 plate reader with data acquisition using Gen 5 software® (Bio-Tek Instruments, Inc., Winooski, VT, USA).

3.5.2 Protein assessment

Protein concentrations were established using the Bradford protein assay, as per manufacturer's instructions. Five micro litres of Bovine serum albumin (BSA) protein standards (0.125, 0.25, 0.5, 0.75, 1, 1.5 and 2.0 mg/mL) were pipetted in the first two

columns (A-B) of a 96-well plate. Thereafter, 10 µL of sample lysates (prepared in section 3.5.1) were pipetted into the respective wells. To the standards and samples, 250 µL of the Bradford reagent was pipetted into the respective wells and mixed by multiple pipetting and then incubated for 10 minutes at RT. Absorbance was read at 570 nm in a BioTek® ELX800 plate reader. Proteins were measured by excluding the blank from the absorbance values of the standards and samples.

3.5.3 Cardiomyoblasts glucose uptake

Assessment of 2-deoxy-[3H]-D-glucose (DOG) uptake in H9c2 cells was performed as per protocol defined by Johnson *et al*. (2016). The principle behind the assay entails the addition of radioactively labelled DOG to H9c2 cardiomyoblasts, followed by quantifying DOG by means of a scintillation counter. To measure glucose uptake, cardiomyoblasts (treated as per section 3.4) were rinsed twice with warm DPBS (1 mL). Subsequently, 250 µL of DMEM comprising of NG, 0.5 µCi/mL DOG and 2% BSA was pipetted to every well followed by incubation under standard TC conditions for 15 minutes. The assay was terminated by a cold wash of DPBS followed by the addition of 1 mL of 3 M sodium hydroxide (NaOH) with 1% sodium dodecyl sulfate solution and then incubated for 45 minutes at 37°C to lyse the cardiomyoblasts. Protein concentrations were established as per section 3.5.2. Cell lysates were then added to scintillation vials containing 1 mL TC grade water. Subsequently, 8 mL of Ready Gel Ultima Gold was pipetted into scintillation vials containing samples and then vigorously mixed. Thereafter, vials were equilibrated overnight at room temperature, in complete darkness, in a liquid scintillation analyser (2200 CA, Parkard Tricarb series). The following day, samples were measure with a 3Hisotope quantifying system. To determine DOG and counter efficiency (CE), the results were computed using counts per minute (CPM) and disintegration per minute (DPM) program (http://www.graphpad.com/quickcalcs/radcalcform.cfm). To establish cpm/fmol, the precise radioactivity of DOG and CE were used. The averaged protein values and CPM were utilized to assess the fmol/mg. Data was presented as fmol DOG/mg of proteins, by means of the GraphPad radioactivity calculator (GraphPad software).

3.5.3 Intracellular lipid content determination

Lipid storage in H9c2 cardiomyoblasts was assessed using an Oil-Red O staining technique adapted from Sanderson *et al.* (2014). Oil red O (ORO) is a widely used lysochrome (fat-soluble) diazo dye for staining and quantifying neutral intracellular lipids. To quantify lipid accumulation, previously treated cardiomyoblasts were fixed with 10% (v/v) neutral buffered formalin for 15 minutes. Cells were washed and then stained with 0.7% (v/v) ORO (made by diluting 1% stock (w/v) in TC grade water) and incubated for 30 minutes at RT. Subsequently, the ORO stain was aspirated and the cardiomyoblasts washed until clear. Images were captured at 20x magnification using a NETI- microscope (Nikon, Kanagawa, Japan). Total cellular lipid accumulation was measured by eluting the dye with 200 µL of isopropanol (100%) after which the absorbance was read at 570 nm by means of a BioTek® ELx800 plate reader equipped with Gen 5® software (BioTek Instruments Inc., Winooski, VT, USA).

Total lipids accumulated in H9c2 cell were standardized as per the methods defined by Sanderson *et al*. (2014). Concisely, following removal of ORO stain, cardiomyoblasts were discolored with ethanol (70% (v/v)) and counterstained with 400 µL crystal violet (CV- 0.5% (v/v). Following 5 minute incubation, cells were washed and then air dried. Absorbance was measured after CV dye was extracted with 70% ethanol, at 570 nm with a BioTek® ELx800 plate reader equipped with Gen 5® software for data attainment. The total lipid content was calculated using the following equation:

$$\boldsymbol{Lipid\ content} = \frac{(\boldsymbol{A_{490\ nm}} / \boldsymbol{A_{570\ nm}})\boldsymbol{sample}}{(\boldsymbol{A_{490\ nm}} - \boldsymbol{A_{570\ nm}})\boldsymbol{control}} \times \mathbf{100}$$

Figure 3.2A: Equation for calculating total lipid content of cells. Total lipid content was calculated as the dividend of oil red o (ORO) over crystal violet (CV) multiplied by the sample over the dividend of the difference between ORO and CV multiplied by the control. Results were represented as percentage.

3.5.4 Quantification of pro- and anti-oxidants

3.5.4.1 Superoxide dismutase activity (SOD)

Superoxide dismutase (SOD) is an endogenous antioxidant which scavenges the superoxide anion into hydrogen peroxide and molecular oxygen. The levels of SOD were measured using an Abcam SOD activity kit as per manufacturer's instructions. Concisely, previously treated H9c2 cardiomyoblasts were lysed with 100 µL of 0.1 M trizma/hydrochloride (Tris/HCl), pH 7.4 (comprising of 0.5% Triton X-100, 5 mM βmethylphenethylamine (β-ME) and 0.1 mg/mL phenylmethylsulfonyl fluoride (PMSF). Lysed cells were then centrifuged at 15 000 x g for 5 minutes at 4°C. Next, 20 µL of cell lysates were pipetted into a new TC plate (96-well) and incubated under standard TC conditions for 20 minutes prior to measuring the activity of SOD. Absorbance was read at 450 nm with a Biotek® ELX 800 plate reader (Gen 5® software). Levels of SOD were computed using the method in table 3.2 and calculated using the following equation:

$$\boldsymbol{SOD\ Activity} = \frac{(\boldsymbol{A_{blank\,1} - A_{blank\,3}}) - (\boldsymbol{A_{sample\,1} - A_{blank\,2}})}{(\boldsymbol{A_{blank1} - A_{blank\,3}})} \times \mathbf{100}$$

Figure 3.2B: Equation for the calculation of SOD activity (inhibition rate %) in H9c2 cardiomyoblasts.

Table 3.2: Preparation of sample for SOD activity

Reagents	Sample (µL)	Blank 1 (µL)	Blank 2 (µL)	Blank 3 (µL)
Sample solution	20	-	20	-
Distilled water	-	20	-	20
Wst working solution	200	200	200	200
Enzyme working solution	20	20	-	-
Dilution buffer	-	-	20	20

3.5.4.2 Total glutathione (GSH) activity

GSH activity assay is a luminescent-based assay which detects and quantifies the antioxidant GSH in various biological samples. Total glutathione content was assessed using a GSH/GSSH-Glo™ assay kit following manufacturer's guidelines. Previously treated H9c2 cardiomyoblasts, in white 96-well TC plates, were lysed in 50 µL GSH lysis reagent and then mixed on an orbital shaker at RT for 5 minutes. Thereafter, 50 µL of a luciferin generation reagent (LGR) was pipetted into the mix. The mix was incubated for a further 30 minutes at RT. 100 µL of luciferin detection reagent was added and mixed on a shaker for 15 minutes at RT. Luminescence was assessed by a Biotek® FLX 800 plate reader using Gen 5® software.

3.5.4.3 Reactive oxygen species generation

Intracellular production of ROS was evaluated by exposing cardiomyoblasts to 100 µL 2', 7'-dichlorfluoresceindiacetatefluorescent dye (DCFH-DA- 1 µM, made up in Hank's balanced solution (HBSS) fluorescent dye and incubated under standard TC conditions for 30 minutes. Thereafter, dye was eluted by the addition of HBSS which was followed by measuring DCFH-DA fluorescent intensity (emission spectra of 528 ± 20 nm) by means of a BioTek® FLx800 plate reader.

3.5.5 Evaluating mitochondrial membrane potential

High glucose-stimulated depolarized mitochondria were evaluated by subjecting the cardiomyoblasts to 5,5',6,6'-tetrachloro-1,1',3,3-tetraethylbenzimidazolyl-carbocyanine iodide (JC-1) cationic dye. The principle behind JC-1 entails the formation of J-aggregates in cells with a normal mitochondrial membrane potential which subsequently produces orange/red fluorescence. Conversely, JC-1 retains its monomeric form and exhibits a bright fluorescence (green) in cells with impaired mitochondrial membrane potential.

Previously treated cardiomyoblasts were stained with 2 µM of JC-1 solution and then incubated in the dark for 30 minutes under TC conditions. Subsequently, the fluorescent intensity of JC-1 was assessed by measuring fluorescence at 485 nm in a BioTek® FLx

800 plate reader. Images were captured at 10x magnification with a NETI- microscope (NIS elements software).

3.5.6 Assessment of lipid peroxidation

The TBARS assay is an established method that quantifies lipid peroxides based on the production of MDA, a biomarker that measures oxidative stress. Lipid peroxidation was assessed by means of an OxiSelect™ TBARS assay Kit as per the instructions of the manufacture.

Previously treated high glucose-induced H9c2 cardiomyoblasts were suspended in a solution containing DPBS (1 mL) and 100x butylated hydroxytoluene (10 µL). Thereafter, cardiomyoblasts were transmitted to a clean 2 mL microfuge tube and homogenized at 250 Hz in a Qiagen TissueLyser (Qiagen, Hilden, Germany) for 1 minute. Homogenates were stored in an ice bucket until MDA standards (125, 62.5, 31.5, 15.25, 7.81, 3.91, 1.95 and 0.98 µM) were prepared. One hundred micro litres of sodium dodecyl sulfate lysis solution was pipetted into new eppendorf's containing 100 µL of standards and treated samples (H9c2 cell lysate). The sample mixtures were then vortexed and incubated for 5 minutes at RT. Subsequently, 250 µL of thiobarbituric acid reagent was pipetted into each tube, thoroughly mixed and incubated for 45-60 minutes at 95°C. The eppendorf's were chilled on ice for 5 minutes before centrifuging for 15 minutes at 1500 x g. Thereafter, supernatants of samples and standards were inserted into a new 96-well plate to measure the absorbance at 532 nm using a BioTek® ELX800 plate reader (Gen 5® software).

3.5.6 Apoptosis Assays

3.5.6.1 Annexin V and propidium iodide

Annexin V and propidium iodide staining assays were conducted to measure early and late apoptosis, as per manufacturer's instructions. Briefly, after pre-determined experimental conditions H9c2 cardiomyoblasts were counterstained with 0.5% annexin V and 1 µg/mL propidium iodide solution and incubated under standard TC conditions for 30 minutes. Thereafter, cells were rinsed once in DPBS before measuring fluorescence at an excitation and emission spectrum of 485 ± 20/ 528 ± 20 nm for Annexin V and 530

± 25/ 590 ± 35 nm for propidium iodide, using BioTek FLx800 plate reader and Gen 5 software for data attainment. Images were captured by means of a NETI- microscope (with NIS-Elements imaging software).

3.5.6.2 TUNEL assay

TUNEL assay is based on terminal deoxynucleotidyl transferase (TdT)-mediated inclusion of a modified dUTP (X-dUTP) to 3'-OH ends of extensive genomic fragmented DNA that are produced as a consequence of apoptosis. High glucose-induced apoptosis was assessed by means of a DeadEnd Fluorometric TUNEL kit (Promega, Madison, Wilsconsin, USA), as per manufacturers protocol.

Previously treated cardiomyoblasts were exposed to 4% paraformaldehyde, to fix cells, followed by 15 minutes incubation at RT. Thereafter, cardiomyoblasts were permeabilized with 0.2% (v/v) Triton X-100 for 5 minutes, then suspended in DPBS for an equal duration followed by the addition of 100 µL of equilibration buffer (EB). The EB was aspirated and a terminal deoxynucleotidyl transferase (TdT) reaction mixture (50 µL) was added and then incubated for 60 minutes under standard TC conditions. The reaction was terminated by the addition of a SSC buffer and incubated for an additional 15 minutes. TUNEL positive cardiomyoblasts were identified by the emission of a bright green fluorescent color at 10x magnification field (of at least 5 fields per well) with the use of a NETI-fluorescent microscope (with NIS Elements imaging software).

3.5.6.3 DAPI Assay

4ˈ,6-diamidino-2-phenylindole-2 (DAPI) is a blue fluorescent dye which binds both dead and live cells, through their A-T rich regions in DNA providing a bright blue fluorescence when viewed under ultraviolet light. DAPI counterstaining allows for the assessment of a nuclear morphology indicator. In this study, DAPI counterstain was used to normalize TUNEL staining. Previously treated H9c2 cardiomyoblasts were fixed in 4% paraformaldehyde and incubated for 15 minutes at RT. Thereafter, the cardiomyoblasts were rinsed (2x) with DPBS and exposed to DPBS Buffer containing 10 µg of DAPI in the dark for a duration of 10 minutes. To stop the reaction, cardiomyoblasts were washed with DPBS for 5 minutes. Nuclear blebbing was detected by the excitation of blue

fluorescence. To quantify nuclear morphology, DAPI images were analyzed with the NETI- fluorescent microscope (NIS Elements imaging software) under 10x magnification field (of at least 5 fields per well) and DAPI positive cells within those fields were calculated.

3.5.6.4 The activity of caspase 3/7

Caspase 3/7 activity is a luminescent assay used to measure pro-apoptotic activity in high glucose-induced H9c2 cells.

Concisely, previously treated cardiomyoblasts were lysed in 360 µL cold lysis buffer containing 10 µL/mL PMSF. The extraction of proteins was according to the methods as per section 3.6.2.1 and 3.6.2.2. Thereafter, 20 µL of the cardiomyoblasts lysates were pipetted into a 96-well plate. Subsequently, 20 µL Caspase-Glo® reagent was pipetted into respective wells and then incubated for 30 minutes in the dark. A BioTek® FLX 800 plate reader with Gen 5® software was used to measure luminescence. Data were normalized to previously acquired protein content using the Reducing agent and Detergent compatible (RC DC™) protein assay (Bio-Rad, Hercules, CA, USA).

3.6 The expression of proteins

3.6.1.1 Total protein concentration

After treatment, cardiomyoblasts cultured in 6-well TC plates were subjected to 350 µL cold cell lysis buffer per 75 cm^2. The cardiomyoblasts were harvested by means of scraping and then transferred to 2 mL Eppendorf tubes with stainless steel beads. Cell suspension were inserted into a pre-cooled TissueLyser blocks and homogenized 3 times at 25 Hz for 60 secs using a Qiagen TissueLyser (Qiagen, Hilden, Germany) (alternating between TissueLyser and ice for 1 minute). Protein lysates were then centrifuged at 4 ºC for 15 minutes at 15 000 x g. Thereafter, protein lysates were collected in 1.5 mL Eppendorf tubes and kept at -20 ºC until required.

3.6.1.2 Assessing the concentrations of proteins

Proteins levels of previously treated cardiomyoblasts were quantified by means of the RC DC™ protein assay kit (Bio-Rad, Hercules, CA, USA) as per manufacturer's guidelines. Five micro litres of respective, BSA standard (0.125, 0.25, 0.5, 0.75, 1, 1.5 and 2.0 mg/mL) and cell lysates were pipetted into a new 96-well plate. Twenty five micro litres of reagent A (entailing 20 µL RC Reagent C and 1 mL of RC reagent A) as well as 200 µL of reagent B was pipetted into every sample and standard in each well. The plate was then mixed on microplate shaker for 10 seconds and incubated at RT for 10 minutes before absorbance was read at 695 nm using a BioTek® ELX800 plate reader and Gen 5® software.

3.6.1.3 Gel electrophoresis

Thirty milligrams of lysed proteins were mixed with equivalent volumes of a 2x sodium borate (SB) buffer (see appendix A). Subsequently, lysates (with 2x SB buffer) were then denatured for 5 minutes at 95ºC`. Thereafter, 30 µg of the protein samples and 12 µL of the Precision Plus Protein Western C standard were loaded onto either 10 or 12% Mini-Protean® TGX™ (Bio-Rad, Hercules, CA, USA) gels and inserted in a Bio-Rad Mini Protein® Tetra Cell tank filled with 1x Tris/Glycine/SDS running buffer. The tetra cell tank was connected to the PowerPac™ Basic power supply to run the SDS-PAGE gel (Figure 3.3). Gel electrophoresis was commenced at 150 V for 60 min.

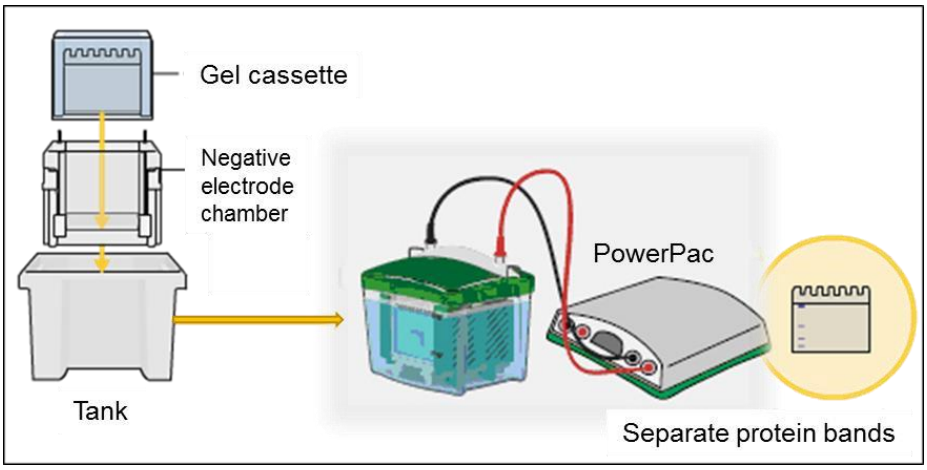

Figure 3.3: Schematic of polyacrylamide gel electrophoresis. 12µL of Western C marker and 30 µg of denatured protein samples were loaded onto either 10 or 12% Mini-Protean® gels. The gels were inserted in a tetra cell tank. The tank was connected to the PowerPac™ Basic power supply and gel electrophoresis initiated at 150 V for 60 min.

3.6.2 Western blot analysis

3.6.2.1 Transfer of gel to PVDF membrane

Western blot analysis is a procedure used for the detection and quantification of the expression of specific proteins using relative antibodies, within a complex mixture of proteins. Following gel electrophoresis, polyvinylidene fluoride (PVDF) membranes were submerged in ethanol for 1 minute. To make the transfer sandwich, membranes and transfer stacks were submerged into a transfer buffer (1x transfer buffer, ethanol and dH_2O) and equilibrated on an orbital shaker for 2-3 minutes. The SDS-PAGE gel was placed on the transfer sandwich and positioned on a cassette. The cassette was inserted into a Trans-Blot® Turbo™ Transfer System (Bio-Rad, Hercules, CA, USA) and run for 8 minutes to transfer the gel contents (proteins) onto the PVDF membrane.

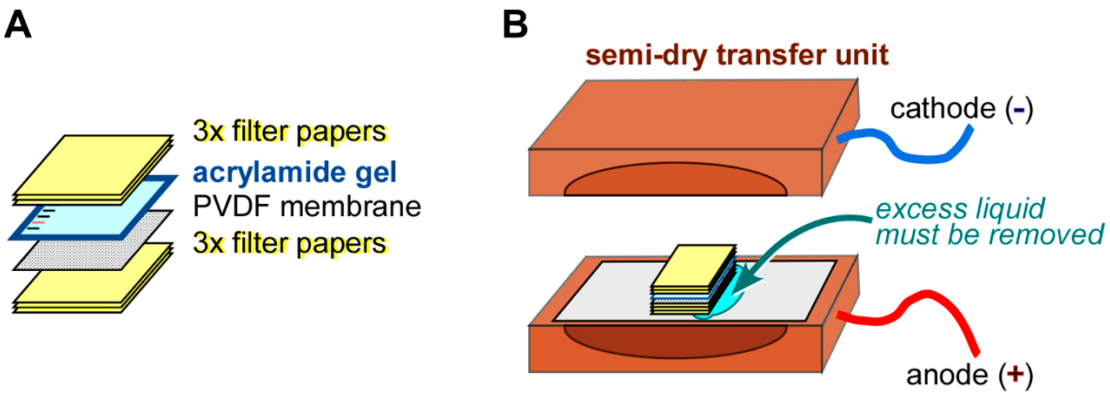

Figure 3.4: Transfer of gel to PVDF membrane. A) A transfer sandwich was made by submerging the polyvinylidene fluoride (PVDF) membranes and transfer stacks into a transfer buffer (1x transfer buffer, ethanol and dH2O) for 2-3 minutes. The SDS-PAGE gel was placed on the transfer sandwich and B) set on a cassette and inserted into a Trans-Blot® Turbo™ Transfer System and run for 8 minutes to transfer the proteins onto the membrane.

3.6.2.2 Ponceau S stain

To guarantee that the transmission of proteins onto the membranes was successful, PVDF membranes were immersed in 50 µL Ponceau S Staining Solution (Sigma-Aldrich, St Louis, MO, USA) before being placed on a shaker for 10 minutes. Following the staining period, membranes were submerged in a 1x Tris-buffered saline containing Tween-20 (TBST-20) to remove all nonspecific binding.

3.6.2.3 Labelling membrane with Antibody

PVDF membranes with the protein samples were blocked in 5% (w/v) skim milk (prepared in 1x TBST-20) at RT for 1-2 hours with constant shaking. Thereafter, the membranes were probed with respective primary antibodies (Table 3.3) in 5 mL 1x TBST-20 at 4 ºC overnight, on an orbital shaker. Subsequently, the membranes were washed with 1x TBST-20 at RT three times at 10 minute intervals. Thereafter, the membranes were probed with the applicable horseradish peroxidase (HRP) conjugated secondary antibody in 2.5% (w/v) skim milk (prepared in 1x TBST-20) for 90 minutes at RT. The wash step was repeated prior to detection and quantification of proteins using a Chemidoc-XRS imager and Quantity One software (Bio-Rad, Hercules, CA, USA). B-actin antibody was used to normalize proteins.

3.6.2.4 Stripping of Blot

Membranes were submerged and incubated for 13 minutes in a Western blot stripping buffer at RT. Subsequently, the membranes were washed 3x in 1x TBST-20 for 10 min.

Table 3.3: List of antibodies and their relative dilution factor

Antibodies	Dilution	Gel (%)	Cat #	Company
Primary Antibody				
Bax	1: 250	12	Sc-493	Santa Cruz
p-IRS (ser307)	1: 1 000	12	2870S	Cell Signaling
GLUT4	1: 1 000	12	4108S	SIGMA
p-Nf-kB	1: 1 000	12	5114S	Cell Signaling
p-PKC	1: 1 000	12	2983S	Cell Signaling
p-AMPK	1: 800	12	3535S	Cell Signaling
β-Actin	1: 1 000	12	Sc-47778	Santa Cruz
Secondary Antibody				
Donkey anti-mouse IgG-HRP	1: 4 000	-	Sc-23181	Santa Cruz
Donkey anti-rabbit IgG-HRP	1: 4 000	-	Sc-2012	Santa Cruz

CHAPTER FOUR

RESULTS

4.1 Triterpenes isolated from *Protorhus longifolia*

Two prominent triterpenes, methyl-3β-hydroxylanosta-9, 24-dienoate (RA3) and 3βhydroxylanosta-9, 24-dien-21-oic acid (RA5) (Figure 4.1A and B), were extracted from the chloroform extract of the stem barks of *P. longifolia.* Structural characterization and spectral analysis of RA3 and RA5 were previously done by Mosa and colleagues (2011). In this study, the presence of RA3 and RA5 was confirmed using thin layer chromatography (Figure 4.1C).

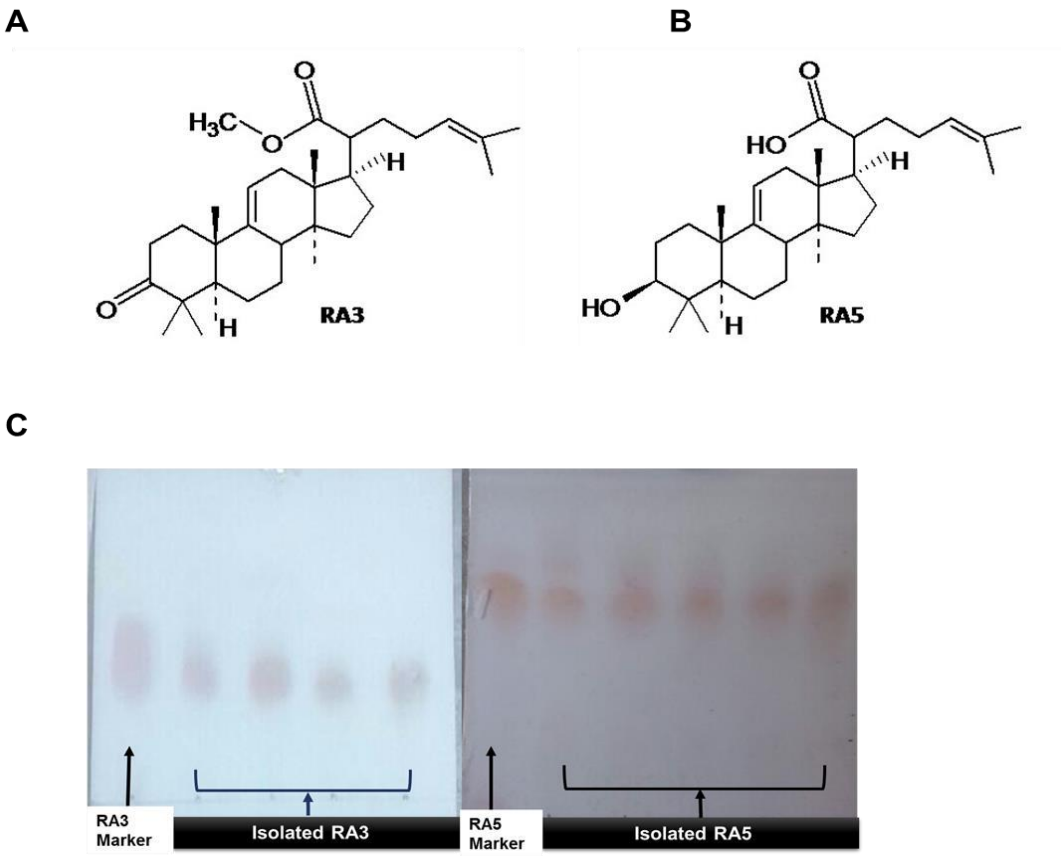

Figure 4.1: Chemical structure and thin layer chromatography of methyl-3β-hydroxylanosta-9, 24dienoate (RA3) and 3β-hydroxylanosta-9, 24-dien-21-oic acid (RA5). Representative images of (A) RA3 and (B) RA5 as well as, (C) thin layer chromatography results of RA3 and RA5, isolated from stembark. The molecular weights of RA3 and RA5 were calculated as 470.736 g/mol and 457.368 g/mol, respectively. Thin layer chromatography confirmed the presence of RA3 and RA5 from the chloroform crude extract when compared to compounds previously isolated by (Mosa *et al.*, 2011).

A. Biochemical Analysis

4.1 Effect of RA3 and RA5 on metabolic activity

4.1.1. RA3 and RA5 time and dose response assessment

ATP, as a quantification of cellular metabolic activity, was used to establish the efficacy of RA3 and RA5. H9c2 cells were exposed to log concentrations (0.001-1000 µM) of either RA3 or RA5 at five varying time intervals (3, 6, 12, 24 and 48 hours) (Figure 4.2). Results obtained showed a concentration dependent increase in cellular metabolic activity for both compounds (RA3 and RA5). While the triterpenes (RA3 and RA5) were effective in improving the metabolic activity of H9c2 cells, the results showed a greater increase in ATP production following treatment with RA3. Furthermore, the efficacy of both RA3 and RA5 was sustained throughout the different time points. However, at the 24 hour time point, we observed a greater efficiency in cellular metabolic activity in response to post-treatment with RA3. From these results, we selected RA3 as our treatment of choice for all subsequent experiments that were conducted in this study.

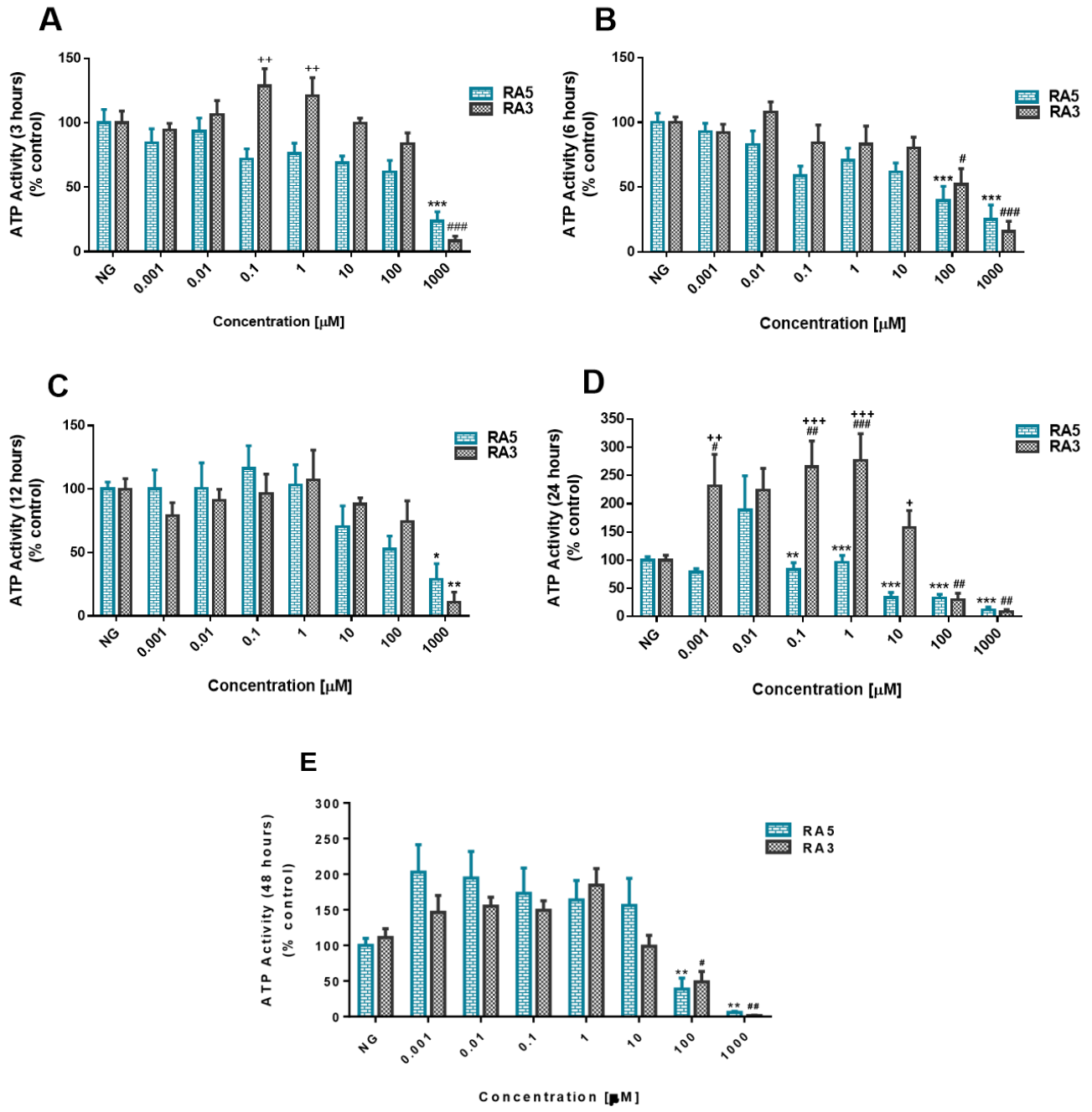

Figure 4.2: Determination of time and dose response of H9c2 cells exposed to methyl-3βhydroxylanosta-9, 24-dienoate (RA3) and 3β-hydroxylanosta-9, 24-dien-21-oic acid (RA5). ATP as a means to quantify metabolic activity cardiomyoblasts exposed to log concentrations of RA3 and RA5 at varying time points. The results represent H9c2 cardiomyoblasts exposed to either RA3 or RA5 for 3-, 6-, 12-, 24- and 48-hours. Data are presented as the mean ± SEM of 3 independent biological experiments with each experiment having 3 technical replicates (n=9). Significance is depicted as #$p \leq 0.05$, $^{\#\#\#}p \leq 0.001$ versus normal glucose (NG) control of RA3 and $^{**}p \leq 0.01$, $^{***}p \leq 0.001$ versus NG control of RA5 and $^{++}p \leq 0.01$ versus RA3.

4.1.2 Effect of RA3 on Metabolic activity

ATP as a measurement of cellular metabolic activity was used to assess the effect of high glucose (HG; 33 mM) on H9c2 cardiomyoblasts over a period of 24 hours. Cells cultured in HG displayed a significant decrease in ATP activity compared to the normal glucose (NG; 5.5 mM) control (46.00 ± 4.344% compared to 100%; $p < 0.001$). No substantial difference was detected in cells treated with NG+RA3 when compared to the NG control (103.3 ± 8.09% compared to 100%). However, treatment with either RA3 (107.1 ± 2.225%, $p < 0.05$), NAC (84.28 ± 20.61%; $p < 0.05$), MET (123.8 ± 18.89%; $p < 0.001$), MET+RA3 (146.1 ± 28.87%; $p < 0.001$) or MET+NAC (133.8 ± 28.89%; $p < 0.001$) was able to significantly improve the metabolic activity of cardiomyoblasts exposed to HG when compared to the HG control (Figure 4.3).

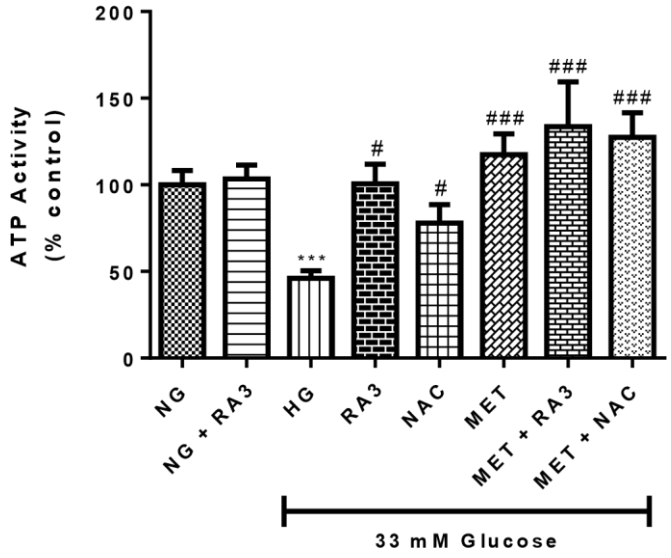

Figure 4.3: The effect of methyl-3β-hydroxylanosta-9, 24-dienoate (RA3) on high glucose-induced metabolic activity. H9c2 cardiomyoblasts were cultured in high glucose (HG; 33 mM) for 24 hours. Thereafter, cardiomyoblasts were treated with RA3 (1 µM), n-acetyl cysteine (NAC) (1 mM), metformin (MET) (1 µM), a combination of MET+RA3 (both at 2 µM) as well as MET+NAC (at 2µM and 2 mM, respectively). Cells treated with normal glucose (NG) served as the vehicle control. Data are presented as the mean ± SEM of 3 distinct biological experiments with each experiment having 3 practical repeats (n=9). Significance is depicted as ***$p \leq 0.001$ versus NG control, $^{\#}p \leq 0.05$, $^{\#\#\#}p \leq 0.001$ versus HG control.

4.2 Effect of RA3 on glucose uptake and lipid accumulation

4.2.1 Glucose uptake in H9c2 cardiomyoblasts

Impaired cardiac glucose regulation is closely linked with the development of heart failure. Glucose uptake (GU) was measured in H9c2 cardiomyoblasts exposed to HG levels. Results obtained showed that cells cultured in HG displayed a significant reduction in GU when compared to the NG control (51.75 ± 6.77% compared to 100.4 ± 11.59%; $p < 0.01$). No significant difference was observed in cells exposed to NG+RA3 in comparison to the NG control (98.75 ± 9.08% compared to 100%). However, treatment with RA3 significantly improved GU compared to the HG control (75.75 ± 6.33% compared to 51.75 ± 6.77%; $p < 0.05$). Interestingly, enhanced GU was displayed by cells treated with the combination of MET+RA3 (171.4 ± 30.31%; $p < 0.001$) and this effect was better than the cells treated with either NAC (54.08 ± 13.51%), MET (88.42 ± 12.56%; $p < 0.01$) or the combinatory treatment of MET+NAC (119.4 ± 24.34%; $p < 0.05$) (Figure 4.4).

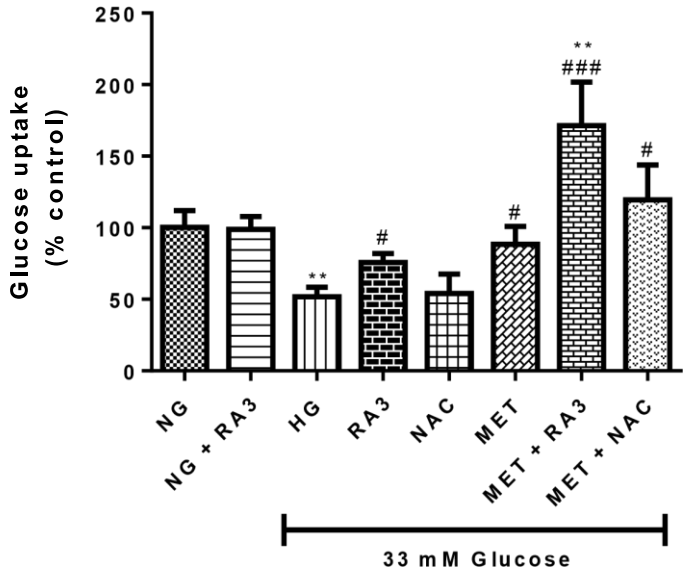

Figure 4.4: The effect of methyl-3β-hydroxylanosta-9, 24-dienoate (RA3) on high glucose-induced H9c2 cells glucose uptake. H9c2 cardiomyoblasts were cultured in high glucose (HG; 33 mM) for 24 hours. Cardiomyoblasts were then co-treated with RA3 (1 µM), n-acetyl cysteine (NAC) (1 mM), metformin (MET) (1 µM), a combination of MET+RA3 (both at 2 µM) as well as MET+NAC (at 2µM and 2 mM, respectively). Cells treated with normal glucose (NG) served as the vehicle control. Data are presented as the mean ± SEM of 3 distinct biological experiments with each experiment having 3 practical repeats (n=9). Significance is depicted as **p ≤ 0.01 versus NG control, $^{\#}$p ≤ 0.05, $^{\#\#\#}$p ≤ 0.001 versus HG control.

4.2.2 Lipid storage in cardiomyoblasts

Increase in cellular lipid accumulation can lead to cardiac dysfunction. H9c2 cardiomyoblasts displayed a significant increase in lipid content in comparison to the NG control (from 100 ± 7.52% to 265.50 ± 7.15%; $p < 0.001$). No substantial change was observed in cells exposed to NG+RA3 in comparison to the NG control (85.00 ± 4.38% compared to 100%). However, treatment with RA3 (100.3 ± 5.57%; $p < 0.001$) as well as the combination of MET+RA3 (132.0 ± 17.64%; $p < 0.001$) were able to significantly reduce lipid accumulation when compared to the HG control. Similarly, NAC (118.8 ± 14.92%; $p < 0.001$), MET (89.75 ± 6.06; $p < 0.001$) and a combination of MET+NAC (93.50 ± 12.82%; $p < 0.001$) effectively decreased lipid accumulation in cardiac cells (Figure 4.5).

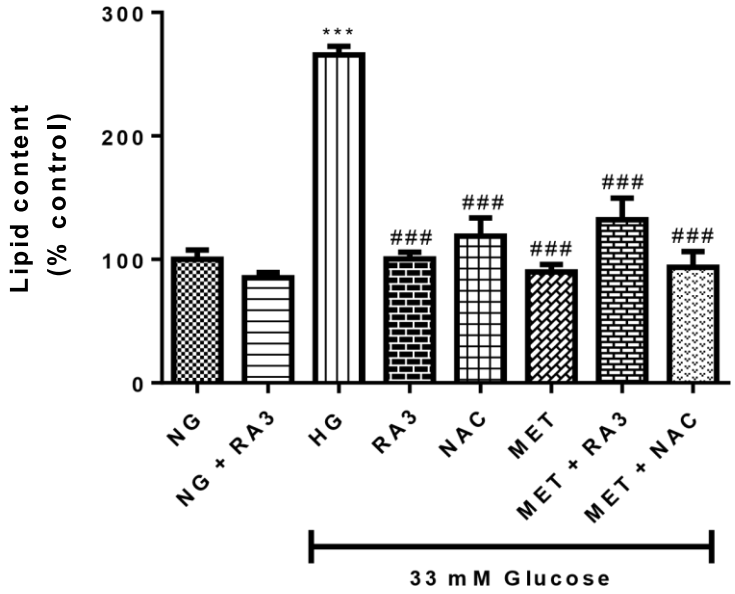

Figure 4.5: Methyl-3β-hydroxylanosta-9, 24-dienoate (RA3) reverse high glucose-induced lipid accumulation. H9c2 cardiomyoblasts were cultured in high glucose (HG; 33 mM) for 24 hours. Cells were then co-treated with RA3 (1 µM), n-acetyl cysteine (NAC) (1 mM), metformin (MET) (1 µM), a combinatory treatment of MET+RA3 (both at 2 µM) as well as MET+NAC (at 2µM and 2 mM, respectively). Cells treated with normal glucose (NG) served as the vehicle control. Results are expressed as the mean ± SEM of 3 independent biological experiments with each experiment having 3 technical replicates (n=9). Significance is depicted as ***$p \leq 0.001$ versus NG control, ###$p \leq 0.001$ versus HG control.

4.3 RA3 attenuates high glucose-induced oxidative stress

4.3.1 Increased ROS production

High glucose-stimulated oxidative stress is related with accelerated cardiovascular disease. H9c2 cardiomyoblasts cultured in HG exhibited a significant increase in intracellular ROS levels, in comparison to the NG control (from 100.0 ± 6.882% to 151.5 ± 9.18%; $p < 0.01$). No significant difference was observed in cells exposed to NG+RA3 when compared to the NG control (95.28 ± 6.42% compared to 100%). Treatment with either RA3 (91.78 ± 4.93%; $p < 0.001$), NAC (103.7 ± 5.67%; $p < 0.001$) MET (95.47 ± 5.58%; $p < 0.001$) or a combination of MET+RA3 (88.75 ± 4.79%; $p < 0.001$) as well as MET+NAC (96.88 ± 6.29%; $p < 0.001$) drastically decreased the production of superoxide radicals when compared to the HG control (Figure 4.6).

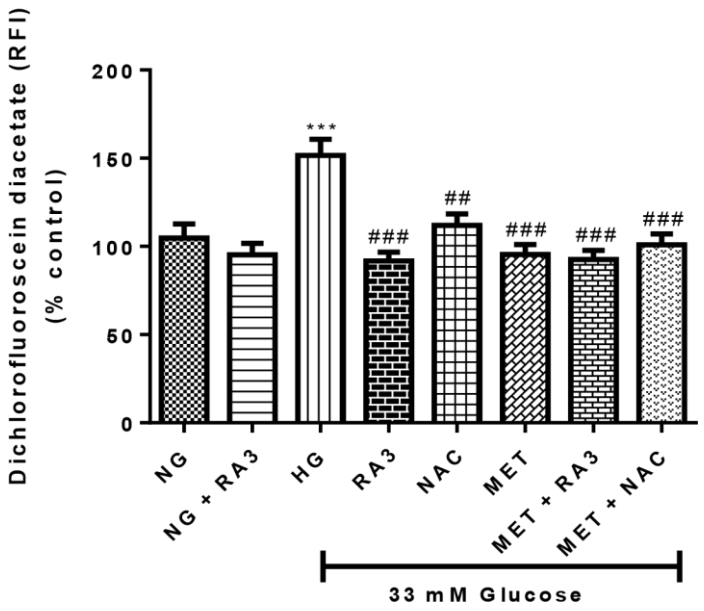

Figure 4.6: The effect of methyl-3β-hydroxylanosta-9, 24-dienoate (RA3) RA3 on high glucose induced oxidative stress. 2′, 7′-Dichlorofluorescin diacetate (DCFH-DA) fluorescence as a measurement of reactive oxygen species production was assessed in H9c2 cardiomyoblasts cultured in high glucose (HG-33 mM) for 24 hours. Cells co-treated with RA3 (1 µM), n-acetyl cysteine (NAC) (1 mM), metformin (MET) (1 µM), a combination of MET+RA3 (both at 2 µM) as well as MET+NAC (at 2µM and 2 mM, respectively) attenuated this effect. Cells treated with normal glucose (NG) served as the vehicle control. Data are expressed as the mean ± SEM of 3 independent ***$p \leq 0.001$ versus NG control, $^{\#\#}p \leq 0.01$, $^{\#\#\#}p \leq 0.001$ versus HG control.

4.3.2 Lipid peroxidation

Hyperglycemia and oxidative stress play a crucial role in the dysregulation of lipid peroxidation (malondialdehyde- MDA) in the diabetic heart. High glucose-induced lipid peroxidation was evident in H9c2 cardiomyoblasts exposed to HG when compared to the NG control (from 100.20 ± 1.33% to 143.70 ± 1.20%; $p < 0.001$). Treatment with RA3 (122.3 ± 1.56%; $p < 0.05$) and the combination of MET+RA3 (111.2 ± 5.05%; $p < 0.01$) significantly decreased the production of MDA when compared to the HG control. Similarly, treatment with NAC (124.7 ± 2.06%; $p < 0.05$), MET (121.0 ± 3.69%; $p < 0.05$) and a combination of MET+NAC (117.7 ± 1.28%; $p < 0.05$) was able to decrease lipid peroxidation (Figure 4.7). No major difference was observed in NG control cells treated with RA3.

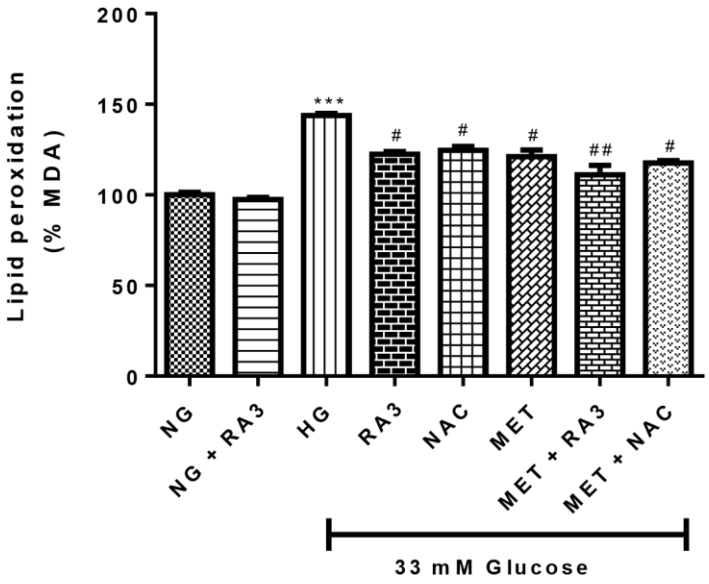

Figure 4.7: The effect of methyl-3β-hydroxylanosta-9, 24-dienoate (RA3) RA3 on high glucose induced lipid peroxidation. Malondialdehyde (MDA) formation is a measurement of lipid peroxidation. H9c2 cardiomyoblasts were cultured in high glucose (HG; 33 mM) for 24 hours. Cells were then co-treated with RA3 (1 µM), n-acetyl cysteine (NAC) (1 mM), metformin (MET) (1 µM), a combination of MET+RA3 (both at 2 µM) as well as MET+NAC (at 2µM and 2 mM, respectively). Data is presented as the mean ± SEM of 3 distinct biological experiments with each experiment having 3 practical repeats (n=9). Significance is depicted as ***p ≤ 0.001 versus NG control, $^{\#}$p ≤ 0.05, $^{\#\#}$p ≤ 0.01 versus HG control.

4.3.3 Superoxide dismutase (SOD) activity

H9c2 cardiomyoblasts cultured in HG displayed a significant reduction in SOD activity in comparison to the NG control (from 100.0 ± 5.46% to 30.66 ± 2.75%; $p < 0.001$). Interestingly, treatment with RA3 (74.19 ± 3.63%; $p < 0.001$), NAC (72.93 ± 2.77; $p < 0.001$), MET (64.18 ± 4.07%; $p < 0.001$), a combination of MET+RA3 (82.77 ± 3.57%; $p < 0.001$) as well as MET+NAC (81.18 ± 1.8%; $p < 0.001$) significantly increased SOD activity when compared to the HG control (Figure 4.8). No significant difference was detected when NG control cardiomyoblasts were treated with RA3.

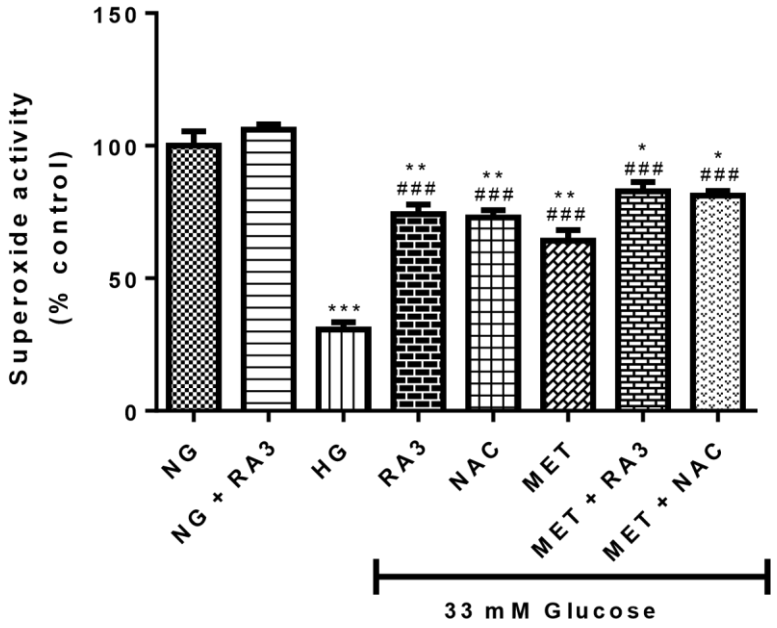

Figure 4.8: The effect of methyl-3β-hydroxylanosta-9, 24-dienoate (RA3) to reverse high glucose induced superoxide dismutase (SOD) activity. H9c2 cardiomyoblasts were cultured in high glucose (HG; 33 mM) for 24 hours. Thereafter, cardiomyoblasts then co-treated with RA3 (1 µM), n-acetyl cysteine (NAC) (1 mM), metformin (MET) (1 µM), a combination of MET+RA3 (both at 2 µM) as well as MET+NAC (at 2µM and 2 mM, respectively). Cells treated with normal glucose (NG) served as the vehicle control. Data is presented as the mean ± SEM of 3 separate biological experiments with each experiment having 3 technical replicates (n=9). Significance is depicted as *p ≤ 0.05, **p ≤ 0.01, ***p ≤ 0.001 versus NG control, ###p ≤ 0.001 versus HG control.

4.3.4 Total Glutathione content

H9c2 cardiomyoblasts presented with a significant decrease in total glutathione content when compared to cells cultured in NG (82.57 ± 5.63%f compared to 100 %; $p < 0.05$). However, treatment with RA3 (121.3 ± 5.43%; $p < 0.001$), NAC (120.3 ± 5.88%; $p < 0.001$), MET (113.9 ± 3.98%; $p < 0.001$), the combination of MET+RA3 (119.0 ± 7.24%; $p < 0.001$) as well as the combination of MET+NAC (115.7 ± 6.57%) were able to significantly improve intracellular glutathione content (Figure 4.9). No major change was observed in NG control cells treated with RA3.

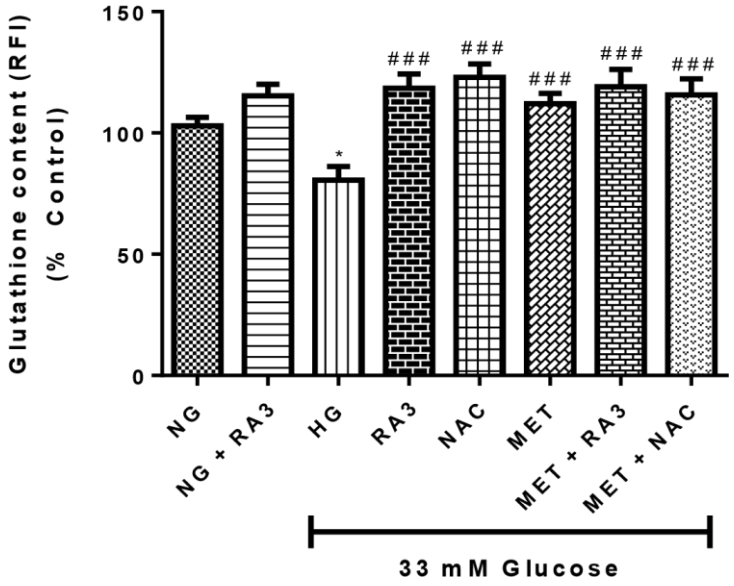

Figure 4.9: The effect of methyl-3β-hydroxylanosta-9, 24-dienoate (RA3) on glutathione (GSH) content. H9c2 cardiomyoblasts were cultured in high glucose (HG; 33 mM) for 24 hours. Cells were cotreated with RA3 (1 µM), n-acetyl cysteine (NAC) (1 mM), metformin (MET) (1 µM), a combination of MET+RA3 (both at 2 µM) as well as MET+NAC (at 2µM and 2 mM, respectively). Cells treated with normal glucose (NG) served as the vehicle control. Data are expressed as the mean ± SEM of 3 distinct biological experiments with each experiment having 3 technical replicates (n=9). Significance is depicted as *$p \leq 0.05$ versus NG control, ###$p \leq 0.001$ versus HG control.

4.4 High glucose-induced apoptosis

4.4.1 Mitochondrial membrane potential (ΔΨm)

Impaired mitochondrial potential as a measurement of early apoptosis was assessed in cardiomyoblasts cultured in HG. A significant increase in depolarized mitochondria, by a ratio of 1.63, was observed in cells exposed to HG when compared to the NG control (from 1.34 ± 0.13 to 2.97 ± 0.24; $p < 0.001$). However, treatment with RA3 (1.29 ± 0.14; $p < 0.001$), MET (1.39 ± 0.11; $p < 0.001$) and the combination of MET+RA3 (1.42 ± 0.12; $p < 0.001$) was able to significantly attenuate depolarization of the mitochondrial membrane. Interestingly, no noticeable difference was observed in cells treated with NAC (2.49 ± 0.22) as well as the combination of MET+NAC (2.81 ± 0.18) (Figure 4.10). Cells treated with NG+RA3 showed no effect as compared to the NG control (1.439 ± 0.11 compared to 1.34 ± 0.13).

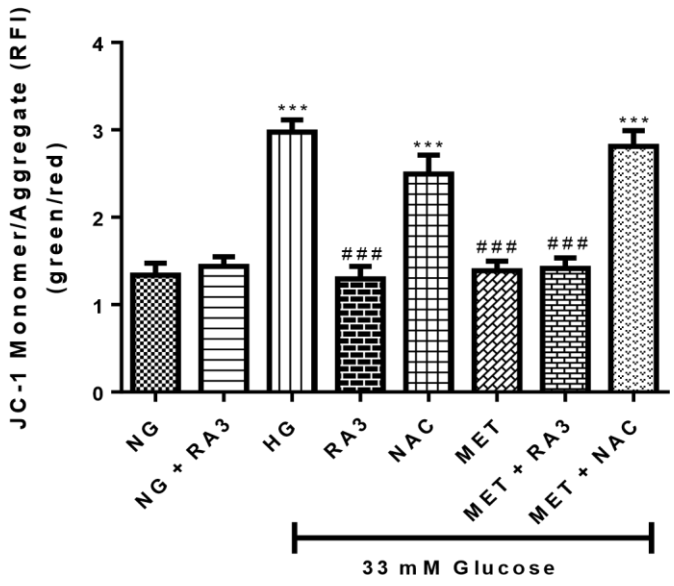

Figure 4.10: The effect of methyl-3β-hydroxylanosta-9, 24-dienoate (RA3) on mitochondrial potential. H9c2 cardiomyoblasts were cultured in high glucose (HG; 33 mM) for 24 hours. Thereafter, cells were co-treated with RA3 (1 µM), n-acetyl cysteine (NAC) (1 mM), metformin (MET) (1 µM), a combination of MET+RA3 (both at 2 µM) as well as MET+NAC (at 2µM and 2 mM, respectively). Cells treated with normal glucose (NG) served as the vehicle control. Data are presented as the mean ± SEM of 3 separate biological experiments with each experiment having 3 technical repeats (n=9). Significance is depicted as ***$p \leq 0.001$ versus NG control, ###$p \leq 0.001$ versus HG control.

4.4.2 Annexin V and Propidium iodide

Annexin V and Propidium iodide are known indicators of cellular apoptosis. In the present study, H9c2 cardiomyoblasts cultured in HG displayed increased levels of fluorescent intensity associated with both early (annexin v) and late (propidium iodide) apoptosis when compared to the NG control (from 99.94 ± 5.69% to 140.42 ± 12.79% and 99.94 ± 1.36% to 148.50 ± 10.88%; $p < 0.001$). However, high glucose induction of early and late apoptosis was significantly attenuated by treatment with RA3 (99.81 ± 5.14%; 94.08 ± 1.5%; $p < 0.001$), NAC (110.03 ± 4.39%; 119.19 ± 6.61%; $p < 0.001$), MET (104.11 ± 5.36%; 99.06 ± 2.26%; $p < 0.0001$) and the combination of MET+RA3 (100.72 ± 5.08%; 97.14 ± 1.77%; $p < 0.001$) when compared to the HG control. No noteworthy change was observed in H9c2 cardiomyoblasts treated with NG+RA3 (100.98 ± 5.53%; 96.75 ±

1.25%) or the combination of MET+NAC (110.78 ± 3.48%; p < 0.001 and 138.58 ± 6.61%) as compared to the NG and HG controls, respectively (Figure 4.11).

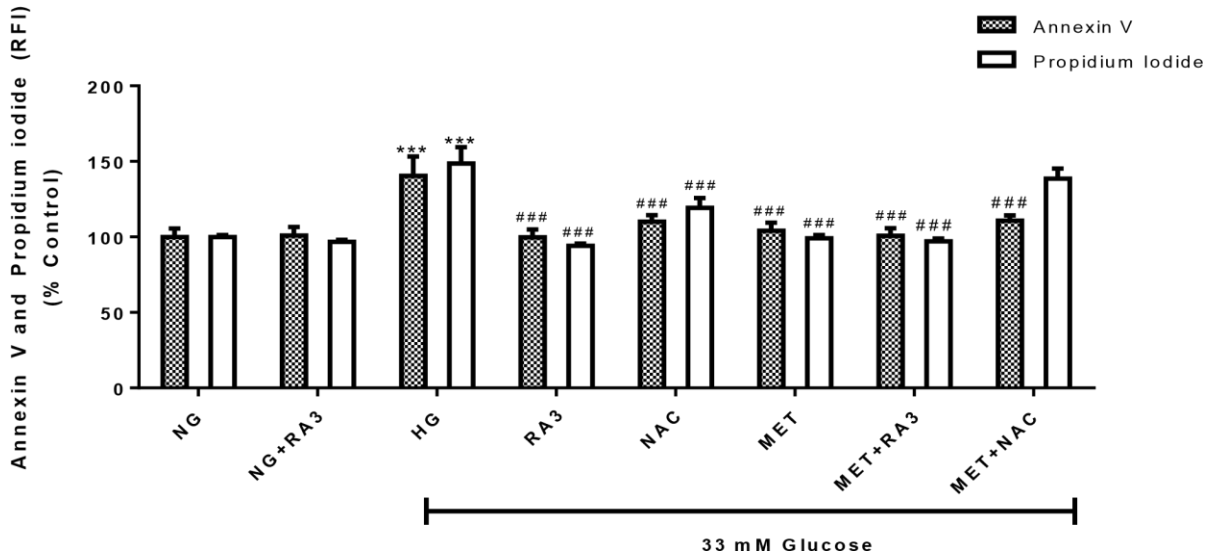

Figure 4.11: The effect of methyl-3β-hydroxylanosta-9, 24-dienoate (RA3) on high glucose-induced cellular apoptosis. H9c2 cardiomyoblasts were cultured in high glucose (HG; 33 mM) for 24 hours. Thereafter, cardiomyoblasts were treated with RA3 (1 µM), n-acetyl cysteine (NAC) (1 mM), metformin (MET) (1 µM), a combination of MET+RA3 (both at 2 µM) as well as MET+NAC (at 2µM and 2 mM, respectively). Cells treated with normal glucose (NG) served as the vehicle control. Data is presented as the mean ± SEM of 3 separate biological experiments with each experiment having 3 practical repeats (n=9). Significance is depicted as ***p ≤ 0.001 versus NG control, ###p ≤ 0.001 versus HG control.

4.4.3 Effect of RA3 on nuclear morphology

To quantify nuclear morphological changes induced by HG, the nucleus of the cells was stained with DAPI. H9c2 cardiomyoblasts exposed to HG displayed significant abnormalities in nuclear morphology when compared to the NG control (from 0.38 ± 0.26 to 10.25 ± 1.33; p < 0.01). However, the results showed that treatment with RA3 (4.38 ± 0.78; p < 0.001), NAC (5.00 ± 0.80; p < 0.001), MET (4.25 ± 0.53; p < 0.001) and the combination of MET+RA3 (4.12 ± 0.72; p < 0.001) were able to significantly ameliorate this effect. Interestingly, a greater improvement was observed in cells treated with the combination of MET+NAC (2.25 ± 0.77; p < 0.001) (Figure 4.12). No significant difference was observed in cells treated with NG+RA3 when compared to the NG control (0.37 ±

0.26 compared to 0.38 ± 0.26).

A

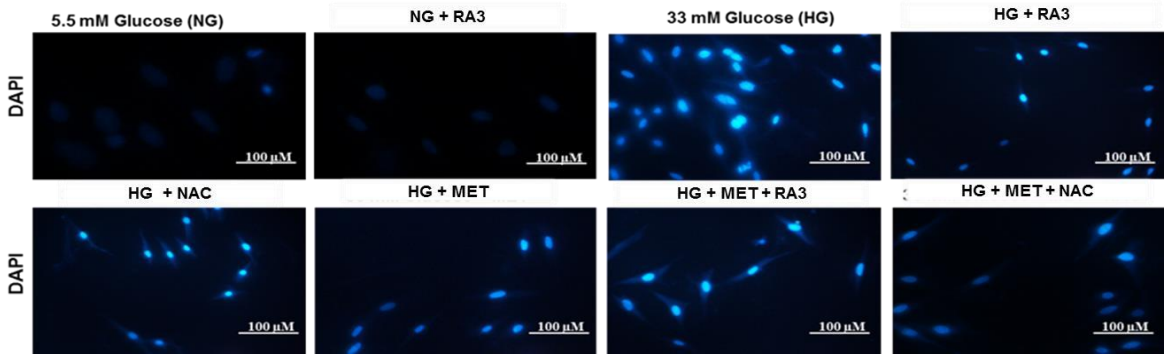

B

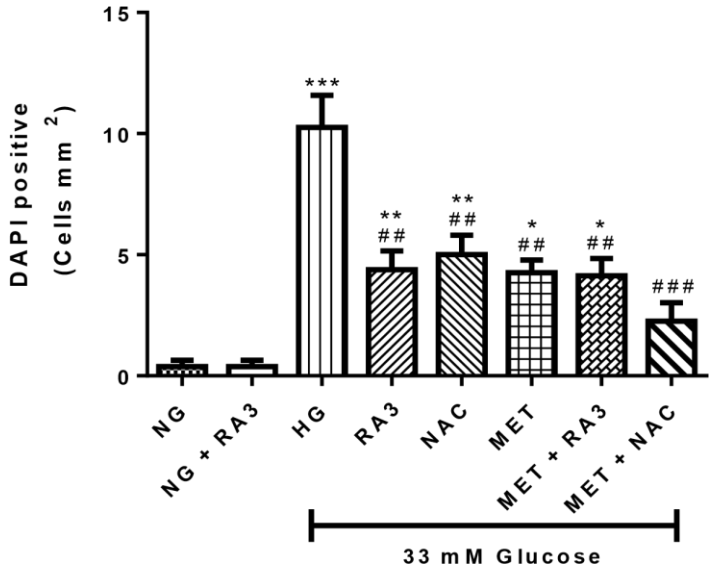

Figure 4.12: Quantification of DAPI-stained nuclear morphology following high glucose exposure with subsequent methyl-3β-hydroxylanosta-9, 24-dienoate (RA3) treatment. A) Representative images of DAPI stained H9c2 cells treated with HG and post treated with RA3. B) Quantification of DAPI stained images. H9c2 cardiomyoblasts were cultured in high glucose (HG; 33 mM) for 24 hours. Thereafter, cells were co-treated with RA3 (1 µM), n-acetyl cysteine (NAC) (1 mM), metformin (MET) (1 µM), a combination of MET+RA3 (both at 2 µM) as well as MET+NAC (at 2µM and 2 mM, respectively). Cells treated with normal glucose (NG) served as the vehicle control. Data is presented as the mean ± SEM of 3 separate biological experiments with each experiment having 3 practical repeats (n=9). Significance is depicted as *p ≤ 0.05, **p ≤ 0.01, ***p ≤ 0.001 versus NG control, $^{\#\#}$p ≤ 0.01, $^{\#\#\#}$p ≤ 0.001 versus HG control.

4.4.4 The effect of RA3 on DNA fragmentation

TUNEL assay was used for the detection of DNA fragmentation, which is a hallmark of apoptosis. In this study, increased TUNEL positive cells were demonstrated in cardiomyoblasts exposed to HG when compared to the NG control (12.63 ± 1.96; $p < 0.001$ compared to 1.75 ± 0.77). Treatment with RA3 (5.88 ± 1.1; $p < 0.001$), MET (6.50 ± 1.99; $p < 0.05$), the combination of MET+RA3 (4.50 ± 0.65; $p < 0.001$) as well as MET+NAC (6.25 ± 1.42; $p < 0.05$) were able to significantly attenuate this effect when compared to the HG control. However, no significant difference was observed in cells treated with NAC (10.00 ± 1.39) (Figure 4.13). Also, no significant difference was observed in cells treated with NG+RA3 when compared to the NG control (1.750 ± 0.6748 compared to 1.750 ± 0.7734).

A

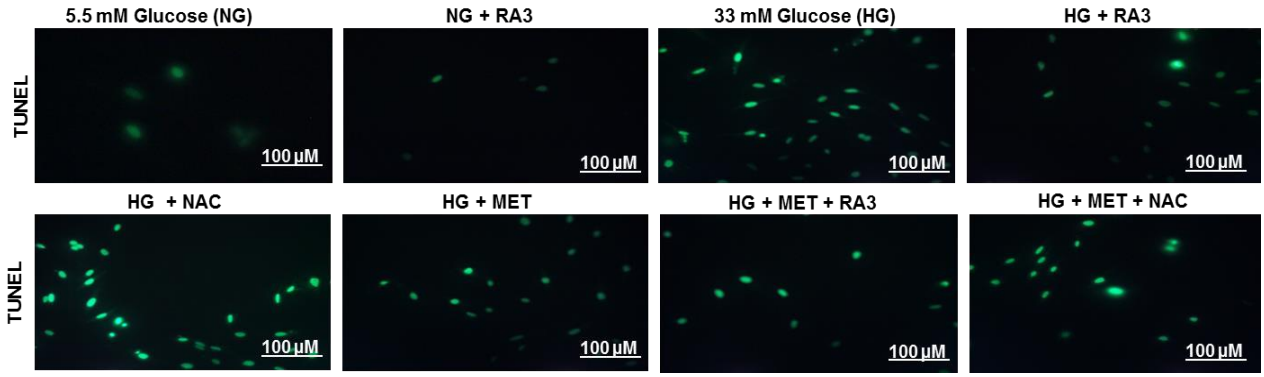

B

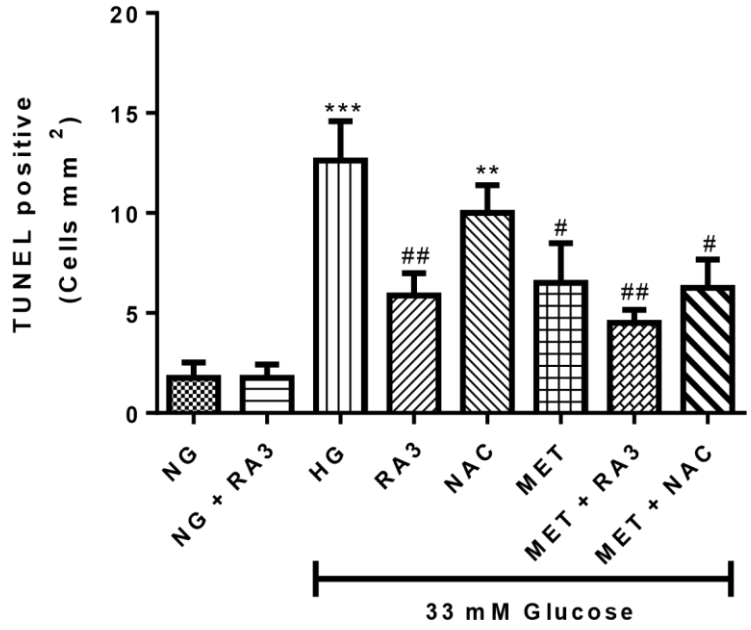

Figure 4.13: The effect of methyl-3β-hydroxylanosta-9, 24-dienoate (RA3) on high glucose-induced DNA fragmentation. H9c2 cardiomyoblasts were cultured in high glucose (HG; 33 mM) for 24 hours. Cells were then co-treated with RA3 (1 µM), n-acetyl cysteine (NAC) (1 mM), metformin (MET) (1 µM), a combination of MET+RA3 (both at 2 µM) as well as MET+NAC (at 2µM and 2 mM, respectively). Cells treated with normal glucose (NG) served as the vehicle control. Data is presented are expressed as the mean ± SEM of 3 separate biological experiments with each experiment having 3 technical repeats (n=9). Significance is depicted as ***$p \leq 0.001$ versus NG control, $^{\#}p \leq 0.05$, $^{\#\#}p \leq 0.01$ versus HG control.

4.4.5 Caspase 3/7 activity

Caspase 3/7 activity assay is a technique used to measure cellular death. High glucose significantly increased Caspase-3/7 activity in H9c2 cardiomyoblasts when compared to the NG control (from 100.0 ± 1.05% to 205.4 ± 5.06%; $p < 0.001$). However, treatment with RA3 (162.9 ± 6.62%; $p < 0.01$), NAC (169.0 ± 7.19%; $p < 0.001$, MET (170.8 ± 7.83%; $p < 0.01$), the combination of MET+RA3 (150.4 ± 7.50%; $p < 0.001$) as well as MET+NAC (163.6 ± 10.15%; $p < 0.001$) was able to significantly mitigate high glucose-induced apoptosis when compared to the HG control (Figure 4.14). No significant difference was observed in cells treated with NG+RA3 when compared to the NG control (97.25 ± 6.34% compared to 100.0 ± 1.05%)

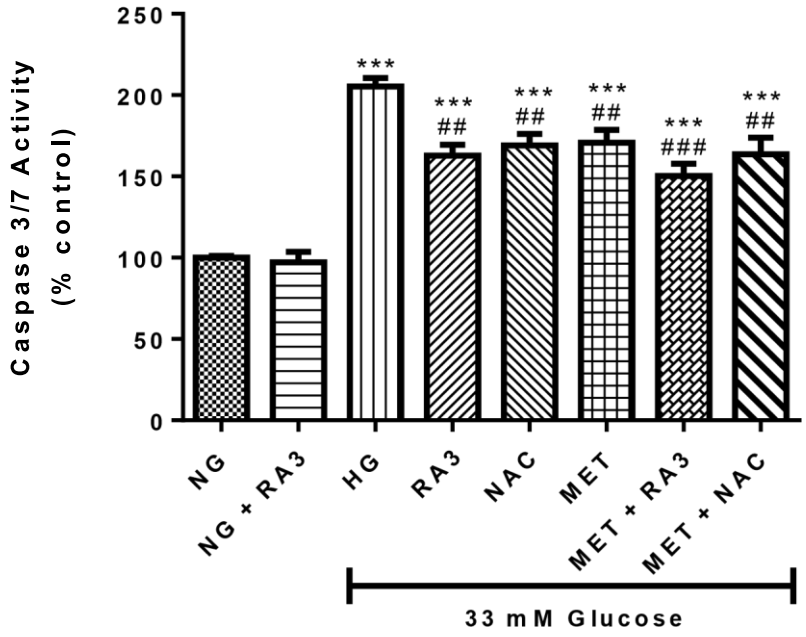

Figure 4.14: The effect of methyl-3β-hydroxylanosta-9, 24-dienoate (RA3) on high glucose-induced caspase 3/7 activity. H9c2 cardiomyoblasts were cultured in high glucose (HG; 33 mM) for 24 hours. Thereafter, cells were co-treated with RA3 (1 µM), n-acetyl cysteine (NAC) (1 mM), metformin (MET) (1 µM), a combination of MET+RA3 (both at 2 µM) as well as MET+NAC (at 2µM and 2 mM, respectively). Cells treated with normal glucose (NG) served as the vehicle control. Results are expressed as the mean ± SEM of 3 independent biological experiments with each experiment having 3 technical replicates (n=9). Significance is depicted as ***$p \leq 0.001$ versus NG control, $^{\#\#}p \leq 0.01$, $^{\#\#\#}p \leq 0.001$ versus HG control.

4.5 Gene and Protein expression

4.5.1. The effect of RA3 on phosphorylated 5' AMP-activated protein kinase (AMPK) expression

The major kinase that plays a role in energy homeostasis is 5' AMP-activated protein kinase (AMPK), which is activated by increased glucose levels. The expression of phosphorylated AMPK (p-AMPK^{Thr172}) in H9c2 cardiomyoblasts was significantly diminished following HG exposure when compared to the NG control (38.73 ± 11.18% compared to 100.0 ±. 22.88%; $p < 0.001$). No significant difference was observed in H9c2 cardiomyoblasts exposed to NG+RA3 (93.45 ± 21.65% compared to 100%). Although no significant increase was observed following treatment with NAC (56.50 ± 8.66%), treatment with RA3 (80.20 ± 17.14%; $p < 0.01$), MET (79.51 ± 14.36%; $p < 0.01$), the combination of MET+RA3 (88.76 ± 17.37%; $p < 0.01$) as well as that of MET+NAC (84.70 ± 22.48%; $p < 0.01$) were able to significantly ameliorate the expression of p-AMPK$^{(Thr172)}$ (Figure 4.15).

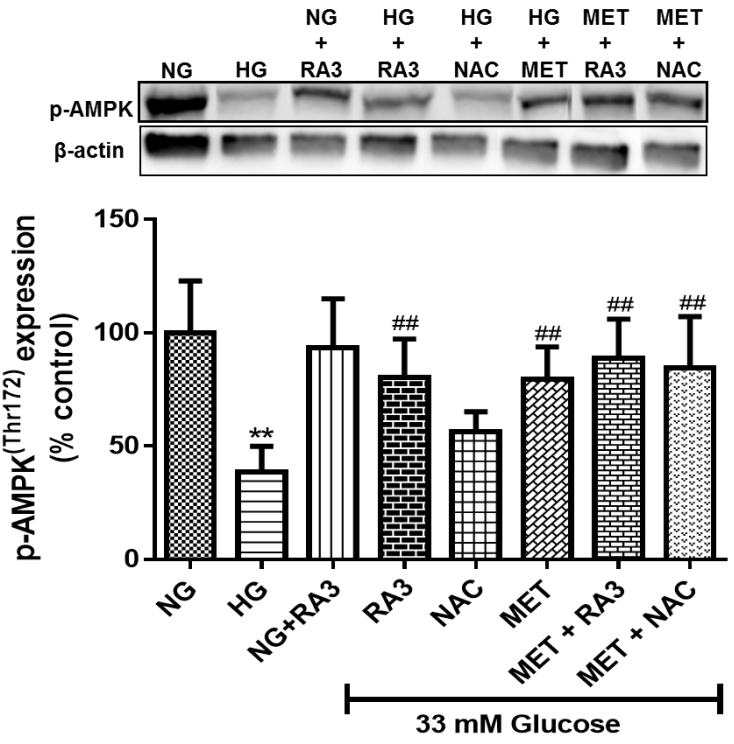

Figure 4.15: The effect of methyl-3β-hydroxylanosta-9,24-dienoate (RA3) on 5' AMP-activated protein kinase phosphorylation at threonine 172 (p-AMPKThr^{172}). H9c2 cardiomyoblasts were cultured in high glucose (HG; 33 mM) for 24 hours. Thereafter, cells were co-treated with RA3 (1 µM), n-acetyl cysteine (NAC) (1 mM), metformin (MET) (1 µM), a combination of MET+RA3 (both at 2 µM) as well as MET+NAC (at 2µM and 2 mM, respectively). Cells treated with normal glucose (NG) served as the vehicle control. Results are expressed as the mean ± SEM of 3 independent biological experiments with each experiment having 3 technical replicates (n=9). Significance is depicted as **p ≤ 0.01 versus NG control, ##p ≤ 0.01 versus HG control.

4.5.2 The effect of RA3 on phosphorylated nuclear factor kappa-β (NF-kβ) expression

H9c2 cardiomyoblasts exposed to HG presented with a significant increase in NF-kβ expression when compared to cells cultured in NG (from 97.98 ± 10.21 to 525.4 ± 40.33; $p < 0.001$). No significant difference was observed in NG cultured H9c2 cardiomyoblasts treated with RA3 when compared to the NG control (113.3 ± 25.25 compared to 97.98 ± 10.21). However, treatment with RA3 (166.7 ± 26.63; $p < 0.001$), NAC (215.4 ± 51.94; $p < 0.001$), MET (345.7 ± 15.76), the combination of MET+RA3 (249.5 ± 73.90; $p < 0.01$)

as well as the combination of MET+NAC (295.4 ± 29.78; $p < 0.05$) were able to significantly attenuate the phosphorylation of NF-kβ (Figure 4.16).

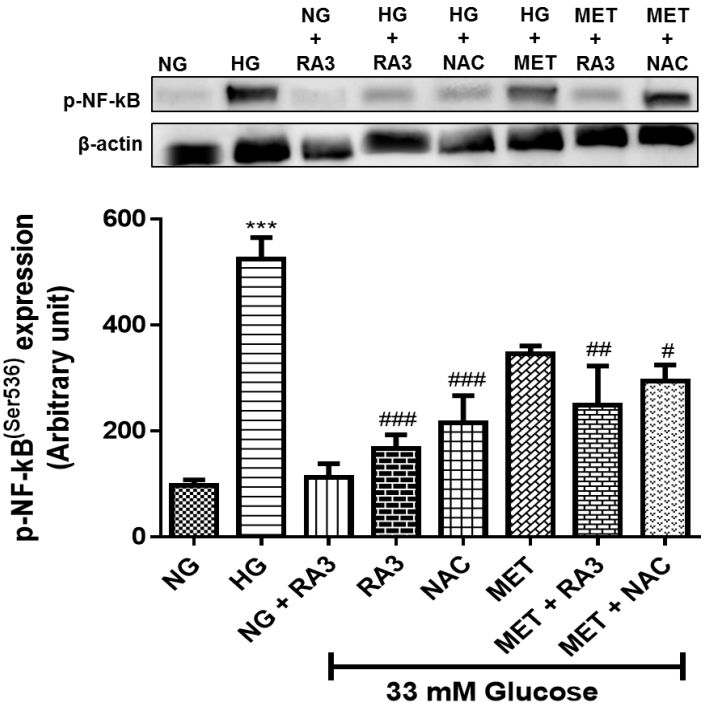

Figure 4.16: The effect of methyl-3β-hydroxylanosta-9,24-dienoate (RA3) on nuclear factor-kappa β phosphorylation at serine 536 (p-NF-kB^{Ser536}). H9c2 cardiomyoblasts were cultured in high glucose (HG; 33 mM) for 24 hours. Cells were then co-treated with RA3 (1 µM), n-acetyl cysteine (NAC) (1 mM), metformin (MET) (1 µM), a combination of MET+RA3 (both at 2 µM) as well as MET+NAC (at 2µM and 2 mM, respectively). Cells treated with normal glucose (NG) served as the vehicle control. Results are expressed as the mean ± SEM of 3 independent biological experiments with each experiment having 3 technical replicates (n=9). Significance is depicted as ***$p \leq 0.001$ versus NG control, $^{\#}p \leq 0.05$, $^{\#\#}p \leq 0.01$, $^{\#\#\#}p \leq 0.001$ versus HG control.

4.5.3 The effect of RA3 on phosphorylated protein kinase C (PKC)

Increased serine phosphorylation of protein kinase (p-PKC^{Ser660}) has been linked with insulin resistance. H9c2 cardiomyoblasts cultured in HG significantly increased the expression of p-PKC$^{(Ser660)}$ when compared to the NG control (from 6604 ± 143.6 to 17054 ± 1000; $p < 0.001$). No significant difference was observed in cells treated with NG+RA3 when compared to the NG control (8379 ± 987.4 compared to 6604 ± 143.6). However,

treatment with RA3 (14644 ± 563.6; $p < 0.05$), NAC (14724 ± 557.1; $p < 0.05$), MET (12749 ± 620.2; $p < 0.01$), the combination of MET+RA3 (7651 ± 412.1; $p < 0.001$) as well as MET+NAC (12125 ± 1063; $p < 0.01$) significantly mitigated the phosphorylation of PKC when compared to the HG control (Figure 4.17).

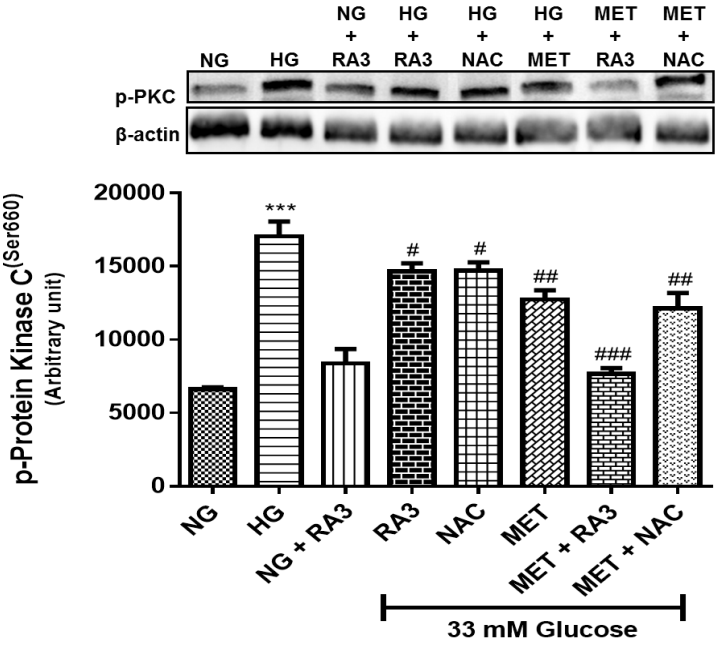

Figure 4.17: The effect of methyl-3β-hydroxylanosta-9,24-dienoate (RA3) on protein kinase C phosphorylation at serine 660 (p-PKC^{Ser660}). H9c2 cardiomyoblasts were cultured in high glucose (HG; 33 mM) for 24 hours. Cells were then co-treated with RA3 (1 µM), n-acetyl cysteine (NAC) (1 mM), metformin (MET) (1 µM), a combination of MET+RA3 (both at 2 µM) as well as MET+NAC (at 2µM and 2 mM, respectively). Cells treated with normal glucose (NG) served as the vehicle control. Results are expressed as the mean ± SEM of 3 independent biological experiments with each experiment having 3 technical replicates (n=9). Significance is depicted as ***$p \leq 0.001$ versus NG control, $^{\#}p \leq 0.05$, $^{\#\#}p \leq 0.01$, $^{\#\#\#}p \leq 0.001$ versus HG control.

4.5.4 The effect of RA3 on phosphorylated insulin receptor substrate-1 (RS-1)

Serine phosphorylation of insulin receptor substrate-1 (p-IRS-1^{Ser307}) inhibits insulin signaling which contributes to peripheral insulin resistance. A significant increase in IRS1$^{Ser(307)}$ activity was observed in H9c2 cardiomyoblasts exposed to HG when compared to the NG control (from 108.8 ± 56.07 to 1861 ± 240.4; $p < 0.001$). However,

treatment with RA3 (911.5 ± 285.6; p < 0.05), NAC (978.2 ± 335.8; p < 0.05), MET (771.5 ± 192.3; p < 0.05), the combination of MET+RA3 (776.9 ± 233.7; p < 0.05) as well as the combination of MET+NAC (1159 ± 449.9) were able to alleviate this effect (Figure 4.18). No significant difference was observed in cells treated with NG+RA3 when compared to the NG control (64.60 ± 35.12 compared to108.8 ± 56.07).

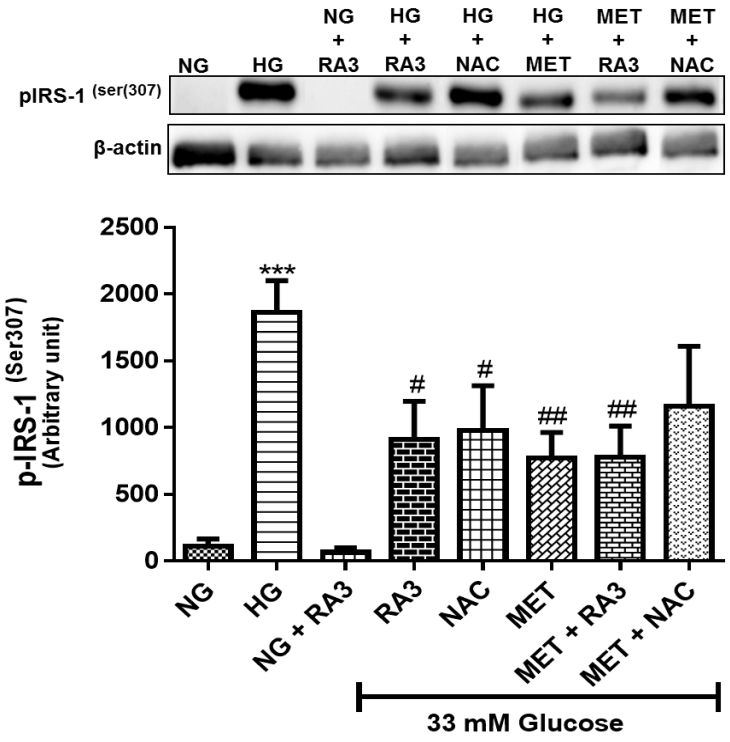

Figure 4.18: The effect of methyl-3β-hydroxylanosta-9,24-dienoate (RA3) on insulin receptor substrate-1 phosphorylation at serine 307 (p-IRS-1^{Ser307}). H9c2 cardiomyoblasts were cultured in high glucose (HG; 33 mM) for 24 hours. Thereafter, cells were co-treated with RA3 (1 µM), n-acetyl cysteine (NAC) (1 mM), metformin (MET) (1 µM), a combination of MET+RA3 (both at 2 µM) as well as MET+NAC (at 2µM and 2 mM, respectively). Cells treated with normal glucose (NG) served as the vehicle control. Results are expressed as the mean ± SEM of 3 Independent biological experiments with each experiment having 3 technical replicates (n=9). Significance is depicted as ***p ≤ 0.001 versus NG control, $^{\#}$p ≤ 0.05, $^{\#\#}$p ≤ 0.01 versus HG control.

4.5.5 The effect of RA3 on phosphorylated protein kinase B (Akt)

Protein kinase B (Akt) signaling plays a central role in insulin stimulated glucose uptake. In the present study H9c2 cardiomyoblasts cultured in HG presented with a significant

decrease in the expression of Akt when compared to the NG control (48.53 ± 11.08 % compared to 100 %). Interestingly, only RA3 was able to significantly ameliorate the expression of Akt (90.29 ± 10.08%; $p < 0.05$), whereas treatment with MET (58.86 ± 8.15%), the combination of MET+RA3 (67.57 ± 6.38%) as well as MET+NAC (70.69 ± 9.87%) increased AKT expression but not significantly when compared to the HG control.

No significant difference was observed in cells treated with NG+RA3 when compared to the NG control (100.7 ± 15.06 % compared to 100.0 ± 13.87 %).

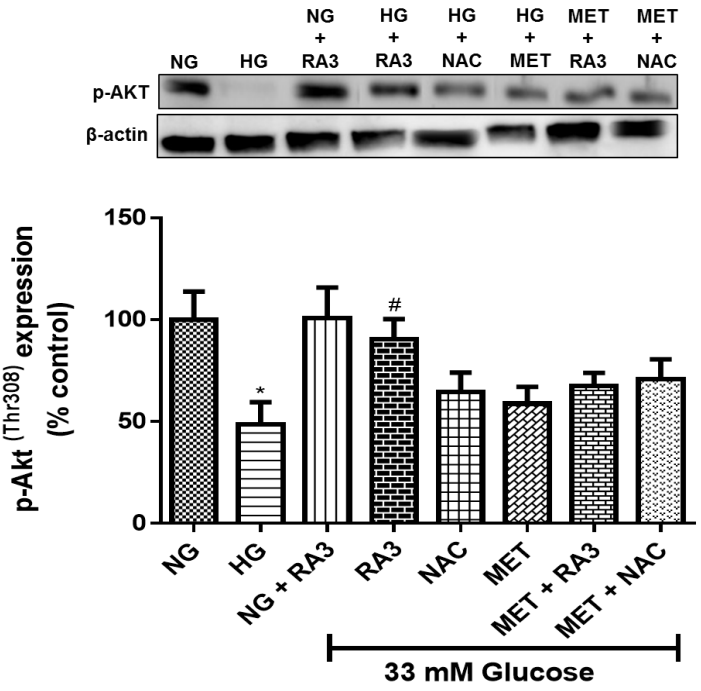

Figure 4.19: The effect of methyl-3β-hydroxylanosta-9, 24-dienoate (RA3) on protein kinase B phosphorylation at threonine 308 (p-Akt^{308}). H9c2 cardiomyoblasts were cultured in high glucose (HG; 33 mM) for 24 hours. Cells were then co-treated with RA3 (1 µM), n-acetyl cysteine (NAC) (1 mM), metformin (MET) (1 µM), a combination of MET+RA3 (both at 2 µM) as well as MET+NAC (at 2µM and 2 mM, respectively). Cells treated with normal glucose (NG) served as the vehicle control. Results are expressed as the mean ± SEM of 3 independent biological experiments with each experiment having 3 technical replicates (n=9). Significance is depicted as *$p \leq 0.05$ versus NG control, $^{\#}p \leq 0.05$ versus HG control.

4.5.5 The effect of RA3 on glucose transporter 4 (GLUT4)

Glucose transporter 4 (GLUT4) is a major transporter of glucose in the heart. Results obtained showed that HG result in a significant decrease in GLUT4 expression when compared to cells cultured in NG (from 100.0 ± 9.32% to 30.82 ± 6.03%; $p < 0.001$). However, this reduction was significantly reversed following treatment with RA3 (91.88 ± 8.10%; $p < 0.001$), NAC (74.61 ± 7.57%; $p < 0.01$), MET (91.09 ± 7.97%; $p < 0.001$), the combination of MET+RA3 (83.79 ± 8.36%; $p < 0.001$) and that of MET+NAC (81.44 ± 9.94%; $p < 0.001$) when compared to the HG control (Figure 4.20). No significant difference was observed in cells treated with NG+RA3 when compared to the NG control (97.44 ± 10.16 compared to 100%).

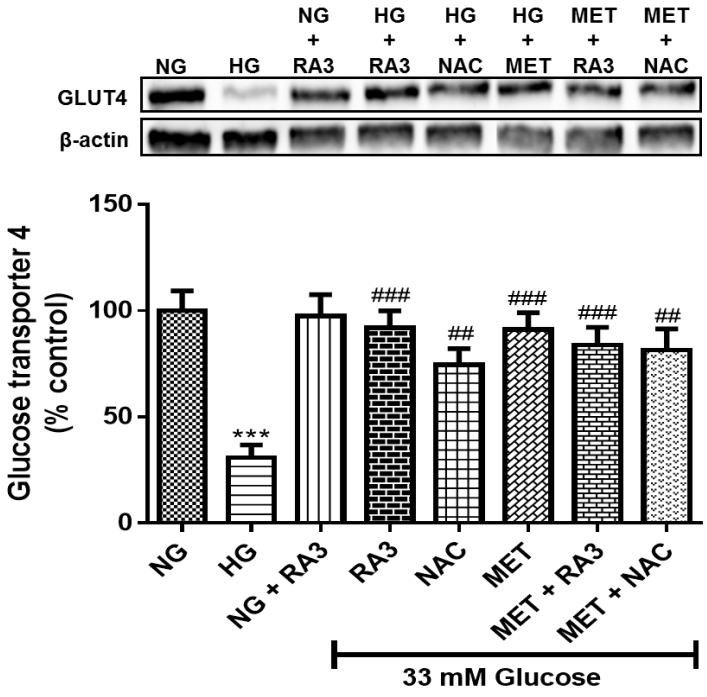

Figure 4.20: The effect of methyl-3β-hydroxylanosta-9, 24-dienoate (RA3) on glucose transporter 4 (GLUT4) activation. H9c2 cardiomyoblasts were cultured in normal glucose (NG; 5.5 mM) and high glucose (HG; 33 mM) for 24 hours. Thereafter, cells were treated with RA3 (1 µM), metformin (MET) (1 µM), n-acetyl cysteine (NAC) (1 mM), a combination of RA3 (2 µM) and MET (2 µM), as well as a combination of NAC (2 mM) and MET (2 µM). Results are expressed as the mean ± SEM of 3 independent biological experiments with each experiment having 3 technical replicates (n=9). Significance is depicted as ***$p \leq 0.001$ versus NG control, $^{\#\#}p \leq 0.01$, $^{\#\#\#}p \leq 0.001$ versus HG control.

CHAPTER FIVE

DISCUSSION

An extensive body of knowledge has shown that diabetes is a known risk factor for the development of CVDs, as chronic hyperglycemia leads to structural and functional modifications in the diabetic heart (Gersh *et al.*, 2010; Dei Cas *et al.*, 2015). Furthermore, a number of studies have demonstrated that chronic hyperglycemia is associated with the development of diabetes-induced cardiomyopathy. By definition, DCM is a nebulous heart disease instigated by resistance to the metabolic actions of insulin and the progression of hyperglycemia in the diabetic heart, characterized by left ventricular dysfunction.

Despite the discovery of DCM more than 4 decades ago by Rubler *et al.* (1972), the exact underlying mechanism leading to its onset remains the subject of extensive research. Decrease in insulin sensitivity and diminished glucose uptake is evident in the diabetic heart through the reduced expression of glucose transporters (GLUT1 and GLUT4). It has been previously proposed that high glucose accompanied by a shift in substrate preference and increased oxidative stress is the primary initiators of diabetes-induced cardiomyopathy. This increased oxidative stress through the overproduction of superoxide in the mitochondria of the diabetic heart activates a cascade of pathways including PKC (Giacco, 2011). Activation of PKC has been implicated in decreased NO production and cardiac apoptosis due to augmented expression of NF-kβ with concomitant fibrosis and insulin resistance, all key feature of DCM (Durpès *et al.*, 2015).

Indeed, the treatment of diabetes as an independent risk factor is crucial for the prevention and management of DCM. However, the current synthetic anti-diabetic drugs (such as metformin, thiazolidinedione's and sulfonylureas) possess far too many sideeffects and over time have been shown to lose their efficacy, thereby exacerbating diabetes and leading to cardiac dysfunction (Erdmann, 2009; García-Compeán *et al.*, 2015). It is for this reason that there is a renewed interest in the use of plant-derived nutraceuticals, such as triterpenes from *Protorhus longifolia*, as an adjunct to current antidiabetic drug therapy (Lozano-Mena *et al.*, 2014). Some lanosteryl triterpenes, RA5 and RA3, from *Protorhus longifolia* have been shown to possess anti-diabetic properties (Machaba *et al.*, 2014; Mosa *et al.*, 2015), anticoagulant and anti-inflammatory (Mosa *et al.*, 2011) activities. Most recently the triterpenes ability to improve myocardial derangements (Mosa *et al.*, 2016) and pancreatic β-cell ultra-structure (Mabhida *et al.*, 2017) has been reported. Based on

these findings, we sought to investigate whether these triterpenes could ameliorate high glucose-induced cardiac injury using embryonic rat heart derived H9c2 cardiomyoblasts.

5.1 Time and dose response of RA3 and RA5.

In the present study we investigated the effect of two prominent triterpenes on the metabolic activity of H9c2 cardiomyoblasts. The results revealed that both compounds were not toxic to the cells at concentrations ranging from 0.001-10 µM, as a concentration dependent increase in metabolic activity was observed. However, at higher concentrations (100-1000µM) an apparent reduction in metabolic activity was observed following treatment with both compounds. The results also revealed that RA3 was more effective than RA5 across various time points, with the most effective dose being 1 µM for a period of 24 hours. Our findings were consistent with a study conducted by Mosa et al. (2011). From these findings, RA3 was selected to conduct all subsequent experiments in the current study.

5.2 The effect of RA3 on the metabolic activity of H9c2 cardiomyoblasts. In normal cardiomyocytes fatty acid oxidation (FAO) and glucose metabolism contribute to approximately 70% and 30% of the total ATP produced, respectively (Rijzewijk *et al.*, 2009; Lopaschuk *et al.*, 2010). This balance in energy production is crucial for optimal contractile function of the heart. However, diabetic hearts cannot use glucose efficiently due to impaired insulin signaling and may consequently be forced to rely completely on FAO (80-90%) as the preferred energy sources (Lorenzo *et al.*, 2013; Bagul *et al.*, 2015). Furthermore, increased reliance on FFAs leads to elevated oxidative stress and reduced cardiac efficiency, subsequently resulting in cardiac dysfunction (Ferrannini *et al.*, 2016; Mizuno *et al.*, 2017).

Literature has identified decreased high energy phosphate levels and flux as consistent features of heart failure (HF) (Chen and Knowlton, 2010). The reduction in ATP levels has been demonstrated in high glucose stimulated H9c2 cells (Johnson *et al.*, 2016). In accordance with these findings, we observed a decrease in ATP production in the H9c2 cardiomyoblasts exposed to HG. However, this effect was significantly ameliorated by treatment with RA3, NAC (an antioxidant stimulant), MET (a first line anti-diabetic drug),

a combination of MET+RA3 as well as that of MET+NAC. Interestingly, we observed a much greater increase in metabolic activity when H9c2 cardiomyoblasts were combinatorial treated. This data suggests that treatment with RA3 or the combination of MET+RA3 as well as MET+NAC can indirectly improve energy efficiency in the diabetic heart which is closely linked to cardiac function.

5.3 The effect of RA3 on glucose metabolism and lipid storage. The physiological balance between glucose and FFA utilization is a crucial component for the maintenance of myocardial contractility and function (Adrian *et al.*, 2017). In diabetic hearts, there is a dramatic shift away from glucose utilization towards a complete reliance on FFAs as an energy source, resulting in loss of metabolic flexibility (Bayeva *et al.*, 2013). While a decrease in glucose utilization is detrimental to the heart, chronic elevated uptake of FFAs can lead to lipid accumulation and subsequent cardiac dysfunction. Johnson and colleagues (2016) demonstrated a significant reduction in glucose uptake with an apparent increase in FFA oxidation in H9c2 cardiomyocytes exposed to high glucose. Correspondingly, Bhatt *et al.* (2014) reported on impaired cardiac function in the hearts of diabetic rats. They further showed that HG and palmitate (a FFA) negatively affected fractional shortening in isolated left ventricular cardiomyocytes.

Similarly, in the present study, a significant increase in lipid accumulation was observed in H9c2 cells exposed to HG, which subsequently led to diminished glucose uptake. However, this effect was mitigated by treatment with RA3, NAC, MET and the combination of MET+NAC. Interestingly, a much greater increase in glucose uptake, with an evident reduction in lipid accumulation, was observed in cardiomyoblasts treated with the combination of MET+RA3, suggesting a potential synergistic effect by the two compounds. These findings are an indication that our compound of interest (RA3) as well as the combinatory treatment (MET+RA3) can potentially protect the diabetic heart by regulating glucose lipid metabolism thereby maintaining cardiac function. Our findings are supported by studies conducted by Machaba *et al.* (2014); Mosa *et al.*, (2015) and Mabhida *et al.*, (2017) in which they demonstrated the ability of RA3 to reducing circulating FFAs and glucose in a diabetic model.

5.4 The effect of RA3 on high glucose-induced oxidative stress and lipid peroxidation. Prolonged vascular exposure to chronic hyperglycemia is a major instigator for increased oxidative stress which is a key factor in the development of diabetes-induced cardiomyopathy (Liu, Wang and Cai, 2014; Jia, Whaley-Connell and Sowers, 2017). The cardiomyocytes have a very low antioxidant capacity and a shift in mitochondrial substrate preference can result in excessive ROS production (Johnson *et al.*, 2016). This has been validated by numerous studies showing a strong correlation between oxidative stress and matrix remodeling in cardiomyocytes isolated from diabetic heart tissue (Dludla *et al.,* 2014; Dludla *et al.*, 2017).

Data from this study showed that cardiomyoblasts exposed to HG triggered increased ROS production and lipid peroxidation, which was evident by elevated levels of superoxide and MDA content. Furthermore, excessive ROS production has been shown to induce intracellular mitochondrial damage which can result in the leakage and subsequent reduction of endogenous antioxidant enzymes, GSH and SOD, as observed in the present study. These results were consistent with a study by Johnson and colleagues (2016) where they demonstrated the effect of high glucose-induced oxidative stress through elevated levels of superoxide with a concomitant reduction in GSH and SOD levels in H9c2 cardiomyoblasts. Similarly, Chen and colleagues (2014) showed that the exposure of H9c2 cells to HG induced cardiac injury as shown by elevated ROS production in these cells. It can be assumed that decreased GSH and SOD activity might result in the accumulation of hydrogen peroxide (H_2O_2) thereby increasing cardiac cells susceptible to oxidative damage. Conversely, in our study, treatment with RA3, NAC, MET, the combination of MET+RA3 as well as MET+NAC was able to significantly attenuate this effect by reducing ROS production and subsequently ameliorating the expression of GSH and SOD in the cardiomyoblasts. Our results are supported by a study by Mabhida *et al.* (2017) where they demonstrated that RA3 could protect against hyperglycemic-induced oxidative damage. These finding suggest that RA3 could be used as a scavenger of ROS and therefore a potent therapeutic agent to protect the diabetic heart against oxidative stress-induced cardiac injury.

5.5 The effect of RA3 on the insulin signaling pathway. In the diabetic state, elevated levels of FFAs with their metabolites, diacylglycerol and ceramides, can inhibit insulin signaling through the activation of PKC. This leads to an increased inflammatory response activating NF-kβ and amplifying insulin resistance through the phosphorylation IRS-$1^{Ser(307)}$. The increased activation of IRS-$1^{Ser(307)}$ results in the disruption of PI3k/Akt signaling cascade, which suppresses GLUT4 mediated glucose uptake in peripheral tissue. Ferrannini *et al.* (2014) have previously attributed the lack of insulin sensitivity and glucose assimilation in the heart to the reduction of glucose transporters (GLUT4). Correspondingly, Mabhida and colleagues (2017) demonstrated accelerated insulin resistance in the skeletal muscles of diabetic rats through the apparent activation of $IRS1^{Ser(307)}$ with reduced GLUT4 expression.

In the current study, we observed an increase in PKC/IRS-$1^{Ser(307)}$ mediated GLUT4 expression in H9c2 cardiomyoblasts, following HG exposure. Furthermore, a noticeable increase in of GLUT4 in the NF-kβ was seen in these cells. However, this effect was attenuated by treatment with RA3, NAC, MET, the combination of MET+RA3 and that of MET+NAC. Interestingly, the combination of MET+RA3 as well as that of MET+NAC provided a greater reduction in PKC and IRS-$1^{Ser(307)}$ expression. Furthermore, we observed a significant amelioration in the phosphorylation of Akt in cardiomyoblasts treated with only RA3. Subsequently, this effect led to upregulation of GLUT4 in the cardiac cells. Our findings are consistent with a study done by Mabhida *et al.* (2017), demonstrating the ability of RA3 to improve insulin signaling by reducing the phosphorylation of IRS-$1^{Ser(307)}$ and increasing the expression of Akt and GLUT4 in the skeletal muscles. Our data is also in agreement with a study conducted by Johnson *et al.*, (2016) in which they reported the increased expression of GLUT4 in H9c2 cells treated with a herbal agent, aspalathin, thereby accentuating the use of natural products in high glucose-induced cardiac dysfunction. Furthermore, the findings from this study suggest that RA3 exerts its anti-hyperglycemic potential in the heart via an insulin dependent (Akt) and can therefore be a used as a potent therapeutic glucose lowering agent.

5.6 The effect of RA3 on AMPK. Apart from insulin-dependent pathways, the regulation of glucose into the cardiomyocytes can also be facilitated by phosphorylated AMPK through the translocation of GLUT4 to the plasma membrane in an insulin-independent manner. AMP-activated protein kinase is a central regulator of cellular energy homeostasis and has been extensively studied as a potential target to ameliorate insulin resistance (Heidrich *et al.*, 2010). A study by Li and colleagues (2014) demonstrated reduced AMPK levels in the hearts of diabetic mice with an accompanied decrease in glucose metabolism (Li *et al.*, 2014). Another study reported on the diminished expression of AMPK in ventricular derived H9c2 cells exposed to 33.3 mM glucose (HG) for 24 hours (Kim *et al.*, 2007). Similarly, data from this study presented with lowered AMPK levels following HG exposure in H9c2 cardiomyoblasts. However, treatment with RA3, MET, MET+RA3 as well as that of MET+NAC were able to ameliorate this effect. These results were particularly interesting as they suggest that RA3 not only exerts its glucose lowering effects via the IRS/PI3k/Akt pathway but also through the AMPK pathway.

5.7 The effect of RA3 on high glucose-induced mitochondrial depolarization and apoptosis. Chronic hyperglycemia stimulates the permeabilization of the mitochondria through the excessive production of ROS leading to apoptosis. In the diabetic heart, the mitochondrial apoptotic pathway is mediated, at least in part, by the activation of the cytochrome c–activated caspase-3/7 pathway (Ares-Carrasco *et al.*, 2009). Activated cytosolic caspase 3/7 translocates to the nucleus where it cleaves DNA repair enzymes and triggers caspase-activated DNase which in turn induces DNA fragmentation, a hallmark of apoptosis (Kim and Kang, 2010). Hyperglycemia-induced apoptosis has been reported to be a key player in cardiac structural remodeling and the subsequent development of left ventricular dysfunction (Rota *et al.*, 2006; C. Y. Tsai *et al.*, 2013). A study by Kain and colleagues (2016) reported on the loss of mitochondrial potential and increased apoptosis through the expression of caspase 3/7 in the H9c2 cells. Similarly, Dludla *et al.* (2016) demonstrated that high glucose exposure impaired mitochondrial potential and augmented DNA damage with subsequent increase in cardiomyocyte apoptosis.

In line with the aforementioned, H9c2 cardiomyoblasts displayed a substantial increase in mitochondrial depolarization, nuclear DNA fragmentation and caspase 3/7 expression following high glucose exposure. In the present study we observed that there was no significant change in mitochondrial potential following treatment with NAC and the combination of MET+NAC. However, the results revealed that treatment with RA3, MET and the combination of MET+RA3 was able to ameliorate mitochondrial potential and attenuate apoptosis in the cardiomyoblasts. The results obtained from this study demonstrate that apoptosis occurs in the diabetic myocardium and provides evidence that high levels of glucose directly cause apoptosis (Webster, 2012; Lorenzo *et al.*, 2013). Importantly, the present study has clearly shown that depolarized mitochondria and caspase-3 activation are associated with hyperglycemia-induced myocardial apoptosis. Our findings are supported by a study by Mosa *et al.* (2016) where they demonstrated that RA3 is able to improve myocardial derangements in the hearts of rats. The data from this study is especially important as accelerated cell death has been implicated in left ventricular dysfunction and the progression of DCM. Therefore, the ability of RA3 to attenuate this effect is suggestive of its cardioprotective potential.

CHAPTER SIX

CONCLUSION

The association between DM and heart failure is a well-recognized global epidemic which has been linked with the development of DCM. Because of the nebulous nature of DCM, the disease is only diagnosed in confirmed diabetic cases when overt heart failure (HF) symptoms manifest (León *et al.*, 2016). Furthermore, there are currently no biomarkers available for early detection or treatment specific for DCM. Adding to the disease burden, current drugs on the pharmaceutical market treat the primary condition and have limited efficacy to protect the diabetic heart. Thus, in an effort to combat the growing burden of DCM our group has engaged in extensive research, involving *in vitro* and *in vivo* models, to further elucidate the pathophysiology of diabetes and its associated cardiovascular complications through the use of natural products. In the present study, we aimed to establish the prospective use of RA3 to attenuate diabetes-induced cardiac dysfunction in an *in vitro* H9c2 cell culture model.

To the best of our knowledge, this is the first study that investigated whether RA3, a lanosteryl triterpene, could alleviate diabetic cardiomyopathy. In our laboratory we previously demonstrated that RA3 has anti-hyperglycemic (Mosa *et al.*, 2015), anti-hyperlipidemic (Machaba *et al.*, 2014) and potentially cardioprotective (Mosa *et al.*, 2016) in an *in vivo* model. Similarly, in the present study we accentuated the anti-diabetic potential and cardioprotective properties exhibited by RA3 in a high glucose stress-induced *in vitro* model. These observations were attributed to the ability of RA3 to inhibit the shift in substrate preference in the H9c2 cardiomyoblasts when compared to a first-line antidiabetic drug, metformin. Furthermore, we demonstrated a synergistic inhibition of hyperglycemia-induced cardiac dysfunction with the combinatory treatment of MET+RA3. Subsequently, we postulated a mechanism by which RA3 protects the diabetic myocardium against hyperglycemia-induced oxidative stress and accelerated cardiac apoptosis (Figure 6.1).

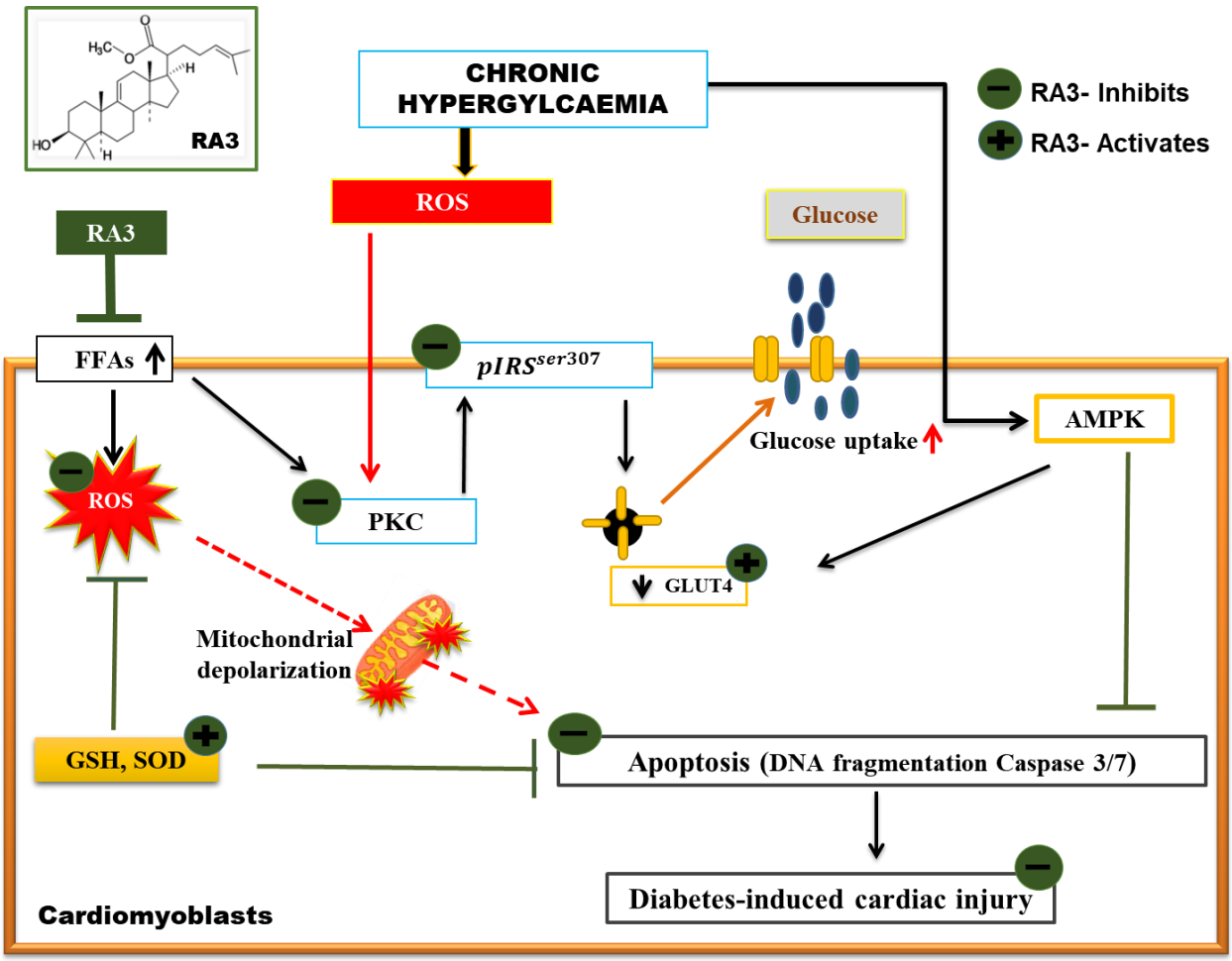

Figure 6.1: Methyl-3β-hydroxylanosta-9,24-dien-21-oate (RA3) protects the diabetic heart against high glucose-induced cardiac dysfunction. Cardiomyoblasts exposed **to h**igh glucose displayed increased levels of lipid content, oxidative stress, lipid peroxidation, mitochondrial depolarization and cardiac apoptosis. Concomitantly, metabolic activity, glucose uptake and insulin signaling were impaired through the activation of protein kinase C **(PKC)** and serine phosphorylated insulin receptor substrate-1 (307) **(IRS-1^{Ser307}).** However, RA3 was able to attenuate these effects by significantly reducing lipid storage while concurrently improving glucose uptake, cellular metabolic activity and insulin sensitivity through the expression of protein kinase B **(Akt)** and glucose transporter 4 **(GLUT4)**. Moreover, RA3 decreased the production of reactive oxygen species and lipid peroxidation by ameliorating the levels of endogenous glutathione content **(GSH)** and superoxide dismutase **(SOD)**. Subsequently, RA3 attenuated myocardial apoptosis by decreasing caspase 3/7 activity and improving mitochondrial potential, thereby preventing hyperglycemia-induced cardiac dysfunction.

RA3 attenuates hyperglycemia-induced oxidative damage: Data from this study provided conclusive evidence that RA3 is able to directly scavenge superoxide radicals through the activation of GSH and SOD. The resultant reduction of oxidative stress diminished the ability of ROS to facilitate lipid peroxidation thereby protecting the cardiac from oxidative damage (Figure 6.1).

RA3 ameliorates insulin signaling: The present study provided conclusive evidence that shift in substrate metabolism impairs the insulin signaling pathway through PKC mediated phosphorylation of IRS-1^{Ser307}. However, we demonstrated the ability of RA3 to ameliorate this effect through the activation of the PI3k/Akt pathway and AMPK-induced expression of GLUT4 (Figure 6.1). This suggests that RA3-mediated insulin signaling could play a significant role in cardioprotection.

RA3 attenuates hyperglycemia-induced apoptosis: Elevated levels of ROS production have been associated with depolarized mitochondria leading to the subsequent release of Cyt c which facilitates apoptosis through the activation of caspase 3/7. Data from this study presented convincing evidence of the capability of RA3 to ameliorate mitochondrial membrane potential thereby regulating apoptosis and preventing DNA fragmentation, a hallmark of cell death, in the cardiomyoblasts (Figure 6.1).

In conclusion, the findings from this study offer plausible validation that RA3 was able to attenuate high glucose-induced oxidative stress, lipid peroxidation, mitochondrial depolarization, DNA damage and subsequent myocardial apoptosis in H9c2 cardiomyoblasts. Furthermore, we presented novel insights on the enhanced efficacy of the combinatory use of metformin with RA3 in the treatment of diabetes-induced cardiomyopathy. Taken together, the data presented in this study provides a credible mechanism by which the combination treatment of MET+RA3 could protect the diabetic heart from developing cardiomyopathy.

Shortcomings of this study:

- Due to time and budget constraints, we were unable to conduct gene expression studies to further support our biochemical observations on oxidative stress and apoptosis. However, protein expression studies, performed in this study, provided conclusive data on the regulation of ROS, insulin signaling and apoptosis.

Future studies will include

- Evaluating gene expression to confirm the mechanism of RA3 on apoptosis.
- Investigating the protective effect of RA3 high glucose-induced cardiac dysfunction in an *in vivo* model.
- Preventative treatment: H9c2 cardiomyoblasts will be treated with RA3 prior to high glucose exposure.

REFERENCES

REFERENCES

Adrian, L., Lenski, M., Todter, K., Hereen, J., Bohm, M., Laufs, U. (2017) 'AMPK Prevents Palmitic Acid- Induced Apoptosis and Lipid Accumulation in Cardiomyocytes', *Lipids*. Springer Berlin Heidelberg, 52(9), pp. 737–750. doi: 10.1007/s11745-017-4285-7.

AGHDR (2016) 'Australian Genetic Heart Disease Registry Information Sheet Hypertrophic Cardiomyopathy (HCM)'. Available at: www.heartregistry.org.au (Accessed: 8 December 2017).

Ansley, D. M. and Wang, B. (2013) 'Oxidative stress and myocardial injury in the diabetic heart', *The Journal of pathology*, 229(2), pp. 232–41. doi: 10.1002/path.4113.

Ares-Carrasco, S., Picatoste, B., Benito-Martı, A., Zubiri, I., Sanz, A.B., Sanchez-Nin,o M.D, Ortiz, A., Egido, J., Tunn, J. and Lorenzo*, O.,* (2009) 'Myocardial fibrosis and apoptosis, but not inflammation, are present in long-term experimental diabetes.', *American journal of physiology. Heart and circulatory physiology*. American Physiological Society, 297(6), pp. H2109-19. doi: 10.1152/ajpheart.00157.2009.

Bagul, P. K., Deepthia, N., Sultanaa, R. and Banerjee, S.K. (2015) 'Resveratrol ameliorates cardiac oxidative stress in diabetes through deacetylation of NFkB-p65 and histone 3', *Journal of Nutritional Biochemistry*. Elsevier Inc., 26(11), pp. 1298–1307. doi: 10.1016/j.jnutbio.2015.06.006.

Balfour, P. C., Rodriguez, C. J. and Ferdinand, K. C. (2014) 'Blood Pressure and Cardiovascular Effects of New and Emerging Antidiabetic Agents', *Current Hypertension Reports*. Springer US, 16(8), p. 455. doi: 10.1007/s11906-014-0455-7.

Battiprolu, P. K.,. Lopez-Crisosto C., Zhao, V., Wang, Z., Nemchenko, A., Lavandero, S. and Hill, J.A. (2013) 'Diabetic cardiomyopathy and metabolic remodeling of the heart', *Life Sciences*. Elsevier B.V., 92(11), pp. 609–615. doi: 10.1016/j.lfs.2012.10.011.

Bayeva, M., Sawicki, K. T. and Ardehali, H. (2013) 'Taking Diabetes to Heart-Deregulation of Myocardial Lipid Metabolism in Diabetic Cardiomyopathy', *Journal of the American Heart Association*, 2(6), pp. e000433–e000433. doi:

10.1161/JAHA.113.000433.

Bhatt, N. M., Aon, M.A., Tocchetti, C.G., Shen, X., Dey, S., Ramirez-Correa, G., Rourke, B.O., Gao, W.D., and Sonia Cortassa, S. (2014) 'Restoring redox balance enhances contractility in heart trabeculae from type 2 diabetic rats exposed to high glucose'. Available at: http://ajpheart.physiology.org/content/ajpheart/308/4/H291.full.pdf (Accessed: 1 December 2017).

Braccini, L., Aon, M.A., Tocchetti, C.G., Shen, X., Dey, S., Ramirez-Correa, G., Rourke, B.O., Gao, W.D., and Cortassa, S. (2015) 'PI3K-C2γ 3 is a Rab5 effector selectively controlling endosomal Akt2 activation downstream of insulin signaling', *Nature Communications*. Nature Publishing Group, 6(May), pp. 1–15. doi: 10.1038/ncomms8400.

Bugger, H. and Dale Abel, E. (2014) 'Molecular mechanisms of diabetic cardiomyopathy'. doi: 10.1007/s00125-014-3171-6.

Cai, L., Li, W., Wang, G., Guo, L., Jiang, Y.,1 and Kang, Y.J. (2002) 'Hyperglycemiainduced apoptosis in mouse myocardium: mitochondrial cytochrome e-mediated caspase-3 activation pathwayNo Title', *Diabetes*, 51(June), pp. 1938–1948. doi: 10.2337/diabetes.51.6.1938.

Cardona, M., López, J. A., Serafín, A., Rongvaux, A., Inserte, J., García-Dorado, D., Flavell, R., Llovera, M. and Cañas, X. (2015) 'Executioner caspase-3 and 7 deficiency reduces myocyte number in the developing mouse heart', *PLoS ONE*, 10(6), pp. 1–21. doi: 10.1371/journal.pone.0131411.

Chait, A. and Bornfeldt, K. E. (2009) 'Diabetes and atherosclerosis: is there a role for hyperglycemia?', *Journal of Lipid Research*, 50(Supplement), pp. S335–S339. doi: 10.1194/jlr.R800059-JLR200.

Chen, L. and Knowlton, A. A. (2010) 'Mitochondria and heart failure: New insights into an energetic problem', *Minerva Cardioangiologica*, 58(2), pp. 213–229. doi: R05102998 [pii].

Chen, N. *et al.* (2014) 'Concerted Cyclization of Lanosterol C-Ring and D-Ring Under

Human Oxidosqualene Cyclase Catalysis: An ab Initio QM/MM MD Study', *Journal of Chemical Theory and Computation*. American Chemical Society, 10(3), pp. 1109–1120. doi: 10.1021/ct400949b.

Cheng, Y., Sheen, J. and Hu, W. (2017) 'Review Article Polyphenols and Oxidative Stress in Atherosclerosis-Related Ischemic Heart Disease and Stroke', 2017.

Dandamudi, S., Slusser, J., Mahoney, D.W., Redfield, M.M., Rodeheffer, R.J., and Chen,H.H. (2014) 'The prevalence of diabetic cardiomyopathy: a population-based study in Olmsted County, Minnesota.', *Journal of cardiac failure*. NIH Public Access, 20(5), pp. 304–9. doi: 10.1016/j.cardfail.2014.02.007.

Dei Cas, A., Fonarow, G.C., Gheorghiade, M., and Butler, J. (2015) 'Concomitant Diabetes Mellitus and Heart Failure', *Current Problems in Cardiology*. Mosby, 40(1), pp. 7–43. doi: 10.1016/j.cpcardiol.2014.09.002.

Dhar, A., Dhar, I., Bhat, A., Desai, K.M. (2016) 'Alagebrium attenuates methylglyoxal induced oxidative stress and AGE formation in H9C2 cardiac myocytes', *Life Sciences*. Elsevier Inc., 146, pp. 8–14. doi: 10.1016/j.lfs.2016.01.006.

Dludla, P.V., Muller, C.J.F., Joubert, E., Louw, J., Essop, M.F., Gabuza, K.B., Ghoor, S., Huisamen, B., and Rabia Johnson, R. (2017) 'Aspalathin Protects the Heart against Hyperglycemia-Induced Oxidative Damage by Up-Regulating Nrf2 Expression', *Molecules*. Multidisciplinary Digital Publishing Institute, 22(1), p. 129. doi: 10.3390/molecules22010129.

Dludla, P. V., Joubert, E., Muller, C.J.F., Louw, J., and Johnson, R. (2017) 'Hyperglycemia-induced oxidative stress and heart disease-cardioprotective effects of rooibos flavonoids and phenylpyruvic acid-2-O-β-D-glucoside', *Nutrition & Metabolism*. Nutrition & Metabolism, 14(1), p. 45. doi: 10.1186/s12986-017-0200-8.

Duarte, F. V., Amorim, J.A., and Palmeira, C.M. (2013) 'Regulation of Mitochondrial

Function and its Impact in Metabolic Stress'. Bentham Science Publishers. Available at: http://www.ingentaconnect.com/content/ben/cmc/2015/00000022/00000020/art00007 (Accessed: 8 December 2017).

Durpès, M. C., Morin, C., Paquin-Veillet, J., Beland, R.I., Pare, M., Marie-Odile Guimond, M., Rekhter, M., King, G.L., and Geraldes, P. (2015) 'PKC-β activation inhibits IL-18binding protein causing endothelial dysfunction and diabetic atherosclerosis', *Cardiovascular Research*, 106(2), pp. 303–313. doi: 10.1093/cvr/cvv107.

El Enshasy, H., Elsayed, E.A., Wadaan, R. and Mohamad A (2013) 'Mushrooms and truffles: historical biofactories for complementary medicine in Africa and in the middle East', *Evidence-based complementary and alternative medicine : eCAM*. Hindawi, 2013, p. 620451. doi: 10.1155/2013/620451.

Erdmann, E. (2009) 'Safety and tolerability of beta-blockers: Prejudices and reality', *European Heart Journal, Supplement*, 11(A), pp. 21–25. doi: 10.1093/eurheartj/sup001.

Esser, N., Legrand-Poels, S., Piette, J., Scheen, A.J., and Paquot, N. (2014) 'Inflammation as a link between obesity, metabolic syndrome and type 2 diabetes', *Diabetes Research and Clinical Practice*, 105, pp. 141–150. doi: 10.1016/j.diabres.2014.04.006.

Evans, J. L., Goldfine, I.D., Maddux, B.A., and Grodsky, G.M. (2002) 'Oxidative Stress and Stress-Activated Signaling Pathways: A Unifying Hypothesis of Type 2 Diabetes'. doi: 10.1210/er.2001-0039.

Faria, A. and Persaud, S. J. (2017) 'Cardiac oxidative stress in diabetes: Mechanisms and therapeutic potential', *Pharmacology and Therapeutics*. Elsevier Inc., 172, pp. 50–62. doi: 10.1016/j.pharmthera.2016.11.013.

Ferrannini, E., Muscelli, E., Frascerra, S., Baldi, S., Mari, A., Heise, T., Broedl, U. C. and Woerle, H.J. (2014) 'Metabolic response to sodium-glucose cotransporter 2 inhibition in type 2 diabetic patients.' *The Journal of clinical investigation*. American Society for Clinical Investigation, 124(2), pp. 499–508. doi: 10.1172/JCI72227.

Ferrannini, E. and DeFronzo, R. A. (2015) ‘Impact of glucose-lowering drugs on cardiovascular disease in type 2 diabetes’, *European Heart Journal*. Oxford University Press, 36(34), pp. 2288–2296. doi: 10.1093/eurheartj/ehv239.

Ferrannini, E., Mark, M. and Mayoux, E. (2016) ‘CV protection in the EMPA-REG OUTCOME trial: A thrifty substrate hypothesis.’ *Diabetes Care*, 39(7), pp. 1108–1114. doi: 10.2337/dc16-0330.

Forbes, J. M. and Cooper, M. E. (2013) ‘Mechanisms of Diabetic Complications’, *Physiological Reviews*, 93(1), pp. 137–188. doi: 10.1152/physrev.00045.2011.

Fotbolcu, H., Yakar, T., Duman, D., Tansu Karaahmet, T., Kursat Tigen, K., Cevik, C., Kurtoglu, U., and Dindar, I. (2010) ‘Impairment of the left ventricular systolic and diastolic function in patients with non-alcoholic fatty liver disease’, *Cardiol J*, 17(5), p. 457–63 ST–Impairment of the left ventricular sy.

Fox, C. S., Golden, S.H, Anderson C., Bray, G.A., Burke, L.E., de Boer, I.H., Deedwania, P., Eckel, R.H., Ershow, A.G., Fradkin J. and Inzucchi, S.E. (2015) ‘Update on Prevention of Cardiovascular Disease in Adults with Type 2 Diabetes Mellitus in Light of Recent Evidence: A Scientific Statement from the American Heart Association and the American Diabetes Association’. *Diabetes care*. American Diabetes Association, 38(9), pp. 1777–803. doi: 10.2337/dci15-0012.

Freire, C. M. and Moura, A. L. (2007) ‘Left Ventricle Diastolic Dysfunction in Diabetes : an Update’, *Arq Bras Endocrinol Metab*, 51(2), pp. 168–175. doi: S00042730200700020005 [pii].

Fueger, P. T., Li, C., and Ayala, J. (2007) ‘Glucose kinetics and exercise tolerance in mice lacking the GLUT4 glucose transporter’, *The Journal of Physiology*. Blackwell Publishing Ltd, 582(2), pp. 801–812. doi: 10.1113/jphysiol.2007.132902.

García-Compeán, D., González-González, J.A., Lavalle-González, F.J., GonzálezMoreno, E.I., Maldonado-Garza, H.J., and Jesús Z. Villarreal-Pérez, J.Z. (2015) ‘The treatment of diabetes mellitus of patients with chronic liver disease’, 14(6), pp. 780–788. doi: 10.5604/16652681.1171746.

Gawli, K. and Lakshmidevi, N. (2015) ‘Antidiabetic and antioxidant potency evaluation of different fractions obtained from Cucumis prophetarum fruit’, *Pharmaceutical Biology*, 53(5), pp. 689–694. doi: 10.3109/13880209.2014.937503.

Gersh, B. J., Sliwa, K., Mayosi, B.M., and Yusuf, S. (2010) ‘Novel therapeutic concepts: The epidemic of cardiovascular disease in the developing world: global implications’, *European Heart Journal*. Oxford University Press, 31(6), pp. 642–648. doi: 10.1093/eurheartj/ehq030.

Giacco, F. (2011) ‘Oxidative stress and diabetic complications’, *Circ Res*, 107(9), pp. 1058–1070. doi: 10.1161/CIRCRESAHA.110.223545.Oxidative.

Goldberg, I. J., Eckel, R. H. and Abumrad, N. A. (no date) ‘Regulation of fatty acid uptake into tissues: lipoprotein lipase-and CD36-mediated pathways’. doi: 10.1194/jlr.R800085JLR200.

Goldstein, J. C., Munoz-Pinedo, C., Ricci, J.E., Adams, S.R., Kelekar, A., M Schuler, M. Tsien, R.Y., and Green, D.R. (2005) ‘Cytochrome c is released in a single step during apoptosis’, *Cell Death and Differentiation*, 12(5), pp. 453–462. doi: 10.1038/sj.cdd.4401596.

Gonzalez-Burgos, E. and Gomez-Serranillos, M. P. (2012) ‘Terpene Compounds in Nature: A Review of Their Potential Antioxidant Activity’, *Current Medicinal Chemistry*, 19(31), pp. 5319–5341. doi: 10.2174/092986712803833335.

Gottlieb, E., Armour, S.M., Harris, M.H., and CB Thompson (2003) ‘Mitochondrial membrane potential regulates matrix configuration and cytochrome c release during apoptosis’, *Cell Death and Differentiation*, 10(6), pp. 709–717. doi: 10.1038/sj.cdd.4401231.

Graveline, D. (2015) ‘Adverse Effects of Statin Drugs : a Physician Patient’s Perspective’, *Journal of American Physicians and Surgeons*, 20(1), pp. 7–11. Available at: http://www.jpands.org/vol20no1/graveline.pdf.

Green, J. B., Bethel, J.B, Armstrong, M.A., Buse, P.W., Engel, J.B., Garg, S.S., Josse, J., Kaufman, R., Doglin, K., Joerg Korn, J., Lachin, S., McGuire, J.M., Pencina, D.K., and Standl, M.J. (2015) 'Effect of Sitagliptin on Cardiovascular Outcomes in Type 2 Diabetes', *New England Journal of Medicine*. Massachusetts Medical Society, 373(3), pp. 232–242. doi: 10.1056/NEJMoa1501352.

Hamid, K., Alqahtani, A., Kim, M., Cho, J., Cui, P., Li, C., Paul W., and Li, G.Q. (2015) 'Tetracyclic triterpenoids in herbal medicines and their activities in diabetes and its complications Tetracyclic Triterpenoids in Herbal Medicines and their Activities in Diabetes and its Complications'. Bentham Science Publishers, (August). Available at: http://www.ingentaconnect.com/content/ben/ctmc/2015/00000015/00000023/art00007 (Accessed: 10 December 2017).

Hansson, G. K. (2005) 'Inflammation, Atherosclerosis, and Coronary Artery Disease', *n engl j med*, 35216(21). Available at: http://www.nejm.org/doi/pdf/10.1056/NEJMra043430 (Accessed: 30 May 2017).

Heidrich, F., Schotola, H., Popov, A.F., Sohns, C., Schuenemann, J., Friedrich, M. Coskun, K.O., von Lewinski, D., Hinz, J., Bauer, M., Mokashi, S.A., Sossalla, S., and Schmitto, J.D. (2010) 'AMPK - Activated Protein Kinase and its Role in Energy Metabolism of the Heart', *Current Cardiology Reviews*, 6, pp. 337–342. doi: 10.2174/157340310793566073.

International Diabetes Federation Diabetes Atlas. Eight edition (2017).

Inzucchi, S. E., Kasia J.M., Hele, B., Clifford J., and McGuire, D.K. and (2014) 'Metformin in Patients with Type 2 Diabetes and Kidney Disease', *JAMA*. American Medical Association, 312(24), p. 2668. doi: 10.1001/jama.2014.15298.

Jia, G., Whaley-Connell, A., and Sowers, J. R. (2017) 'Diabetic cardiomyopathy: a hyperglycemia- and insulin-resistance-induced heart disease', *Diabetologia*. Diabetologia, pp. 1–8. doi: 10.1007/s00125-017-4390-4.

Johnson, R., Dludla, P.V., Joubert, E., February, F., Mazibuko, S., Ghoor, S., Muller,

C.J.F., and Louw, J. (2016) 'Aspalathin, a dihydrochalcone C-glucoside, protects H9c2 cardiomyocytes against high glucose induced shifts in substrate preference and apoptosis', *Molecular Nutrition and Food Research*, 60(4), pp. 922–934. doi: 10.1002/mnfr.201500656.

Johnson, R., Dludla, P.V.D, Christo, C.J.F, Huisamen, B., Essop, M., and Louw, J. (2017) 'The Transcription Profile Unveils the Cardioprotective Effect of Aspalathin against Lipid Toxicity in an In Vitro H9c2 Model', *Molecules*. Multidisciplinary Digital Publishing Institute, 22(2), p. 219. doi: 10.3390/molecules22020219.

Joubert, E. and de Beer, D. (2011) 'Rooibos (Aspalathus linearis) beyond the farm gate: From herbal tea to potential phytopharmaceutical', *South African Journal of Botany*. Elsevier, 77(4), pp. 869–886. doi: 10.1016/J.SAJB.2011.07.004.

Kayama, Y., Raaz, U., Jagger, A., Adam, M., Schellinger, I.N., Sakamoto, M., Hirofumi Suzuki, H., Toyama, K., Spin, J.M., and Tsao, P.S. (2015) 'Diabetic Cardiovascular Disease Induced by Oxidative Stress', *Int. J. Mol. Sci*, 16, pp. 25234–25263. doi: 10.3390/ijms161025234.

Khathi, A., Serumula, M.R., Myburg, R.B., Van Heerden, F.R., and Musabayane, C.T. (2013). 'Effects of Syzygium aromaticum-Derived Triterpenes on Postprandial Blood Glucose in Streptozotocin-Induced Diabetic Rats Following Carbohydrate Challenge', *PLoS ONE*, 8(11). doi: 10.1371/.

Khavandi, K., Khavandi, A., Asghar, O., Greenstein, A., Withers, S., Heagerty, A.M., and Malik, R.A. (2009) 'Diabetic cardiomyopathy – a distinct disease'. *Best Practice & Research Clinical Endocrinology & Metabolism*, 23, pp. 347–360. doi: 10.1016/j.beem.2008.10.016.

Khavjou, O., Phelps, D. and Leib, A. (2016) 'Projections of Cardiovascular Disease Prevalence and Costs: 2015-2035', (214680), pp. 1–54.

Kiencke, S., Handschin, R., von Dahlen, R., Muser, J., Peter Brunner-LaRocca, H., Schumann, J., Barbara Felix, B., Berneis, K., and Rickenbacher, P. (2010) 'Pre-clinical diabetic cardiomyopathy: Prevalence, screening, and outcome', *European Journal of Heart Failure*, 12(9), pp. 951–957. doi: 10.1093/eurjhf/hfq110.

Kim, N. H. and Kang, P. M. (2010) 'Apoptosis in cardiovascular diseases: Mechanism and clinical implications', *Korean Circulation Journal*, 40(7), pp. 299–305. doi: 10.4070/kcj.2010.40.7.299.

Kim, W. H., Lee, J.W., Suh, Y.H., Lee, H.J., Lee, S.H., Oh, Y.K., Gao, B., and Jung, M.H. (2007) 'AICAR potentiates ROS production induced by chronic high glucose: Roles of AMPK in pancreatic β-cell apoptosis', *Cellular Signaling*, 19(4), pp. 791–805. doi: 10.1016/j.cellsig.2006.10.004.

Kitazumi, I. and Tsukahara, M. (2011) 'Regulation of DNA fragmentation: The role of caspases and phosphorylation', *FEBS Journal*, 278(3), pp. 427–441. doi: 10.1111/j.17424658.2010.07975.x.

Komatsu, M., Takei, M., Ishii, H., and Yoshihiko Sato, Y. (2013) 'Glucose-stimulated insulin secretion: A newer perspective', *Journal of Diabetes Investigation*, 4(6), pp. 511–516. doi: 10.1111/jdi.12094.

Kowaltowski, A. J., de Souza-Pinto, N.C., Castilho, R.F., and Vercesi, A.E. (2009) 'Mitochondria and reactive oxygen species'. doi: 10.1016/j.freeradbiomed.2009.05.004.

Lawson, K. (2017) *Botanical and Plant-derived Drugs: Global Markets: BIO022H | BCC Research*. Available at: https://www.bccresearch.com/market-research/biotechnology/botanical-and-plant-derived-drugs-global-markets-bio022h.html (Accessed: 10 December 2017).

Leon, B. M. (2015) 'Diabetes and cardiovascular disease: Epidemiology, biological mechanisms, treatment recommendations and future research', *World Journal of Diabetes*, 6(13), p. 1246. doi: 10.4239/wjd.v6.i13.1246.

León, L. E., and Maddox, T.M. (2016) 'Subclinical Detection of Diabetic Cardiomyopathy with MicroRNAs: Challenges and Perspectives', *Journal of Diabetes Research*, 2016, pp. 1–12. doi: 10.1155/2016/6143129.

Li, H., Wang, X., Mao, Y., Hu, R., Xu, W., Lei, Z., Zhou, N., Jin, L., Guo, T., Li, Z., Irwin,

D.M., Niu, G., and Tan, H. (2014) ‘Long term liver specific glucokinase gene defect induced diabetic cardiomyopathy by up regulating NADPH oxidase and down regulating insulin receptor and p-AMPK’, *Cardiovascular Diabetology*, 13, p. 24. doi: 10.1186/1475-284013-24.

Liu, Q., Wang, S. and Cai, L. (2014) ‘Diabetic cardiomyopathy and its mechanisms: Role of oxidative stress and damage’, *Journal of Diabetes Investigation*, 5(6), pp. 623–634. doi: 10.1111/jdi.12250.

Long, Y. C. and Zierath, J. R. (2006) ‘Review series AMP-activated protein kinase signaling in metabolic regulation’, *The Journal of Clinical Investigation*, 116(7), pp. 1776–1783. doi: 10.1172/JCI29044.1776.

Loor, G. and Schumacker, P. T. (2008) ‘Role of hypoxia-inducible factor in cell survival during myocardial ischemia-reperfusion’, *Cell Death and Differentiation*, 15(4), pp. 686–690. doi: 10.1038/cdd.2008.13.

Lopaschuk, G. D. *et al.* (2010) ‘Myocardial fatty acid metabolism in health and disease’, *Physiol Rev.*, 90(1522–1210 (Electronic)), pp. 207–258. doi: 10.1152/physrev.00015.2009.

Lorenzo, O., Ramírez, E., Picatoste, B., Egido, J., and Tuñón, J. (2013) ‘Alteration of energy substrates and ROS production in diabetic cardiomyopathy’, *Mediators of Inflammation*, 2013. doi: 10.1155/2013/461967.

Low Wang, C. C., Hess, C.N., Hiatt, W.R.; Allison B., and Goldfin, A.B. (2016) ‘Clinical update: Cardiovascular disease in diabetes mellitus’, *Circulation*, 133(24), pp. 2459–2502. doi: 10.1161/CIRCULATIONAHA.116.022194.

Lozano-Mena, G., Sánchez-González, M., Juan, M. E., and Planas, J.M. (2014) ‘Maslinic acid, a natural phytoalexin-type triterpene from olives - A promising nutraceutical’, *Molecules*, 19(8), pp. 11538–11559. doi: 10.3390/molecules190811538.

Mabhida, S. E., Mosa, R.A., Dambudzo, P., Osunsanmi, F.O., Dludla, P.V., Djarova, T.G., and Opoku, A.R. (2017) ‘A lanosteryl triterpene from protorhus longifolia improves

glucose tolerance and pancreatic beta cell ultrastructure in type 2 diabetic rats', *Molecules*, 22(8), pp. 1–11. doi: 10.3390/molecules22081252.

Machaba, K. E., Cobongela, S.Z., Rebamang A Mosa, R.A., Lawal A Oladipupo, L.A., Djarova, T.G., and Opoku, A.R. (2014) 'In vivo anti-hyperlipidemic activity of the triterpene from the stem bark of Protorhus longifolia (Benrh) Engl', *Lipids in Health and Disease*, 13(1), p. 131. doi: 10.1186/1476-511X-13-131.

Mannucci, E., Dicembrini, I., Lauria, A., and Pozzilli, P. (2013) 'Is glucose control important for prevention of cardiovascular disease in diabetes' *Diabetes care*. American Diabetes Association, 36 Suppl 2(Suppl 2), pp. S259-63. doi: 10.2337/dcS13-2018.

Marica Bakovic, N. H. (2015) 'Biologically Active Triterpenoids and Their Cardioprotective and Anti- Inflammatory Effects', *Journal of Bioanalysis & Biomedicine*, 1(s12). doi:

10.4172/1948-593X.S12-005.

May, M. and Schindler, C. (2016) 'Clinically and pharmacologically relevant interactions of antidiabetic drugs', *Therapeutic Advances in Endocrinology and Metabolism*, 7(2), pp. 69–83. doi: 10.1177/2042018816638050.

Mazibuko, S. E. *et al.* (2013) 'Amelioration of palmitate-induced insulin resistance in C2C12 muscle cells by rooibos (Aspalathus linearis)', *Phytomedicine*, 20. doi: 10.1016/j.phymed.2013.03.018.

Mazibuko, S. E., Muller, C.J.F., Joubert, E., De Beer, D., Johnson, R., Opoku, A.R., and Louw, J. (2015) 'Aspalathin improves glucose and lipid metabolism in 3T3-L1 adipocytes exposed to palmitate', *Molecular Nutrition & Food Research*, 59(11), pp. 2199–2208. doi: 10.1002/mnfr.201500258.

Menard, S. L., Croteau, E., Sarrhini, O., Gelinas, R., Brassard, P., Ouellet, R., Bentourkia, M., van Lier, J. E., Rosiers, C. D., Lecomte, R., and Carpentier, A. C. (2010) 'Abnormal in vivo myocardial energy substrate uptake in diet-induced type 2 diabetic cardiomyopathy in rats', *AJP: Endocrinology and Metabolism*, 298(5), pp. E1049–E1057. doi: 10.1152/ajpendo.00560.2009.

Miki, T., Yuda, S., Kouzu, H., and Miura, T. (2013) 'Diabetic cardiomyopathy: Pathophysiology and clinical features', *Heart Failure Reviews*, 18(2), pp. 149–166. doi: 10.1007/s10741-012-9313-3.

Mizuno, Y., Harada, E., Nakagawa, H., Morikawa, Y., Shono, M., Kugimiya, F., Yoshimura, M., and Yasue, H. (2017) 'The diabetic heart utilizes ketone bodies as an energy source', *Metabolism*, pp. 65–72. doi: 10.1016/j.metabol.2017.08.005.

Montessuit, C. and Lerch, R. (2013) 'Regulation and dysregulation of glucose transport in cardiomyocytes', *Biochimica et Biophysica Acta - Molecular Cell Research*, pp. 848– 856. doi: 10.1016/j.bbamcr.2012.08.009.

Mosa, R. A., Lazarus, G.G., Gwala, P.E., Oyedeji, A.O., and Opoku, A.R. (2011) 'In Vitro Anti-platelet Aggregation , Antioxidant and Cytotoxic Activity of Extracts of Some Zulu Medicinal Plants', *Journal of Natural Products*, 4, pp. 136–146.

Mosa, R. A., Oyedeji, A.O., Shode, F.O., Singh, M. and Opoku, A.R. (2011) 'Triterpenes from the stem bark of Protorhus longifolia exhibit anti-platelet aggregation activity', *African Journal of Pharmacy and Pharmacology*, 5(24), pp. 2698–2714. doi: 10.5897/AJPP11.534.

Mosa, R. A., Naidoo, J.J., Nkomo, F.S., Mazibuko, S.E., Muller, C.J.F., and Andy R. Opoku, A.R. (2014) 'In vitro antihyperlipidemic potential of triterpenes from stem bark of Protorhus longifolia', *Planta Medica*, 80(18), pp. 1685–1691. doi: 10.1055/s-00341383262.

Mosa, R. A., Cele, N.D., Mabhida, S.E., Shabalala, S.C., Penduka, D., and Andy R. Opoku, A.R. (2015) 'In vivo antihyperglycemic activity of a lanosteryl triterpene from Protorhus longifolia', *Molecules*, 20(7), pp. 13374–13383. doi: 10.3390/molecules200713374.

Mosa, R. A., Hlophe, N.B., Ngema, N.T., Penduka, D., Lawal, O.A., and Andy R. Opoku, A.R. (2016) 'Cardioprotective potential of a lanosteryl triterpene from Protorhus longifolia', *Pharmaceutical Biology*, 54(12), pp. 3244–3248. doi: 10.1080/13880209.2016.1223144.

Naito, R. and Kasai, T. (2015) 'Coronary artery disease in type 2 diabetes mellitus: Recent treatment strategies and future perspectives', *World J Cardiol March World J Cardiol*, 26(73), pp. 119–124. doi: 10.4330/wjc.v7.i3.119.

Napolitano, J.G., Gödecke, T., Lankin, D.C., Jaki, B.U., McAlpine, J.B., Chen, S., and Pauli, G.F. (2014) 'Orthogonal analytical methods for botanical standardization: Determination of green tea catechins by qNMR and LC–MS/MS', *Journal of Pharmaceutical and Biomedical Analysis*. Elsevier, 93, pp. 59–67. doi: 10.1016/J.JPBA.2013.06.017.

Neri, M., Fineschi, V., Di Paolo, M., Pomara, C., Riezzo, I., Turillazzi, E., and Cerretani, D. (2015) 'Cardiac Oxidative Stress and Inflammatory Cytokines Response after Myocardial Infarction'. Bentham Science Publishers. Available at: http://www.ingentaconnect.com/content/ben/cvp/2015/00000013/00000001/art00007 (Accessed: 8 December 2017).

Penduka, D., Gasa, N.P., Hlongwane,M.S., Mosa, R.A., Osunsanmi, F.O., and Opoku, A.R. (2015) 'The antibacterial activities of some plant-derived triterpenes', *African Journal of Traditional, Complementary and Alternative Medicines*, 12(6), pp. 180–188. doi: 10.4314/ajtcam.v12i6.19.

Peng, C., Ma, J., Gao, X., Tian, P., Li, W., and Zhang, L. (2013) 'High glucose induced oxidative stress and apoptosis in cardiac microvascular endothelial cells are regulated by FoxO3a', *PLoS ONE*, 8(11). doi: 10.1371/journal.pone.0079739.

Pergola, P. E., Raskin, P., Toto, R.D., Meyer, C. J., Huff, J.W., Grossman, E.B., Krauth, M., Ruiz, S., Audhya, P., Christ-Schmidt, H., Wittes, J., Warnock, D.G. (2011) 'Bardoxolone Methyl and Kidney Function in CKD with Type 2 Diabetes', *New England Journal of Medicine*. Massachusetts Medical Society, 365(4), pp. 327–336. doi: 10.1056/NEJMoa1105351.

Randle, P.J., Garland, P.B., Hales, C.N., and Newsholme, E.A. (1963) 'The glucose fattyacid cycle, its role in insulin sensitivity and the metabolic disturbances of diabetes

mellitus', *The Lancet*. Elsevier, 281(7285), pp. 785–789. doi: 10.1016/S01406736(63)91500-9.

Rijzewijk, L.J., van der Meer, R.W., Lamb, H.J., de Jong, H.W.A.M., Lubberink, M., Romijn, J.A., Bax, J.J., de Roos, A., Twisk, J.W., Heine, R.J., Lammertsma, A.A., Smit, J.W.A., and Diamant, M. (2009) 'Altered Myocardial Substrate Metabolism and Decreased Diastolic Function in Nonischemic Human Diabetic Cardiomyopathy', *Journal of the American College of Cardiology*. Elsevier Inc., 54(16), pp. 1524–1532. doi: 10.1016/j.jacc.2009.04.074.

Rodriguez-Rodriguez, R. (2015) 'Oleanolic Acid and Related Triterpenoids from Olives on Vascular Function: Molecular Mechanisms and Therapeutic Perspectives', *Current Medicinal Chemistry*. Bentham Science Publishers, 22(11), pp. 1414–1425. doi: 10.2174/0929867322666141212122921.

Rojas, J., Arraiz, N., Aguirre, M.,Velasco, M., and Bermúdez, V. (2011) 'AMPK as target for intervention in childhood and adolescent obesity', *Journal of Obesity*, 2011. doi: 10.1155/2011/252817.

Rota, M., LeCapitaine, N., Hosoda, T., Boni, A., De Angelis, A., Padin-Iruegas, M.E., Esposito, G., Vitale, S., Urbanek, K., Casarsa, C., Giorgio, M., Luscher, Thomas F., Pelicci, P.G., Anversa, P., Leri, A., Kajstura, J. (2006) 'Diabetes promotes cardiac stem cell aging and heart failure, which are prevented by deletion of the p66shc gene', *Circulation Research*, 99(1), pp. 42–52. doi: 10.1161/01.RES.0000231289.63468.08.

Rubler, S., Dlugash, J., Yuceoglu, Y.Z., Kumral, T., Branwood, A.W., Grishman, A. (1972) 'New type of cardiomyopathy associated with diabetic glomerulosclerosis', *The American Journal of Cardiology*. Excerpta Medica, 30(6), pp. 595–602. doi: 10.1016/00029149(72)90595-4.

Sanchis-Gomar, F., Quilis, C.P., Leischik, R., and Alejandro Lucia, A. (2016). 'Epidemiology of coronary heart disease and acute coronary syndrome', *Annals of Translational Medicine*, 4(13), pp. 256–256. doi: 10.21037/atm.2016.06.33.

Sanderson, M., Mazibuko, S.E., Joubert, E., De Beer, D., Johnson, R., Pheiffer, C., Louw,

J., Muller, C.J.F. (2014) ‘Effects of fermented rooibos (Aspalathus linearis) on adipocyte differentiation’, *Phytomedicine*, 21. doi: 10.1016/j.phymed.2013.08.011.

Satta, S., Mahmoud, A.M., Wilkinson, F.L., Alexander, Y.M., White, S. J. (2017) ‘The Role of Nrf2 in Cardiovascular Function and Disease’, *Oxidative Medicine and Cellular Longevity*, 2017. doi: 10.1155/2017/9237263.

Schloms, L., Storbeck, K.H., Swart, P., Gelderblom, W.C.A., Swart, A.C. (2011) ‘The influence of Aspalathus linearis (Rooibos) and dihydrochalcones on adrenal steroidogenesis: Quantification of steroid intermediates and end products in H295R cells’, *Journal of Steroid Biochemistry and Molecular Biology*, 128, pp. 128–138. doi: 10.1016/j.jsbmb.2011.11.003.

Dludla, P.V., Joubert, E., Muller, C.J.F., Louw, J., and Johnson, R. (2016) ‘Nutrition & Metabolism The diabetic heart : role of oxidative stress and the cardioprotective potential of rooibos flavonoids and phenylpyruvic acid-2-O-β-D-glucoside the diabetic heart : role of oxidative stress and the cardioprotective’.

Sharma, K. and Kass, D. A. (2014) ‘Heart failure with preserved ejection fraction: Mechanisms, clinical features, and therapies’, *Circulation Research*, 115(1), pp. 79–96. doi: 10.1161/CIRCRESAHA.115.302922.

Srivastava, S., Lal, V. K. and Pant, K. K. (2012) ‘Polyherbal formulations based on Indian medicinal plants as antidiabetic phytotherapeutics’, *Diabetes*, 2(1), pp. 1–15.

Stanley, W. C., Recchia, F. A. and Lopaschuk, G. D. (no date) ‘Myocardial Substrate Metabolism in the Normal and Failing Heart’. Available at: http://physrev.physiology.org/content/physrev/85/3/1093.full.pdf (Accessed: 13 November 2017).

STATS SOUTH AFRICA (2017) *Media release: Mortality and causes of death, 2015* | *Statistics South Africa*. Available at: http://www.statssa.gov.za/?p=9604 (Accessed: 8 December 2017).

Stone, N.J., Robinson, J.G., Lichtenstein, A.H., Bairey Merz, C.N., Blum, C.B., Eckel,

R.H., Goldberg, A.C., Gordon, D., Levy, D., Lloyd-Jones, D.M., McBride, P., Schwartz, J.S., Shero, S.T., Smith, Sidney C., Watson, K., and Wilson, P.W.F. (2014). '2013 ACC/AHA guideline on the treatment of blood cholesterol to reduce atherosclerotic cardiovascular risk in adults: A report of the American college of cardiology/American heart association task force on practice guidelines', *Journal of the American College of Cardiology*, 63(25 PART B), pp. 2889–2934. doi: 10.1016/j.jacc.2013.11.002.

Street, R. A. and Prinsloo, G. (2013) 'Commercially Important Medicinal Plants of Zimbabwe: A Review', *Journal of Chemistry*, 2013(205048), pp. 1–16. doi: 10.1155/2013/205048.

Szwejkowski, B. R., Gandy, S.J., Rekhraj, S., Houston, J.G., Lang, C.C., Morris, A.D., George, J., Struthers, A.D. (2013) 'Allopurinol Reduces Left Ventricular Mass in Patients With Type 2 Diabetes and Left Ventricular Hypertrophy'. doi: 10.1016/j.jacc.2013.07.074.

Taegtmeyer, H., McNulty, P. and Young, M. E. (2002) 'Adaptation and maladaptation of the heart in diabetes: Part I: general concepts', *Circulation*. American Heart Association, Inc., 105(14), pp. 1727–33. doi: 10.1161/01.CIR.0000012466.50373.E8.

Tarquini, R., Lazzeri, C., Pala, L., Rotella, C.M., and Gensini, G.F. (2011) 'The diabetic cardiomyopathy', *Acta Diabetologica*, 48(3), pp. 173–181. doi: 10.1007/s00592-0100180-x.

Tendera, M., Fox, K., Ferrari, R., Ford, I., Greenlaw, N., Abergel, H., Macarie, C., Tardif, J., Vardas, P., Zamorano, J., and Steg, P.G. (2014) 'Inadequate heart rate control despite widespread use of beta-blockers in outpatients with stable CAD: findings from the international prospective CLARIFY registry, on behalf of the CLARIFY Registry Investigators', *International Journal of Cardiology*, 176, pp. 119–124. doi: 10.1016/j.ijcard.2014.06.052.

Tsai, C.Y., Wang, C.C., Lai, T.Y., Tsu, H.N., Wang, C.H., Liang, H.Y., and Kuo, W.W. (2013) 'Antioxidant effects of diallyl trisulfide on high glucose-induced apoptosis are mediated by the PI3K/Akt-dependent activation of Nrf2 in cardiomyocytes', *International*

Journal of Cardiology. Elsevier Ireland Ltd, 168(2), pp. 1286–1297. doi: 10.1016/j.ijcard.2012.12.004.

Unlu, A., Nayir, E., Kirca, O., and Ozdogan, M. (2016) 'Ganoderma Lucidum (Reishi Mushroom) and cancer', *Journal of B.U.ON. : official journal of the Balkan Union of Oncology*, 21(4), pp. 792–798. Available at: http://www.ncbi.nlm.nih.gov/pubmed/27685898 (Accessed: 10 December 2017).

Valen, G., Yan, Z. and Hansson, G. K. (2001) 'Nuclear Factor Kappa-B and the Heart'. doi: 10.1016/S0735-1097(01)01377-8.

Varga, Z. V., Giricz, Z., Liaudet, L., Haskó, G., Ferdinandy, P., and Pacher, P. (2015) 'Interplay of oxidative, nitrosative/nitrative stress, inflammation, cell death and autophagy in diabetic cardiomyopathy ☆', *BBA - Molecular Basis of Disease*, 1852, pp. 232–242. doi: 10.1016/j.bbadis.2014.06.030.

Velagaleti, R.S., Gona, P., Pencina, M.J., Aragam, J., Wang, T.J., Levy, D.D., Ralph B., Lee, D.S., Kannel, W.B., Benjamin, E.J. and Vasan, R.S., (2014) 'Left Ventricular Hypertrophy Patterns and Incidence of Heart Failure with Preserved Versus Reduced Ejection Fraction', *The American Journal of Cardiology*, 113, pp. 117–122. doi: 10.1016/j.amjcard.2013.09.028.

Velayutham, M., Pandey, D., Denicola, A., Xing, Y., Shang, H., Yang, X., Li, Y., Li, Y., Ren, X., Zhang, X., Hu, D., and Gao, Y. (2017) 'Oxidative Stress-Mediated Atherosclerosis: Mechanisms and Therapies', *Frontiers in Physiology Article Front. Physiol*, 8(8). doi: 10.3389/fphys.2017.00600.

Volkers, M., Doroudgar, S., Nguyen, N., Konstandin, M.H., Quijada, P., Din, S., Ornelas, L., Thuerauf, D.J., Gude, N., Friedrich, K., Herzig, S., Glembotski, C.C., and Sussman, M.A. (2014) 'PRAS40 prevents development of diabetic cardiomyopathy and improves hepatic insulin sensitivity in obesity', *EMBO Mol Med*, 6(1), pp. 57–65. doi: 10.1002/emmm.201303183.

Webster, K. (2012) ‘Mitochondrial membrane permeabilization and cell death during myocardial infarction: roles of calcium and reactive oxygen species’, *Future cardiology*, 8(6), pp. 863–884. doi: 10.2217/fca.12.58.Mitochondrial.

WHO (2017) ‘World Health Statistics’, *World Health Organization*. Available at: http://apps.who.int/iris/bitstream/10665/255336/1/9789241565486-eng.pdf?ua=1 (Accessed: 8 December 2017).

World Health Organization (2016) ‘WORLD HEALTH STATISTICS - MONITORING HEALTH FOR THE SDGs’, *World Health Organization*, p. 1.121. doi: 10.1017/CBO9781107415324.004.

Yoshikawa, K., Inoue, M., Matsumoto, Y., Sakakibara, C., Miyataka, H., Matsumoto, H., and Arihara, S. (2005) ‘Lanostane Triterpenoids and Triterpene Glycosides from the Fruit Body of *Fomitopsis p inicola* and Their Inhibitory Activity against COX-1 and COX-2’, *Journal of Natural Products*, 68(1), pp. 69–73. doi: 10.1021/np040130b.

Younce, C. W., Burmeister, M. A. and Ayala, J. E. (2013) ‘Exendin-4 attenuates high glucose-induced cardiomyocyte apoptosis via inhibition of endoplasmic reticulum stress and activation of SERCA2a’, *American Journal of Physiology - Cell Physiology*, 304(6), pp. C508–C518. doi: 10.1152/ajpcell.00248.2012.

APPENDIX A

LIST OF REAGENTS, CONSUMABLES AND EQUIPMENT

Table A1: Reagents and Chemicals

Chemical/Reagent	Catalogue number	Company
ATP ViaLight assay kit	LT27-008	Lonza, Walkersville, MD, USA
Cell counting chamber slides	C10228	Life Technologies Corporation, Carlsbad, CA, USA
Cell lysis Buffer	FNN0011	Life Technologies Corporation, Carlsbad, CA, USA
Chloroform	136112-00-0	Sigma-Aldrich , St Louis, MO, USA
Coomassie blue stain	161-0437	Bio-Rad, Hercules, CA, USA
Cryotubes	430659	Corning, MA, USA
DeadEnd colometric TUNEL system	PRG3250	Promega,Madison, Wilsconsin, USA
Dimethyl sulfoxide (DMSO)	276855	Sigma-Aldrich , St Louis, MO, USA
Dulbecco`s modified Eagle`s medium (DMEM) with phenol red	B12-604F	Lonza, Walkersville, MD, USA

Dulbecco`s modified Eagle`s medium (DMEM) without phenol red	B12-917F	Lonza, Walkersville, MD, USA
Dulbecco`sphosphate buffered saline (DPBS)	B17-513F	Lonza, Walkersville, MD, USA
Ethanol	2875	Sigma-Aldrich , St Louis, MO, USA

Fetal bovine serum	BC/S0615-HI	Lonza, Walkersville, MD, USA
Hybond-P PVDF Membrane	RNP1416F	Amersham
Iso-propanol	I9516	Sigma-Aldrich , St Louis, MO, USA
Methanol	1070182511	Merck, Whitehouse Station, NJ, USA
Fat-free milk powder	N/A	Clover, Johannesburg, SA
Paraformaldehyde	158127	Sigma-Aldrich , St Louis, MO, USA
Penicillin-streptomycin mixture	DE17-602E	Lonza, Walkersville, MD, USA
Phenylmethanesulfonyl fluoride (PMSF)	11206893001	Roche, Basel, Switzerland
Ponceau S Stain	P23295	Sigma-Aldrich, St Louis, MO, USA

Propidium iodide	P4170	Sigma-Aldrich , St Louis, MO, USA
Protease Inhibitors	11206893001	Roche, Basel, Switzerland
Qiazol	79306	Qiagen, Hilden, Germany
RNase free water	Am9937	Ambion, Austin, TX, USA
Running buffer SDS	161-0772	Bio-Rad, Hercules, CA, USA
SDS-PAGE gels	161-0993	Bio-Rad, Hercules, CA, USA
Sodium bicarbonate (NaHCO3)	M2645	Sigma-Aldrich , St Louis, MO, USA
Sodium hydroxide (NaOH)	109140	Merck, Whitehouse Station, NJ, USA
Stainless steel beads 5mm	69989	Qiagen, Hilden, Germany
Sterile TC water	59900C	Lonza, Walkersville, MD, USA
SYBR Green mix	4385612	Applied Biosystems, Foster City, CA, USA
Tris-base	93352	Sigma-Aldrich , St Louis, MO, USA

Trypan blue	15050-065	Invitrogen, Carlsbad, CA, USA
Trypsin	17-161F	Lonza, Walkersville, MD, USA
Tween 20	58980C	Sigma-Aldrich , St Louis, MO, USA
Restore plus Western blot stripping buffer	46430	Thermo Fisher Scientific, Waltham, MA, USA

Table A2: Consumables

Consumables	Catalogue number	Company
0. 2 PCR tubes, flat cap	AX/PCR-02-C/S	Axgyen, Corning, NY
0.5 mL Eppendorf safe-lock tubes	0030 123.301	Eppendorf, Hamburg, Germany
1.5 mL Eppendorf safe- lock tubes	0030 123.328	Eppendorf, Hamburg, Germany
2 mL Eppendorf safe- lock tubes	0030 123. 344	Eppendorf, Hamburg, Germany
15 mL centrifuge tubes	602072	NEST Biotechnology, Jiangsu China Wuxi
50 mL centrifuge tubes	601001	NEST Biotechnology, Jiangsu China Wuxi
CELLBIND 24- well plates	3337	Corning, MA, USA
CELLBIND 6- well plates	3335	Corning, MA, USA

CELLBIND 96-well clear plates	3300	Corning, MA, USA
Cryotubes	430659	Corning, MA, USA
Filter Pads	23385	Sigma-Aldrich , St Louis, MO, USA
T75 Flasks	658975	Greiner bio-one, Frickenhausen, Germany

Table A3: Experimental kits

Experimental kits	Catalogue no	Company
ViaLight ATP assay kit	LT27-008	Lonza, Walkersville, MD, USA
Biorad RC DC protein kit	500-0201	Bio-Rad, Hercules, CA, USA
Caspase-Glo 3/7 Assay	PRG8091	Promega,Madison, Wilsconsin, USA
Catalase kit	707002	Cayman chemical, Ellsworth
DeadEnd Fluorometric TUNEL system	G3250	Promega, Madison, Wilsconsin, USA
GSH/GSSH assay kits	PRV6612	Promega, Madison, Wilsconsin, USA
High Capacity cDNA kit	PN 4375575	Applied biosystem, Foster City, CA, USA

Turbo DNase kit	AM1907	Ambion, Austin, TX, USA
SOD activity kit	ab65354	Abcam, Pretoria, SA
RNeasy mini kit	74106	Qiagen, Hilden, Germany
TBARS assay kit	STA-330	Cell Biolabs, San Diego,US
Clarity™ Western ECL substrate	1705060	Bio-Rad, Hercules, CA, USA

Table A4: Antibodies

Primary Antibodies	Catalogue number	Company
p-AMPK (Thr172)	2535	Cell signaling, Danvers, MA, US
p-Akt	Sc-493	Cell signaling, Danvers, MA, US
p-IRS-1 (Ser307)	2381	Cell signaling, Danvers, MA, US
GLUT4	G4173	Sigma-Aldrich , St Louis, MO, USA
p-NF-kB p65 (Ser468)	3039	Cell signaling, Danvers, MA, US
p-PKC (Tyr311)	2055	Cell signaling, Danvers, MA, US
B-actin	Sc-47778	Santa Cruz Biotechnology, Santa Cruz, CA, USA
Donkey anti-mouse IgG-HRP	Sc-2318	Santa Cruz Biotechnology, Santa Cruz, CA, USA

Donkey anti-rabbit IgG-HRP	Sc-2012	Santa Cruz Biotechnology, Santa Cruz, CA, USA

Table A5: Equipment

Equipment	Product Number	Supplier
Agilent Bioanalyser	G2946-90004	Agilent Technologies,Santa Clara, California
CountessTM Automated Cell Counter	C10227	Invitrogen, Carlsbad, CA, USA
D1200-230V Heating block	S62927099	Labnet, Adison,NJ,USA
IKA® MS 3 digital shakers	IKA 331900X	Sigma-Aldrich , St Louis, MO, USA
Benchtop Centrifuge	SL16R	Thermo Fisher Scientific, Waltham, MA, USA
Micro-centrifuge	001977	Eppendorf, Hamburg, Germany
Mini Protean casting frame	165-3304	Bio-Rad, Hercules, CA, USA
Mini Protean casting stand	165-3303	Bio-Rad, Hercules, CA, USA
Mini Protein tetra cell	165-8030	Bio-Rad, Hercules, CA, USA
Mini Trans-blot cell	170-4070	Bio-Rad, Hercules, CA, USA
NanoDrop™1000 Spectrophotometer	A984	Thermo Fisher Scientific, Waltham, MA, USA
Orbital shaker ITPSIC 10	20197	Torrey pines Scientific
PowerPac HC	165-8025	Bio-Rad, Hercules, CA, USA
TissueLyser	85300	Qiagen, Hilden, Germany
ABI 7500 Real time PCR system	4351104	Applied Biosystem, Foster City, CA, USA
2720 Thermal cycler	4413750	Applied Biosystem, Foster City, CA, USA
Nikon Eclipse Ti inverted microscope	Ti inverted	Nikon, Tokyo, Japan

Biotek® FLX 800 plate reader	FLX 800	BioTek Instruments Inc., Winooski, VT, USA
BioTek® ELX800 plate reader	ELX800	BioTek Instruments Inc., Winooski, VT, USA
Orbital shacker	20197	Stoval life Sciecne

APPENDIX B PREPARATION OF REAGENTS

I. Preparation of DMEM: Stored at 4°C in 50 mL tubes

500mL of DMEM with phenol red and glutamate was supplemented with;

- 50 mL of FBS (Final FBS concentration of 10%)
- 5.5mL of pen-strep (Final concentration of 1%)

II. Preparation of treatment media: Stored at 4°C in 50 mL tubes

- 33 mM glucose containing; 1000 mg/L DMEM powder and 1 % BSA
- 5.5 mM glucose containing: 1000 mg/L DMEM powder and 1 % BSA

III. Preparation of 10x Tris-buffered saline (TBS) wash buffer: Stored at 4°C

The 10x TBS wash buffer was prepared by dissolving:

- 200 mM of Tris (24.22 g)
- 1.37 mM NaCl (80.06 g)
- Topped up with distilled to a total volume of 1L.

IV. 1X TBS and Tween 20 (1X TBST-20): Stored at 4°C

1X TBST-20 was prepared by added:

- 100 mL of 10 x TBST
- 900 mL of distilled water (v/v)
- 1 mL Tween 20

V. Transfer buffer for Western Blot

The buffer was prepared by adding:

- 25 mM of Tris (3.03 g)
- 192 mM glycine (14.4 g)
- 800 mL of distilled water,
- 200mL of methanol to make up a total volume of 1L.
-

VI. RIPA Buffer

The buffer consisted of the following:

- 25mM Tris (10 mM sodium phosphate may be used instead), pH 7–8
- 150 mM NaCl
- 0.1% SDS (optional)
- 0.5% sodium deoxycholate
- 1% Triton X-100 or NP-40